093650

Memoir 46

New Mexico Bureau of Mines & Mineral Resources

A DIVISION OF
NEW MEXICO INSTITUTE OF MINING & TECHNOLOGY

Field excursions to volcanic terranes in the western United States, Volume I: Southern Rocky Mountain region

Edited by Charles E. Chapin and Jiri Zidek
New Mexico Bureau of Mines & Mineral Resources, Socorro, New Mexico 87801

Published for
IAVCEI GENERAL ASSEMBLY
Santa Fe, New Mexico, USA
June 25–July 1, 1989

RECEIVED
AUG 25 2006
By

14366

INTERNATIONAL ASSOCIATION OF VOLCANOLOGY AND CHEMISTRY OF THE EARTH'S INTERIOR (IAVCEI)
1989 GENERAL ASSEMBLY

Sponsors

U.S. Geological Survey
Institute for the Study of Earth and Man, Southern Methodist University
Los Alamos National Laboratory
New Mexico Bureau of Mines and Mineral Resources
University of New Mexico
Institute for Geophysics and Planetary Physics, University of California
National Science Foundation
American Geophysical Union
U.S. Department of Energy
Sandia National Laboratories

Organizing Committee

Chairman: MICHAEL DUNGAN, *Dallas*
Secretary: SCOTT BALDRIDGE, *Los Alamos*
Program: PETER LIPMAN, *Denver*
Field Trips: WOLFGANG ELSTON, *Albuquerque*
Publications: CHARLES CHAPIN, *Socorro*
Local Arrangements: GRANT HEIKEN, *Los Alamos*
KENNETH WOHLETZ, *Los Alamos*
IAVCEI Secretary General: HANS-ULRICH SCHMINCKE, *Bochum*

FRONT COVER—Shiprock, in northwestern New Mexico, is a 500 m high erosional remnant of an Oligocene diatreme. It consists mainly of minette (a potassic lamprophyre) tuff breccia cut by a few thin, irregularly shaped dikes. The tuff breccia contains abundant inclusions of the sedimentary rocks through which the vent penetrated as well as fragments of plutonic rocks from the Precambrian basement, approximately 2.7 km beneath the present summit. Mantle xenoliths are also present. Crude bedding formed by fallback of pyroclastic ejecta defines a shallow, saucer-shaped structure near the top and indicates that the original crater was not much higher. The tuff breccia is strongly cemented with calcite and is much more resistant to erosion than surrounding Cretaceous shales. Conspicuous vertical jointing, exploited by weathering and erosion, has produced a castellated appearance. Three dikes radiate from Shiprock; the south dike, shown here, extends 9 km from the vent. Photo H. L. James.

BACK COVER—Digitally enhanced multispectral Landsat image of north-central New Mexico centered on the Jemez Mountains and Valles caldera (Quaternary). The northern suburbs of Albuquerque are just visible along the Rio Grande at bottom edge of image. Santa Fe can be seen at lower right and Taos at upper right. The Sangre de Cristo Mountains form the right margin and the early Tertiary San Juan Basin occupies the left one-third of the image. The very straight Nacimiento oblique-slip fault is conspicuous at left center and trends N4°W along the west edge of the Nacimiento Range. The snow-covered mountains at top center are the Tusas Mountains. The Albuquerque, Española, and San Luis Basins form a right-stepping chain of en-echelon rift basins between the Sangre de Cristo Mountains on the right (east) and the Jemez and Tusas Mountains on the left (west). The Rio Grande Gorge and scattered stratovolcanoes of the Taos Plateau volcanic field (4.5–2 Ma) are prominent geomorphic features in the San Luis Basin at upper right. A southwest-trending prong of Servilleta Basalt from the Taos Plateau caps Black Mesa near the confluence of the Rio Grande and Chama River at right center. Black Mesa parallels the Embudo fault zone, an accommodation zone between the east-tilted San Luis Basin to the north and the west-tilted Española Basin to the south. The Embudo fault, the Valles caldera, and basalt-capped Mesa Prieta and Cebolleta Mesa at lower left lie on the Jemez lineament, a crustal flaw of Precambrian ancestry which has been one of the most active magmatic zones in the United States for the past 5 m.y. See Excursion 17B for details of the Valles caldera and Jemez volcanic field. Excursions 5A and 8A cover the southwestern projection of the Jemez lineament; Excursion 18B visits the Embudo fault zone, the Taos Plateau, and the northeastern extension of the Jemez lineament. Excursion 15B examines the Questa caldera (26 Ma) with its plutons and molybdenum mines (just visible at far upper right). The Dulce swarm of early-rift mafic dikes (23.5–27 Ma) is visible at upper left.

GEOPIC image provided by Earth Satellite Corporation, 7222 47th Street, Chevy Chase, Maryland 20815.

chemistry of the Handkerchief Mesa mixed magma complex, San Juan Mountains, Colorado: Journal of Volcanology and Geothermal Research, 26: 251–274.

Tweto, O., and Sims, P. K., 1963, Precambrian ancestry of the Colorado mineral belt: Geological Society of America, Bulletin, 74: 991–1014.

Tweto, O., Steven, T. A., Hail, W. J., Jr., and Moench, R. H., 1976, Preliminary geologic map of the Montrose 1 × 2° quadrangle, southwestern Colorado: U.S. Geological Survey, Miscellaneous Field Studies Map MF-761.

Varnes, D. J., 1963, Geology and ore deposits of the South Silverton mining area, San Juan County, Colorado: U.S. Geological Survey, Professional Paper 378-A: 56 pp.

Webber, K. L., 1988, The Mammoth Mountain and Wason Park Tuffs: Magmatic evolution in the central San Juan volcanic field, southwestern Colorado: Unpublished Ph.D. thesis, Rice University, Houston, 244 pp.

Wetlaufer, P. H., Bethke, P. M., Barton, P. B., Jr., and Rye, R. O., 1977, The Creede Ag–Pb–Zn–Cu–Au district, central San Juan Mountains, Colorado: A fossil geothermal system: Nevada Bureau of Mines, Report 33: 159–164.

Whitney, J. A., and Stormer, J. C., Jr., 1986, Mineralogy, petrology, and magmatic conditions from the Fish Canyon Tuff, central San Juan volcanic field, Colorado: Journal of Petrology, 26: 726–762.

Whitney, J. A., and Stormer, J. C., Jr., 1988, The Carpenter Ridge Tuff: The development of chemical and thermal gradients through magma mixing in a periodically replenished magma chamber: American Journal of Science, 228A: 16–44.

EXCURSION 17B: Volcanic and hydrothermal evolution of Valles caldera and Jemez volcanic field

Fraser Goff[1], Jamie N. Gardner[1], W. Scott Baldridge[1], Jeffrey B. Hulen[2], Dennis L. Nielson[2], David Vaniman[1], Grant Heiken[1], Michael A. Dungan[3], and David Broxton[1]

[1]*Earth and Space Sciences Division, Los Alamos National Laboratory, Los Alamos, New Mexico 87545;*
[2]*University of Utah Research Institute, 391 Chipeta Way, Suite C, Salt Lake City, Utah 84108;*
[3]*Department of Geological Sciences, Southern Methodist University, Dallas, Texas 75275*

Introduction

Valles caldera has become world famous as an example of a resurgent caldera and as the location of a high-temperature geothermal system of volcanic origin (Smith and Bailey, 1968; Dondanville, 1978). Although the caldera and its modern hydrothermal system result from events that have happened during the last 1.12 Ma, the Jemez volcanic field has experienced continuous volcanism for more than 13 Ma and is known to have had at least three major periods of distinct hydrothermal activity (Gardner et al., 1986; WoldeGabriel and Goff, 1989). The field-trip guide presented here will emphasize the results of volcanic, tectonic, and geochemical research pertaining not only to the Valles caldera but to the entire history of the Jemez volcanic field. The last one and one-half days of the trip will also emphasize drill-hole data that have recently given researchers a wealth of information on extra- and intracaldera structure, stratigraphy, hydrothermal alteration, and fluid chemistry in the most explored Quaternary caldera complex in the United States. The accompanying paper is not intended to review exhaustively all aspects of research on the Jemez volcanic field; rather, it stresses significant discoveries and interpretations that have occurred since about 1980.

Geologic overview and summary of earlier research

The Jemez volcanic field (Figs. 1, 2) contains a diverse suite of basaltic through rhyolitic rocks that were erupted from >13 to 0.13 Ma, although the field is best known for the Valles caldera (1.12 Ma) and the Bandelier Tuff (Smith and Bailey, 1966, 1968; Gardner et al., 1986; Self et al., 1986). The volcanic field overlies the western edge of the Rio Grande rift (RGR) at the intersection of the rift and the Jemez volcanic lineament (JVL). The lineament is defined by a chain of Miocene to Quaternary volcanic centers stretching from southeast Colorado across New Mexico to central Arizona (Mayo, 1958; Laughlin et al., 1976; Aldrich, 1986). The largest volume and diversity of volcanic rocks

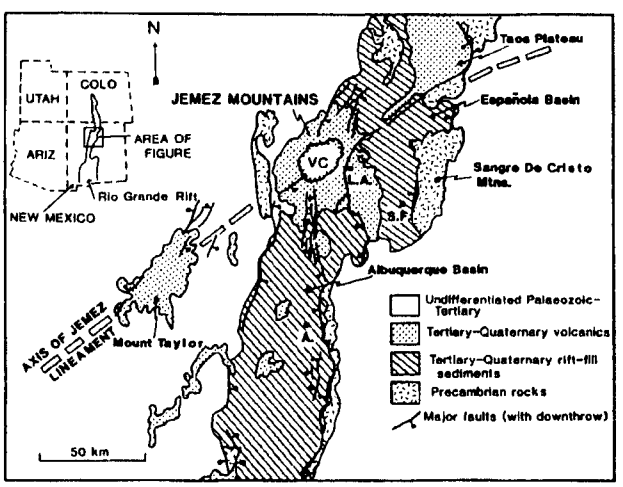

FIGURE 1—Regional map showing generalized relations of the Jemez volcanic field (Jemez Mountains) to basins of the north-central Rio Grande rift. VC is the Valles caldera; major fault zones of the region are shown. LA, SF, and A are the cities of Los Alamos, Santa Fe, and Albuquerque, respectively (from Self et al., 1987).

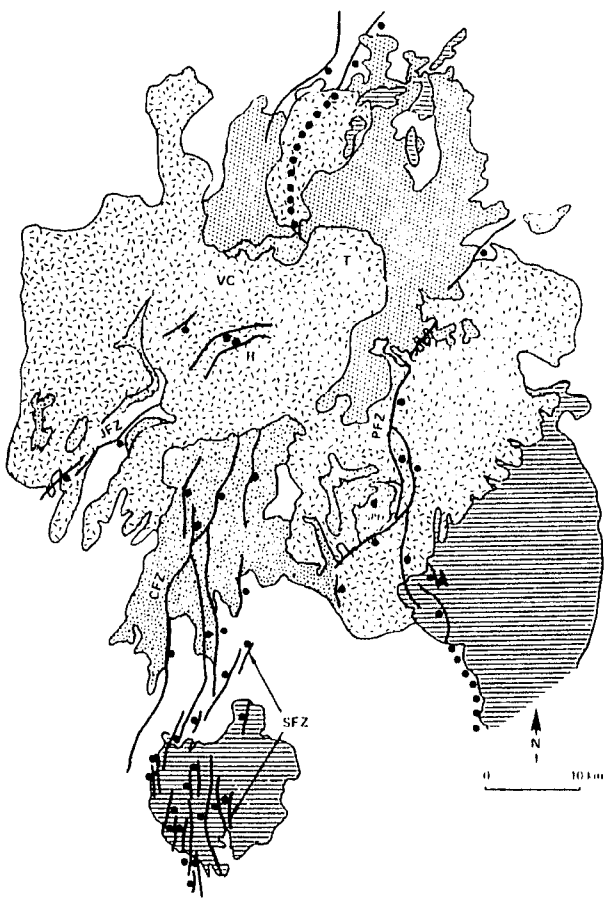

FIGURE 2—Generalized geologic map of the Jemez volcanic field showing distribution of major stratigraphic groups. Irregular stipple = Keres Group formations; coarse, regular stipple = Polvadera Group formations; random dash = Tewa Group formations; horizontally ruled pattern = young basalt fields. Major fault zones are Jemez fault zone (JFZ), Santa Ana Mesa fault zone (SFZ), Cañada de Cochiti fault zone (CFZ), and Pajarito fault zone (PFZ). VC = Valles caldera, R = resurgent dome of Valles caldera, T = Toledo embayment, SPD = St. Peter's Dome (from Gardner and Goff, 1984).

along the JVL have been erupted in the Jemez Mountains. Tertiary basin-fill rocks of the Española and Santo Domingo Basins of the RGR underlie volcanic rocks on the eastern side of the volcanic field, whereas Paleozoic to Mesozoic sedimentary rocks and Precambrian crystalline rocks of the Colorado Plateau underlie volcanic rocks on the west.

Early reconnaissance studies of the geology and petrology of the Jemez Mountains were conducted by J. P. Iddings and J. W. Powell (Iddings, 1890; Powell, 1961). Gold claims were first staked in the Cochiti Mining District in the southeast Jemez Mountains in 1893 and ore was mined from 1897 to 1903 and from 1914 to 1916 (L. C. Graton *in* Lindgren et al., 1910). Sulfur was mined from the Sulphur Springs area, inside the caldera, from 1902 to 1904 (Mansfield, 1918). There have been various topical studies of the hot springs of the Jemez Mountains (Fig. 3) during the last 100 years, beginning with O. Loew in 1875 (see Summers, 1976).

Comprehensive investigations of the geology, volcanism, and hydrology of the Jemez Mountains began in the 1920's and were intensified during the 1940's by members of the U.S. Geological Survey. These studies continued through the 1960's and, in limited fashion, to the present day (Ross and Smith, 1961; Smith et al., 1961; Griggs, 1964; Doell et al., 1968; Bailey et al., 1969; Smith et al., 1970; Smith, 1979). Valles caldera contains the type locality of the Jaramillo normal-polarity magnetic event (Doell and Dalrymple, 1966).

Although a limited number of geophysical studies were performed in the region before 1980, many were conducted by oil companies in the RGR or by UNOCAL (formerly Union Oil Company of California) in the caldera and were,

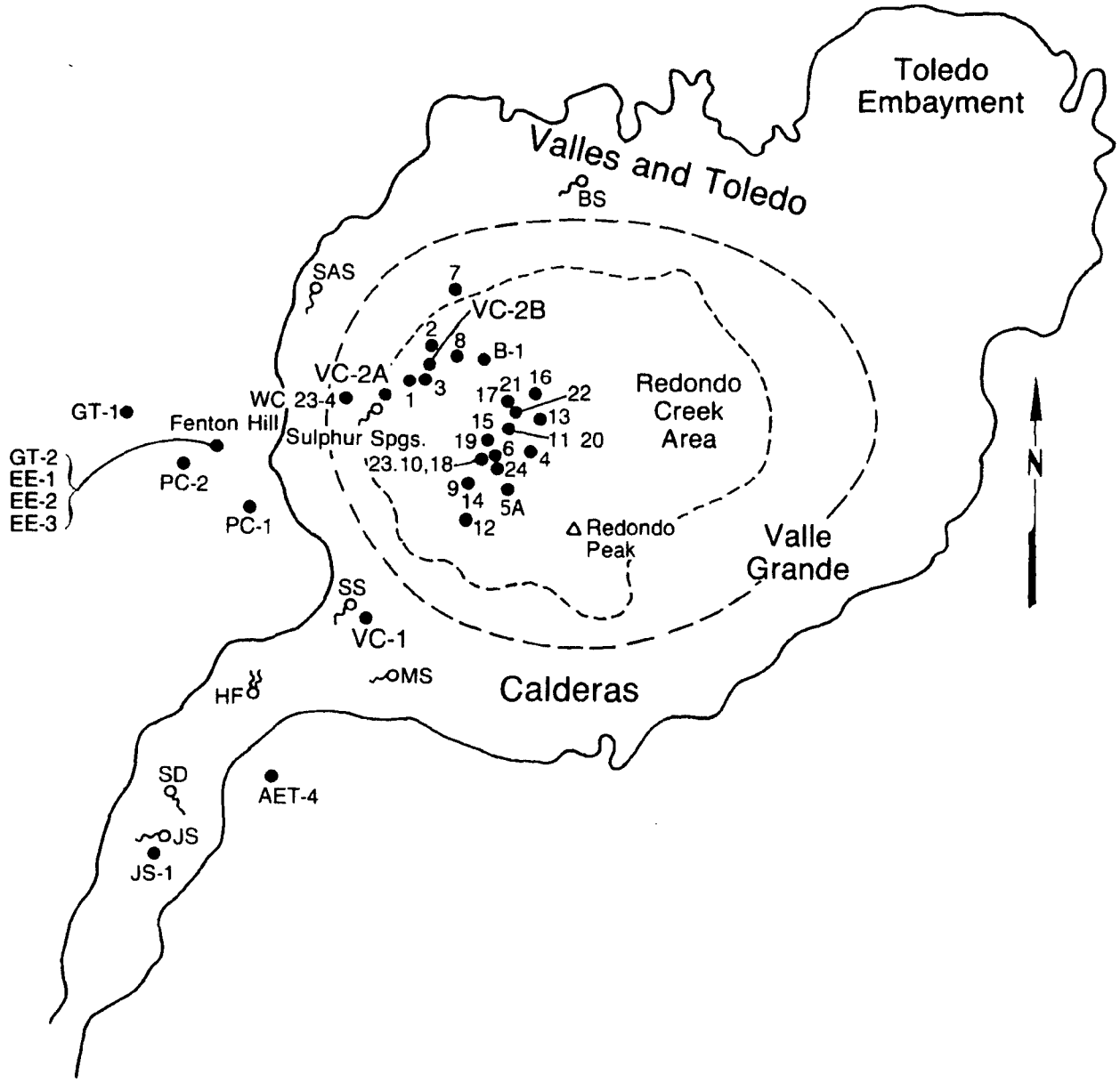

FIGURE 3—Map of Valles caldera region showing locations of hot-spring areas and geothermal wells. Hot springs: BS = Bathhouse Spring; SAS = San Antonio Hot Spring; SS = Spence Hot Spring; MS = McCauley Spring; SD = Soda Dam; JS = Jemez Spring; HF = Hummingbird Fumarole. All wells with number only have "Baca" prefix. B-1 = Westates-Bond #1.

therefore, proprietary. Nonetheless, it was known in the 1970's that large gravity anomalies were associated with the caldera and the RGR (Cordell, 1978), as were substantial heat-flow anomalies (Reiter et al., 1975, 1976).

Geothermal development and research

The first "geothermal" well was drilled in Valles caldera in 1960 as an oil test on the west flank of the resurgent dome. Instead of oil, the Westates-Bond #1 well struck superheated water (~200°C) at shallow depths (Dondanville, 1971). Three more wells were drilled during the 1960's in the same general area, achieving maximum temperatures of 220°C at a depth of 430 m (Fig. 3). UNOCAL drilled their first well in the central resurgent dome (Baca 4) in 1970 (278°C at a depth of 1435 m) and 20 more wells were drilled before the geothermal project was terminated in 1984 because of insufficient reservoir permeability (Kerr, 1982; Goldstein and Tsang, 1984).

As the prospect of geothermal development brightened during the 1970's, there were more investigations of the hot springs and caldera hydrology (Trainer, 1975, 1978). Attempts were made (with mixed success) to drill wells to extract fluids for space heating at Jemez Springs, southwest of the caldera, and on the Pajarito Plateau east of the caldera (Goff and Grigsby, 1982). Exploration efforts by GEO Operator Corporation (formerly Geothermal Resources International, Inc.) and SUNEDCO (Sun Energy Development Corporation), west and south of the caldera, respectively, resulted in two more deep wells (Shevenell et al., 1988). The body of scientific and engineering data gained from these various drilling programs is immense. Because of partial U.S. Department of Energy (DOE) funding for the UNOCAL effort (Spencer and Tsang, 1984; Mills et al., 1987), virtually all data from all wells mentioned above are in the public domain.

Fenton Hill, located on the western margin of Valles caldera, is the site of the first Hot Dry Rock (HDR) geothermal research experiment in the world (Heiken et al., 1981; Laughlin, 1981; Smith, 1983). Although intended to develop the technology for commercially extracting heat from hot, impermeable rock, the HDR project provides an extensive geologic data base from relatively unfaulted Precambrian and Paleozoic rocks just west of the caldera depression. Eleven heat-flow holes and seven intermediate to deep wells have been drilled for this project. Maximum temperatures are 325°C at a depth of 4.5 km in complex Precambrian basement lithologies. The commercial applications of HDR technology are still under investigation at Fenton Hill, but this research has spawned other HDR efforts of varying scope in Great Britain, France, Germany, and Japan.

Significant geologic research since 1980

Starting in about 1980, results from diversified research in the Valles caldera region began to appear in the geological literature. In addition to graduate-thesis projects (e.g., Stein, 1983; Gardner, 1985), much of the research was stimulated by geologic investigations of the HDR program (Kolstad and McGetchin, 1978; Laughlin et al., 1983; Heiken and Goff, 1983) or from data and samples released from the "Baca" project of UNOCAL (Faust et al., 1984; Nielson and Hulen, 1984). The largest single source of funding for new Valles research has come through the Continental Scientific Drilling Program (CSDP) (Goff and Gardner, 1988). Because the Valles caldera has been discussed for nearly 20 years as a high-priority site for the investigation of fundamental processes in magmatism, hydrothermal systems, and ore depositional mechanisms, the DOE/Office of Basic Energy Sciences has sponsored scientific investigations, task groups, and workshops to identify critical data gaps, drilling objectives, and sites (e.g., Luth and Hardee, 1980; Taschek, 1981; Heiken, 1985). The extensive subsurface data base at Valles caldera (nearly 40 deep wells) makes it the best explored Quaternary caldera complex in the USA and allows for very precise planning and realistic expectations to meet scientific goals. For example, the known composite stratigraphic section in the Valles region is nearly 7 km (wells Baca 12 and EE-2), consisting of 1950 m of Quaternary caldera fill, over 300 m of Tertiary precaldera volcanic and sedimentary rocks, over 800 m of Paleozoic sedimentary rocks, and 3700 m of Precambrian basement (Laughlin et al., 1983; Nielson and Hulen, 1984). The support of the CSDP has resulted in continuous coring of three scientific holes in the caldera (VC-1, VC-2A, and VC-2B) and the creation of a scientific constituency and long-range plan for future scientific drilling (Goff et al., 1986, 1987; Goff and Nielson, 1986).

All this new surface and subsurface work resulted in important discoveries and refinements of previous knowledge in the Valles caldera region. We categorize these discoveries and refinements in the following sections, and our field trip touches on many of the recent research topics.

Stratigraphy, petrology, and tectonic associations in Jemez volcanic field

Stratigraphy—The formalized stratigraphy for volcanic and volcaniclastic rocks in the Jemez volcanic field was developed by Griggs (1964), Bailey et al. (1969), and Smith et al. (1970). These authors divided the volcanic field into three stratigraphic groups, from oldest to youngest the Keres, Polvadera, and Tewa. The Keres Group is dominated by two-pyroxene andesite, the Polvadera Group is dominated by dacite, and the Tewa Group is dominated by high-silica rhyolite. Bailey, Smith, and coworkers believed that each group represented discrete time intervals and petrologic entities. After considerably more detailed geologic mapping, acquisition of radiometric dates, and analysis of the various rock types by several groups of researchers, it is now realized that temporal and petrologic overlap occurs among all groups and many formations (Gardner et al., 1986; Loeffler et al., 1988), although the three stratigraphic groups still retain much of their original petrologic significance.

Fig. 4 shows the generalized stratigraphic relations of major units in the Jemez volcanic field as defined by Gardner et al. (1986), compared with the age relations of the three groups as originally defined by Bailey et al. (1969). Many significant changes appear in this figure, which are summarized as follows (see Gardner et al., 1986):

1. The inception of volcanism in the Jemez Mountains region began at least 16.5 Ma ago (alkalic basalts in the Santa Fe Group), but the oldest rocks in formal units of the volcanic field were erupted between 13 and 14 Ma.

2. Hydrothermally altered volcanic and hypabyssal rocks of the Cochiti mining district (Bland group of Stein, 1983) are not Eocene or Oligocene as previously thought. They represent the altered and eroded interior of Keres Group andesitic volcanoes that were intruded by Bearhead Rhyolite and later cut by epithermal quartz veins. Ages on all units

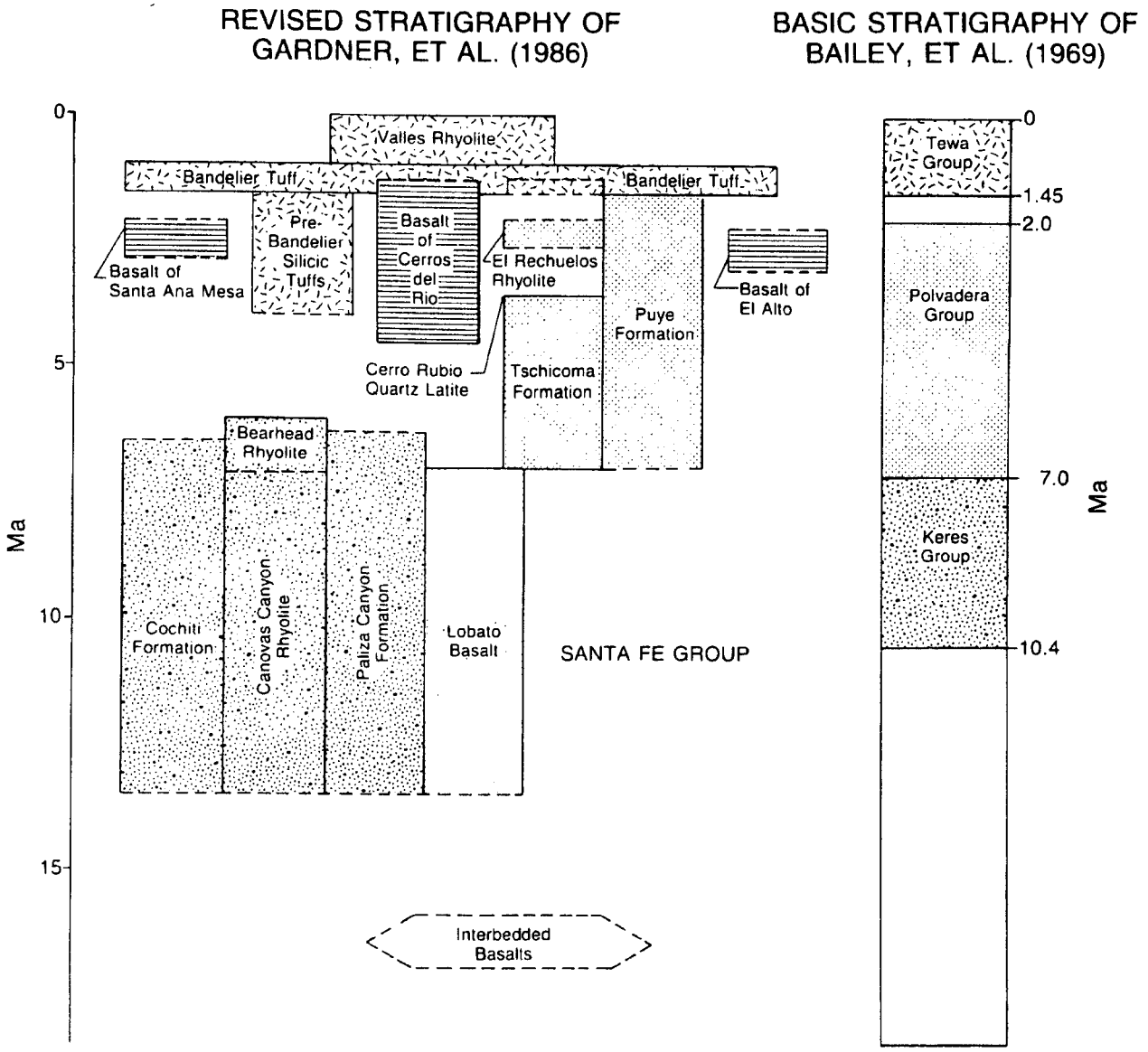

FIGURE 4—Basic stratigraphy of the Jemez volcanic field (Bailey et al., 1969) compared to revised stratigraphy of Gardner et al. (1986); patterns are the same as Fig. 2. Dashed lines indicate uncertainty and more revisions may be forthcoming (see Fig. 27, Day 2). The figure is also a schematic south-to-north (left-to-right) section through the volcanic field.

and events within this altered sequence range from 11.2 to 5.6 Ma (Stein, 1983; Wronkiewicz et al., 1984; Gardner et al., 1986; WoldeGabriel and Goff, 1989).

3. The Basalt of Chamisa Mesa (10.4 Ma) is indistinguishable from basalts of the Paliza Canyon Formation chemically, temporally, or petrographically.

4. The Cochiti Formation is included within the Keres Group because of intimate spatial, temporal, genetic, and tectonic relations to formations in the group.

5. The Lobato Basalt occupies a much wider time range (14–7 Ma) than previously thought (~8–7 Ma). Lobato basalts are petrographically and chemically similar to basalts of the Paliza Canyon Formation and the age range of the two units is practically identical, indicating that the distinction between the units is merely geographical.

6. Dacitic rocks of the Tschicoma Formation (7–3 Ma) are chemically and petrographically similar to some mapped dacites in the Paliza Canyon Formation. On the other hand, the Tschicoma Formation, originally defined by Griggs (1964) to consist only of dacite, contains large unmapped areas of two-pyroxene andesite grossly similar to andesites in the Paliza Canyon Formation. Overlap in chemistry, petrography, and age of these formations is significant and the age break between them shown in Fig. 4 acknowledges the geographical distinction built into the formal stratigraphy of Bailey et al. (1969).

7. The El Rechuelos Rhyolite, on the northern side of the volcanic field, is restricted to two domes west of Polvadera Peak dated at 2 Ma. Other rhyolites in the northern Jemez Mountains are older (5.8–7.5 Ma) (Loeffler et al., 1988). The older rhyolites resemble Bearhead Rhyolite on the southern side of the volcanic field.

8. The Tewa Group contains recently characterized ignimbrites that predate the Bandelier Tuff and temporally overlap the waning stages of Polvadera Group volcanic activity (Self et al., 1986).

9. The Cerro Rubio Quartz Latite, located in the Toledo embayment, chemically and temporally resembles Tschicoma Formation dacites and is now included in the Tschicoma Formation (Heiken et al., 1986; Gardner et al., 1986).

10. Post-Toledo caldera moat volcanism is more complicated than previously thought (e.g., Smith, 1979). Several rhyolites formerly thought to be post-Valles in age are now realized to be post-Toledo in age (Heiken et al., 1986). Chemical and petrologic variation within the Cerro Toledo Rhyolite define subgroups of rhyolite types and show restoration of compositional zonation of the Bandelier magma chamber between two caldera-forming eruptions (Stix et al., 1988).

11. Post-Valles caldera moat volcanism is far more complicated than previously thought (e.g., Smith, 1979). Several distinct magma batches gave rise to the Valles Rhyolite (Gardner et al., 1986; Spell, 1987; Self et al., 1988).

Volcanic petrology—Chemical data for selected rocks from all major stratigraphic units of the Jemez volcanic field show a wide range of compositions (Table 1; Gardner et al., 1986). Both chemical and modal classification schemes tend to obscure the diversity of rock types in the volcanic field (Gardner, 1985). With few exceptions, the rocks of the volcanic field are subalkaline (Fig. 5) and are of the calc-alkaline series. In fact, most andesites of the Jemez Mountains satisfy the criteria suggested by Gill (1981) for high-potassium orogenic andesites. A noteworthy result of recent work is that rocks previously termed dacite, latite, quartz latite, and rhyodacite are best referred to as dacite.

Fig. 6A shows a representation of dates in the volcanic field plotted with respect to magma type, while Fig. 6B shows a plot of rate of volcanism vs. time for the Jemez volcanic field (Gardner and Goff, 1984; Gardner, 1985). Several features are revealed by these figures:

1. Eruptions of mantle-derived basalt span the entire history of the volcanic field with the exception of a tectonic lull from 7 to 4 Ma (mentioned below).

2. Magmas derived by differentiation of mantle-derived material were erupted early in the history of the field with a voluminous pulse occurring from 10 to 7 Ma. These magmas are represented primarily by two-pyroxene andesites and some dacites of the Paliza Canyon Formation and constitute over half the original volume of the volcanic field (~2000 km^3). Similar rocks of similar age are now recognized in units previously mapped as Tschicoma Formation and Lobato Basalt on the north side of the volcanic field (see Table 5, Day 2 of this guide).

3. High-silica rhyolitic magmas, derived from partial melts of lower crust, were continuously erupted in the period 13–6 Ma with a pronounced volumetric pulse at 7–6 Ma (Gardner et al., 1986). These melts are represented by the Canovas Canyon and Bearhead rhyolites of the Keres Group. On the other hand, the "early rhyolite" of Loeffler et al. (1988) (formerly called El Rechuelos) is derived primarily by fractional crystallization of basalt with addition of about 5% of lower crust. El Rechuelos Rhyolite requires less than 2% of lower crust. Thus, the origin of rhyolite in the Jemez Mountains is still the subject of intense investigation.

4. Dacites formed by mixing of basalt or basaltic andesite and high-silica rhyolite were erupted beginning at about 7 Ma. Onset of eruption of these mixed magmas was contemporaneous with cessation of eruption of basalt, differentiates of basalt, and high-silica rhyolites discussed above. Most of these mixed magmas are represented by the dacites of the Tschicoma Formation, but some occur in the Paliza Canyon Formation.

5. Onset of Tewa Group volcanism, including the caldera cycles and Bandelier Tuff, was essentially contemporaneous with revival of basaltic volcanism at 4 Ma. Some overlap with eruptions of mixed magma continued to 2 Ma.

Tectonic history—Following a mid-Miocene volcanic hiatus (Chapin and Seager, 1975), revival of rifting in the vicinity of the Jemez Mountains began at roughly 16.5 Ma (Gardner and Goff, 1984). From 13 to 10 Ma, tectonic activity was intense and was accompanied by basalt and rhyolite eruptions along the Cañada de Cochiti fault zone. These eruptive rocks are interbedded with immature basin-fill gravels and laharic breccias of the Cochiti Formation

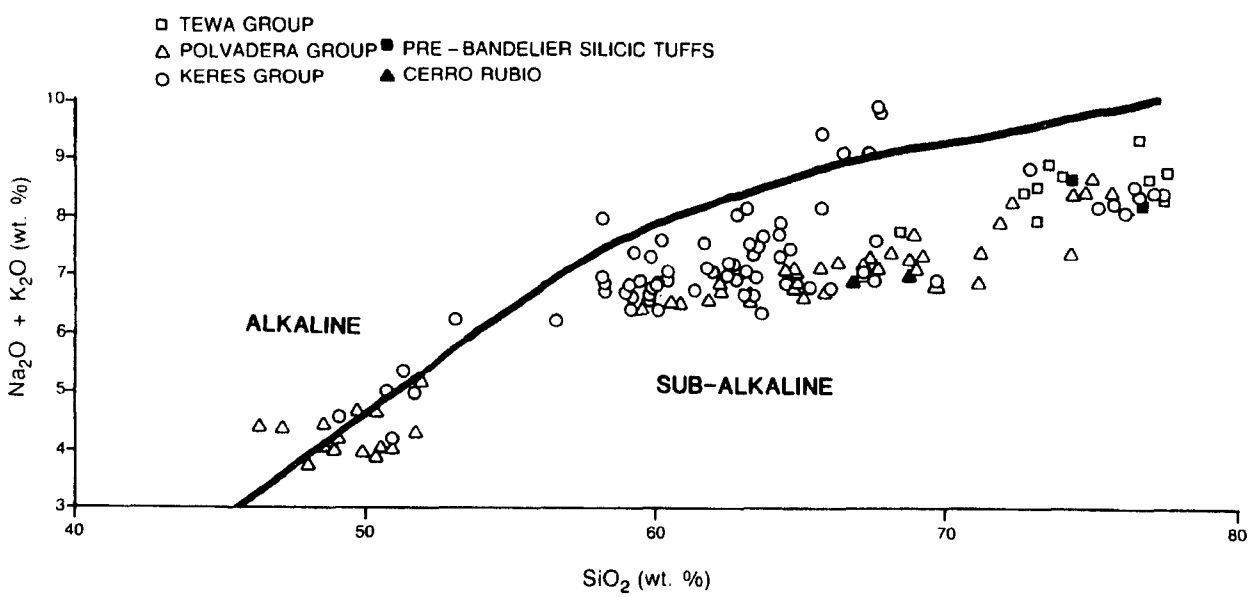

FIGURE 5—Plot of total alkalies vs. SiO_2 for rocks of the Jemez volcanic field. Curve separating alkaline and subalkaline fields is from Irvine and Baragar (1971). From Gardner et al. (1986).

that thicken dramatically from west to east into the Rio Grande rift. In the period 10–7 Ma, basalt, rhyolite, and basaltic differentiates were rapidly vented along the Cañada de Cochiti zone to form half the volume of the entire volcanic field. From 7 to 6 Ma, eruption of differentiates of basalt and rhyolite ceased and eruption of dominantly mixed magma began with a sharp reduction in the volumetric rate of volcanic activity. At 7–4 Ma, a lull in basaltic volcanism occurred and the Cañada de Cochiti fault zone became inactive.

We believe the events at about 7 through 4 Ma reflect petrogenetic response to a significant reduction in the intensity of tectonic activity in the vicinity of the Jemez Mountains. Instead of being rapidly vented along active faults as in earlier stages of the volcanic field's development, pockets of these mantle- and lower-crust-derived magmas coalesced, giving rise to the hybrid dacite volumetrically dominant in the Tschicoma Formation (Polvadera Group). Additionally, the geometry of the Puye Formation, a broad volcaniclastic alluvial fan shed off the Polvadera Group's constructive highland, strongly suggests building of most of the fan in a period of relative tectonic inactivity from 7 to 4 Ma.

Major tectonic activity shifted from the Cañada de Cochiti fault zone to the Pajarito fault zone at about 5–4 Ma. This shift was accompanied by renewed basaltic activity at 4 Ma, peripheral to and basinward of the volcanic field. By about 3.5 Ma, dacitic eruptions in the central field began to be intermixed with small-volume rhyolitic ignimbrite eruptions. Dacitic eruptions ceased by about 2 Ma and the first large-volume ignimbrite of the Tewa Group, the Otowi Member of the Bandelier Tuff, was erupted at 1.45 Ma from the Toledo caldera. The Toledo and Valles caldera (1.12 Ma) cycles, with attendant postcaldera rhyolite dome eruptions, continued to 0.13 Ma.

Tectonic activity on the Pajarito and Jemez fault zones has continued through the Quaternary (Smith et al., 1970; Golombek, 1983; Gardner and House, 1987; Goff and Shevenell, 1987). Vertical displacement on the Tshirege Member of the Bandelier Tuff is typically about 100–200 m along the Pajarito fault zone in Los Alamos County and in Bandelier National Monument. Offset of the Tshirege Member is 50 m along the Jemez fault zone in the west wall of San Diego Canyon. Numerous localities show faulting of Quaternary units younger than the Bandelier Tuff along both of these faults (Gardner and House, 1987; Goff and Shevenell, 1987).

TABLE 1—Chemical analyses of rocks from each major stratigraphic unit of the Jemez volcanic field (from Gardner et al., 1986). See Gardner (1985) for analytical methods and quality of data. [a]Chemical data from Loeffler (1984). [b]Total iron as Fe_2O_3 from analysis.

	Santa Fe Group Basanite	Paliza Canyon Basalts		Canovas Canyon Rhyolite		Paliza Canyon Andesite		Paliza Canyon Dacite		Bear-head Rhyolite	Lobato[a] Basalt	Tschicoma[a] Andesite	Tschicoma Dacite
						Type 1	Type 2	Type 1	Type 2				
	F81-50	JG80-53	F81-22	JG81-51	JG80-47C	JG80-28	JG81-4B	JG81-31	JG81-20A	JG80-49	SB224	IM153	JG80-12
Approx. age, Ma	16.5	13.2	11	11	8.7	8	8	9	8	6.18	8	6.5	5
Major elements													
SiO_2	43.82	50.62	50.95	76.08	76.63	59.98	63.47	66.48	67.45	76.16	50.51	60.76	67.21
TiO_2	2.36	1.76	1.37	0.12	0.12	1.09	0.83	0.68	0.48	0.11	1.47	0.93	0.51
Al_2O_3	13.74	17.77	15.65	11.77	12.36	16.37	16.75	15.75	15.43	12.11	16.00	16.54	15.28
Fe_2O_3[b]	12.35	10.27	9.34	0.68	0.77	6.40	4.45	3.27	3.89	0.68	11.05	6.02	3.68
MnO	0.17	0.15	0.13	0.05	0.04	0.08	0.09	0.07	0.05	0.07	0.16	0.09	0.06
MgO	10.65	3.91	7.96	0.07	0.09	2.66	1.65	0.58	1.12	0.04	6.71	2.54	1.69
CaO	10.00	9.08	8.33	0.54	0.47	5.27	3.87	1.91	3.10	0.40	9.56	4.62	3.40
Na_2O	3.26	3.99	3.25	3.71	3.80	4.25	4.23	5.49	3.79	3.92	3.11	3.74	3.90
K_2O	1.47	1.29	1.01	4.57	4.62	2.55	3.18	3.81	3.14	4.61	0.93	2.82	3.18
P_2O_5	0.87	0.66	0.34	—	0.03	0.40	0.24	0.19	0.12	0.05	0.40	0.22	0.14
LOI	2.16	1.16	1.43	0.43	0.41	0.47	1.33	0.57	0.60	0.37	0.61	0.82	1.46
Total	100.85	100.66	99.76	98.02	99.34	99.52	100.10	98.80	99.17	98.52	100.51	99.10	100.51
Trace elements													
Cl	—	—	—	300	480	—	620	—	200	380	n.a.	n.a.	500
Sc	24.9	23	26.3	1.9	3.2	12.9	8.1	6.1	5.5	3.1	30.5	13	5.1
V	260	254	176	—	—	144	78	31	56	—	220	104	58
Cr	350	27	280	—	—	25	11	—	31	—	250	29	22
Zn	—	72	—	—	21	71	52	52	30	—	n.a.	n.a.	—
Rb	65	30	n.a.	185	139	55	68	95	64	154	14	50	79
Sr	1058	1053	n.a.	56	60	718	769	505	470	62	716	649	510
Zr	—	151	n.a.	116	112	241	360	454	232	127	133	201	189
Nb	n.a.	20	n.a.	27	20.6	19.6	25.3	39	14.7	27.3	13	20	17.3
Cs	94	—	4.7	5.5	3.9	—	2.2	2.1	0.7	3.1	—	0.6	1.4
Ba	1400	710	590	n.a.	810	1280	1440	2400	1390	800	483	1157	1180
La	48	52	21.6	41.1	27.3	50.2	57.9	114	42.9	30.4	30	49	44.1
Ce	96	73	43	54	54	73	83	129	56	52	54	97	54
Nd	50	n.a.	—	n.a.	n.a.	n.a.	n.a.	n.a.	n.a.	n.a.	n.a.	n.a.	n.a.
Sm	9.4	7.0	4.5	2.5	3.9	5.8	6.1	13	5.3	4.4	5.8	7	4.4
Eu	2.3	2.2	1.21	0.25	0.40	1.6	1.6	2.1	0.93	0.51	1.50	1.43	1.0
Dy	5.2	5.5	4.2	1.4	3.8	4.3	5.1	12.2	3.2	5.0	5.0	5.1	3.0
Yb	2.0	2.9	1.9	1.7	3.0	2.2	3.3	5.3	1.5	2.6	2.6	2.7	1.5
Hf	4.9	4.1	3.4	3.5	3.5	5.4	6.3	9.0	3.8	3.2	3.5	5.5	3.5
Th	4.4	6.1	2.0	22.5	12.9	7.7	9.4	14.3	3.4	12.0	3.0	8.4	7.5
U	1.47	2.18	0.72	6.19	3.94	2.62	2.92	5.22	1.38	4.12	0.85	2.56	3.29

TABLE 1, continued.

	Cerro Rubio Dacite F83-245	San Diego Canyon Ignimbrite "B" F82-92	El Rechuelos' Rhyolite ER 3-3	Otowi Mbr. Bandelier Pumice F82-11	Cerro Toledo Rhyolite: Cerro Toledo F81-145	Cerro Toledo Rhyolite: Cerro Trasquilar F81-139	Tshirege Mbr. Bandelier, Tsankawi Pumice F82-94	Redondo Creek Rhyolite F81-109	Valles Rhyolite: San Antonio Mountain F80-74	Valles Rhyolite: Banco Bonito F82-7
Approx. age, Ma	3.6	2.85	2.02	1.45	1.38	1.27	1.12	1.0	0.54	0.13
Major elements										
SiO_2	66.9	74.4	74.8	73.6	77.0	75.2	72.7	73.2	74.0	73.2
TiO_2	0.47	0.10	0.08	0.04	0.08	0.08	0.08	0.36	0.14	0.29
Al_2O_3	15.2	11.8	12.4	11.9	12.2	11.9	12.2	12.8	13.2	13.5
Fe_2O_3[b]	3.43	1.54	0.55	1.40	1.19	1.01	1.47	1.04	1.09	1.84
MnO	0.05	0.06	0.06	0.07	0.05	0.07	0.08	0.03	0.05	0.05
MgO	1.42	0.08	0.05	0.10	0.02	0.03	0.05	0.09	0.15	0.63
CaO	3.32	0.33	0.45	0.24	0.14	0.26	0.33	0.69	0.67	1.58
Na_2O	3.60	4.00	3.74	4.36	4.21	4.22	3.08	3.66	3.76	3.84
K_2O	3.20	4.67	4.74	4.61	4.47	4.49	5.36	4.86	5.03	4.11
P_2O_5	0.15	0.005	—	0.005	0.005	0.005	0.005	0.01	0.01	0.06
LOI	1.37	3.35	3.17	4.26	0.25	3.19	4.01	3.63	1.96	0.24
Total	99.11	100.34	100.04	100.59	99.62	100.46	99.37	100.37	100.06	99.34
Trace elements										
Cl	390	1620	—	2800	790	1990	2200	680	680	500
Sc	6.5	2.7	3.11	0.58	1.09	1.16	1.01	2.9	2.2	4.0
V	64	—	—	16	12	14	—	—	—	19
Cr	51	5	—	5	—	4.2	—	3.6	4.0	12
Zn	73	40	—	20	60	80	33	30	40	30
Rb	52	155	139	330	205	230	330	110	160	165
Sr	500	—	—	9.9	—	10	—	—	—	—
Zr	160	180	58	190	130	150	350	210	125	160
Nb	n.a.	n.a.	40	n.a.	n.a.	n.a.	n.a.	n.a.	n.a.	n.a.
Cs	0.8	4.1	5.3	10.5	4.6	8.1	18	3.8	5.4	5.2
Ba	1170	—	17	—	—	—	—	1000	320	900
La	34	59	17.2	52	31	36	91	57	47	46
Ce	68	113	44	109	72	80	117	106	89	77
Nd	19	30	—	47	18	29	60	21	21	25
Sm	4.4	8.0	3.6	13.9	7.0	7.4	16.6	5.5	5.6	4.5
Eu	1.08	0.16	0.17	2.4	0.10	0.09	0.05	0.68	0.27	0.51
Dy	2.6	8.0	3.6	18.5	10.2	11.6	28	5.3	6.8	3.8
Yb	1.56	5.6	2.6	12.2	5.7	8.1	15.4	3.0	4.9	3.5
Hf	5.0	8.2	3.7	12.0	8.6	8.8	14.0	8.2	4.9	5.2
Th	4.6	21.1	20.4	43	24	26	40	15.6	23	23
U	1.16	6.7	8.0	15.9	8.5	8.2	11.8	4.2	6.3	5.7

Volcanic activity of Toledo–Valles caldera complex

Ignimbrite plateaus surrounding the Jemez volcanic field are mostly the product of two caldera-forming eruptions that occurred during the last 1.45 Ma. With an estimated minimum cumulative volume of 600 km^3, the two members of the Bandelier Tuff are the most evident products of silicic volcanism of the central Jemez Mountains volcanic field. Concurrent with the eruption of these two batches of rhyolitic tephra were the formation, by collapse, of the Toledo and Valles calderas. Many modern concepts of pyroclastic-flow deposits and facies, caldera formation, caldera resurgence, and zoned magma chambers were developed here (Ross and Smith, 1961; Smith and Bailey, 1966, 1968; Smith, 1979; Wright et al., 1981). What are believed to be shallow magma bodies associated with the caldera-forming and postcaldera volcanism are also responsible for the much-sought-after geothermal resources of this volcanic field.

San Diego Canyon ignimbrites—Underlying the Bandelier Tuff and extending southwest of the present-day rim of the Valles caldera are erosional remnants of at least two ignimbrites. The largest of these ignimbrites were previously designated "Pre-Bandelier ignimbrite A" and "Pre-Bandelier ignimbrite B" (Self et al., 1986) and are now called the San Diego Canyon ignimbrites (Turbeville and Self, 1988). These are best exposed along the walls of San Diego Canyon, to a distance of 18 km from the Valles caldera wall. The full extent of these deposits is unknown, but they are estimated to have a volume of >5 km^3 (Turbeville and Self, 1988).

The tuffs are lithic-rich (>30% lithic clasts) and overlie an erosion surface covered with fluvial gravels or a poorly developed soil. The ignimbrites are nonwelded, but "B" has incipient welding associated with fossil fumarole pipes. Ignimbrite "A" has very distinctive gray pumice clasts with highly elongated tube vesicles (Self et al., 1986). Co-ignimbrite lithic breccias are found within these ignimbrites and are believed to indicate proximity to source vents. These ignimbrites have been dated, with K–Ar (sanidine) ages of 2.84 ± 0.07 Ma ("B") and 3.64 ± 1.64 Ma ("A"). Chemically, they are similar to, but slightly more mafic than, the two members of the Bandelier Tuff (Table 1; Self et al., 1986; Turbeville and Self, 1988).

Field evidence indicates that these ignimbrites were once extensive, were erupted from what is now the western mar-

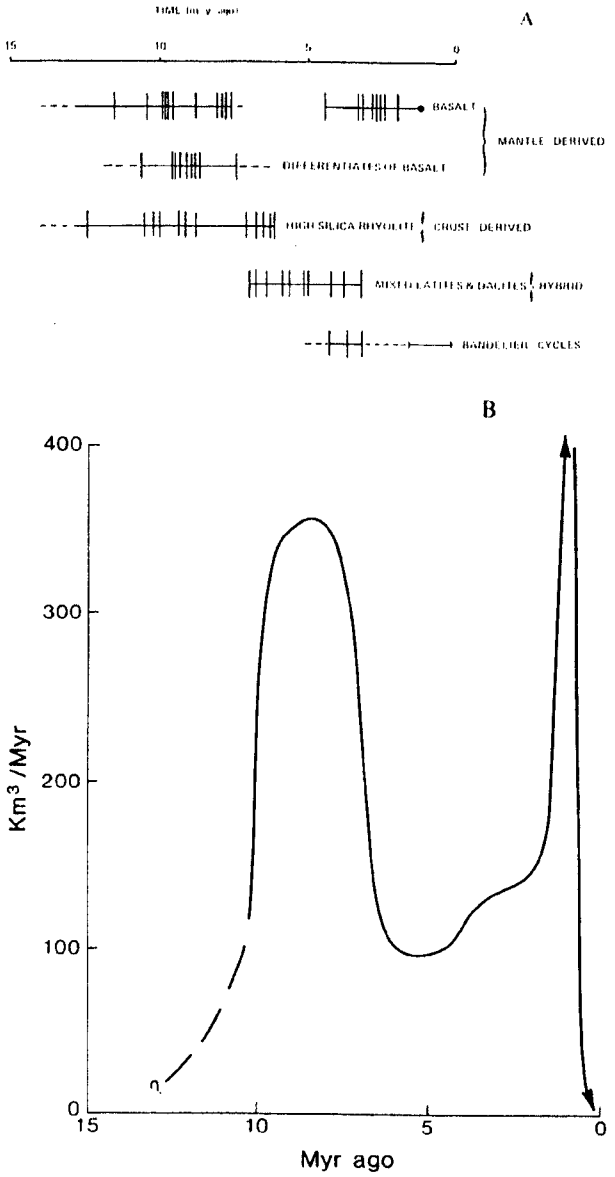

FIGURE 6—**A**, Dates of the Jemez volcanic field plotted with respect to dominant rock type (Gardner and Goff, 1984). Each vertical line represents a K–Ar date. Solid lines indicate continuous eruption of a given magma type inferred from field relations, and dashed lines indicate uncertainty. Numerous dates from Tewa Group (solid line for Bandelier "cycles") not plotted for clarity. **B**, Rate of volcanism (volume per unit time) vs. time for Jemez volcanic activity. Plot goes off-scale with major Bandelier ignimbrite eruptions (from Gardner and Goff, 1984).

gin of the Valles caldera, and may have formed a small caldera, which is now buried within the present-day caldera complex (Fig. 7A). The San Diego Canyon ignimbrites have been described from the geothermal wells drilled within the caldera (the "Lower Tuffs" of Nielson and Hulen, 1984). They appear to thicken eastward in the Redondo Creek area, reaching a thickness of nearly 400 m in geothermal well Baca-4.

Otowi Member of Bandelier Tuff and Toledo caldera—The Otowi Member of the Bandelier Tuff consists of a Plinian pumice-fall deposit (Guaje Pumice Bed), which is overlain by thin surge beds and massive pyroclastic-flow units (Fig. 8). The age of this eruption, based upon several K–Ar dates on sanidine, is 1.45 Ma (Doell et al., 1968).

The Guaje pumice-fall deposits are distributed to the east of the caldera complex. Five fall units have been defined and cumulatively have a maximum thickness of over 8 m (Fig. 7B) (Self et al., 1986). Dispersal axes obtained from isopleth maps of maximum lithic-clast diameters for these fall units may suggest that this pumice deposit was erupted from a central vent or closely spaced vents located near the center of the present Valles caldera.

Surge beds and massive ignimbrite of the Otowi Member are distributed symmetrically about the Valles caldera (Fig. 7C). Multiple flow units have cumulative thicknesses outside the caldera of as much as 180 m and within the caldera of <60 m to 800 m (possibly twice that in the eastern, undrilled half of the caldera complex). The orangish-tan, nonwelded to densely welded ignimbrite contains abundant lithic clasts and pumice clasts in a vitric-crystal or crystal-vitric ash matrix (30–35% phenocrysts of mostly sanidine and quartz). Lithic clasts, which make up from a trace to 30% of the tuffs, are mostly derived from older volcanic rocks but also contain rare fragments of Precambrian basement (Eichelberger and Koch, 1979).

Lithic ("lag") breccias are interbedded with the ignimbrite and are best exposed along the southwestern caldera margin. Lithic blocks, up to 2 m in diameter, within the breccias imply that these deposits are close to vents for the Otowi Member. Gas-escape pipes are present above some of the breccias.

The distribution and thickness of the Otowi Member ignimbrite, distribution of lag breccias, flow-direction indicators such as aligned pumices (Potter and Oberthal, 1983), and K–Ar dates on an intracaldera arc of four domes (Goff et al., 1984) support the interpretation that the Otowi Member was erupted from ring fractures more or less coincident with those of the younger Valles caldera. These features do not support the interpretation that the Otowi Member of the Bandelier Tuff was erupted from the Toledo embayment, a structure 9 km in diameter located on the northeast margin of the Valles caldera. The Toledo embayment may be of tectonic origin or may be a small crater formed at a slightly earlier time; in either case, it is mostly filled with Cerro Toledo Rhyolite. The Toledo caldera, formed during eruption of the Otowi Member of the Bandelier Tuff, is nearly coincident with the younger Valles caldera.

Within the caldera, the Otowi Member has a maximum thickness of 833 m in Baca-12 and thins to 177 m in Baca-4 (Fig. 3) (Nielson and Hulen, 1984). Thus, the unit thins toward the center of the proposed Toledo caldera. We cannot explain this contradiction with prevailing theories of caldera development. However, the data suggest that maximum subsidence was centered over the eastern ring-fracture system.

Intracaldera volcanic activity, Toledo caldera—The Cerro Toledo Rhyolite is a sequence of rhyolitic domes, flows, and associated pyroclastic deposits which postdate collapse of the Toledo caldera (Izett et al., 1981; Heiken et al., 1986). Exposed Cerro Toledo Rhyolite domes are clustered mostly within the Toledo embayment, and along the north rim and just beyond the southeast rim of the Valles caldera (Fig. 7D). K–Ar ages of these domes range from 1.5 Ma to 1.2 Ma, placing them in time between the two, large-volume members of the Bandelier Tuff. The domes consist primarily of gray, flow-banded to massive rhyolite which contains small sanidine and rare quartz phenocrysts.

Contemporaneous with the Cerro Toledo domes are tuffs and epiclastic rocks, which are best exposed in two areas:

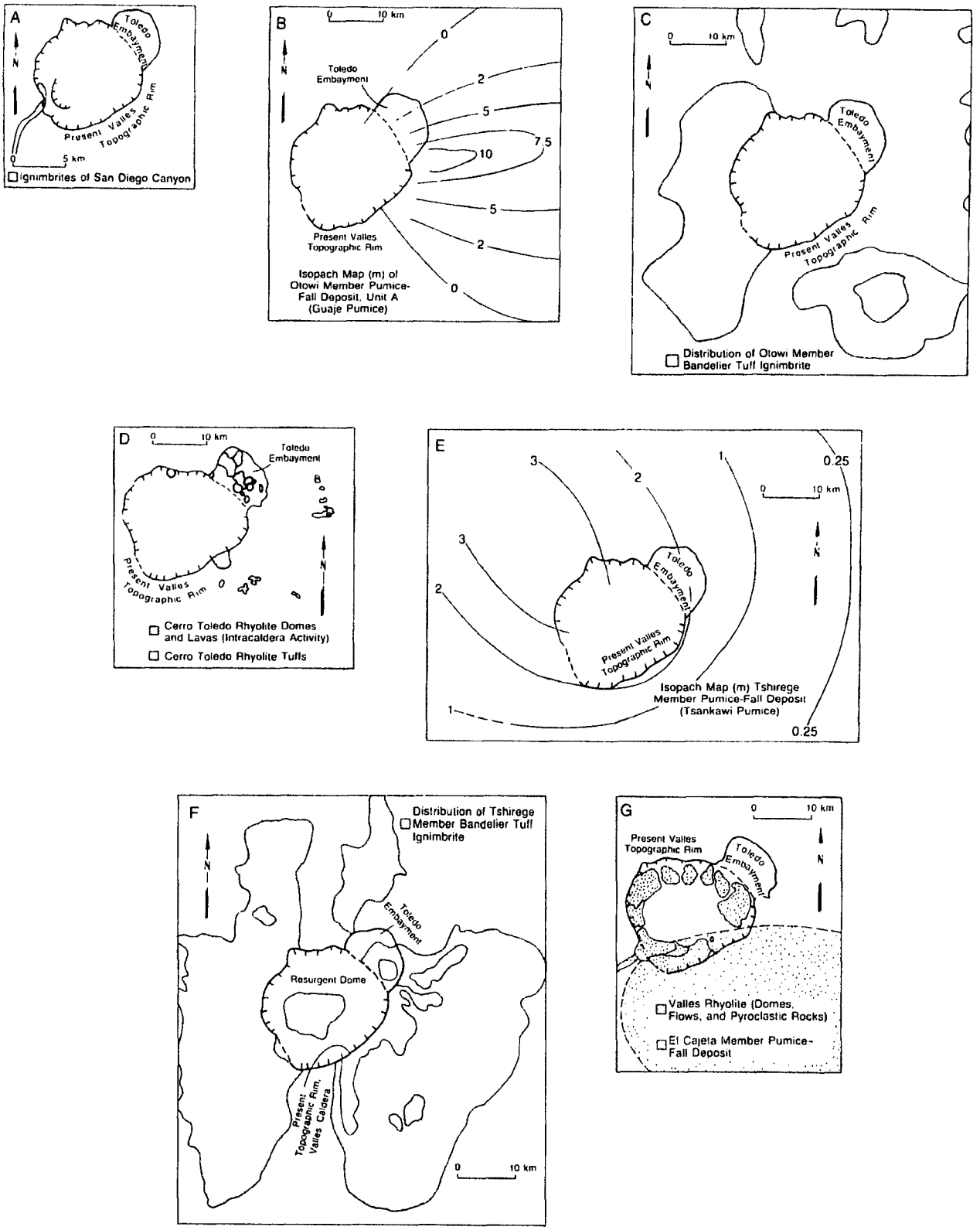

FIGURE 7—Simplified maps showing distribution of major rhyolitic tuffs and lava domes and flows erupted in the central Jemez Mountains during the last 3 Ma. For reference, the present topographic rim of the Valles caldera and the Toldeo embayment are shown on each map. **A**, Distribution of San Diego Canyon ignimbrites (from Turbeville and Self, 1988). **B**, Isopach map, in meters, of unit A of the Otowi Member, Bandelier Tuff pumice-fall deposit (Guaje Pumice) (from Self et al., 1986). **C**, Distribution of the Otowi Member, Bandelier Tuff ignimbrite (from Smith et al., 1970). **D**, Distribution of Cerro Toledo Rhyolite domes, lava flows and tuffs (from Heiken et al., 1986). **E**, Isopach map of fall unit A, Tshirege Member, Bandelier Tuff pumice-fall deposit (Tsankawi Pumice) (from Self et al., 1986). **F**, Distribution of the Tshirege Member, Bandelier Tuff ignimbrite (from Smith et al., 1970). **G**, Distribution of domes, lava flows, and pyroclastic rocks of the Valles Rhyolite (from Smith et al., 1970) and the El Cajete Member pumice-fall deposit (from Self et al., 1988).

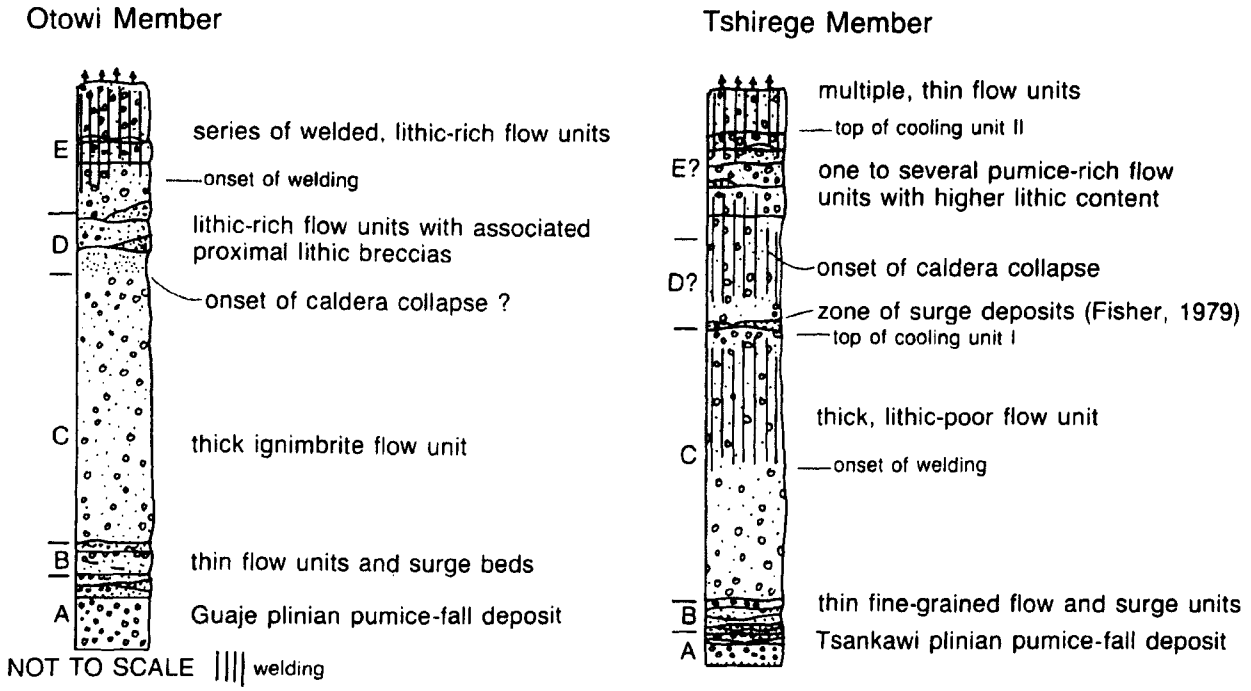

FIGURE 8—Idealized lithology of the Tshirege and Otowi Members of the Bandelier Tuff.

(1) east of the caldera on the Pajarito Plateau, and (2) southeast of the Rabbit Mountain dome (southeast caldera rim, Fig. 7D). East of the caldera, seven eruption sequences of rhyolitic tephra have been studied; most consist of very fine-grained phreatomagmatic ash, overlain by interbedded pumice-fall beds and fine-grained ash-fall beds. The tuffs are nearly aphyric, with only traces of K-feldspar and plagioclase. At isolated outcrops, the nearly aphyric nature of these tuffs can be used to separate them from the phenocryst-rich Bandelier Tuff.

Using cuttings from many deep wells, Nielson and Hulen (1984) identify a clastic deposit within the caldera fill, the S_3 Sandstone, as being correlative with the Cerro Toledo tuffs. The S_3 Sandstone reaches a maximum thickness of 70 m and separates the Otowi and Tshirege Members of the Bandelier Tuff. This unit appears to be composed of interbedded tuffs and epiclastic sandstones.

Tephra-fall patterns of the Cerro Toledo tuffs indicate sources located in the eastern Valles caldera and the Toledo embayment. The pyroclastic breccias and surge deposits along the southeast caldera margin were erupted from the same vent that erupted the Rabbit Mountain dome. Many of the tuff sequences began as phreatomagmatic eruptions, perhaps having been erupted through a caldera lake.

Stix et al. (1988) used the stratigraphy, geochemistry, and geochronology of Cerro Toledo rhyolite domes and tephra to investigate the petrogenesis of the unit and the evolution of compositional zonation within the Bandelier magma chamber. These authors found that compositional (chemical) gradients were restored over a period of 0.33 Ma after eruption of the Otowi Member of the Bandelier Tuff and that crystal fractionation of quartz, alkali feldspar, zircon, and a light-rare-earth-element-enriched phase (probably allanite) was the most likely mechanism by which these gradients were re-established.

Tshirege Member of Bandelier Tuff and Valles caldera—The Valles caldera was formed during eruption of the Tshirege Member of the Bandelier Tuff at 1.12 Ma (Doell et al., 1968). The eruption sequence consists of a basal pumice-fall deposit overlain by thin surge beds and pyroclastic-flow units that make up the ignimbrite (Fig. 8) (Self et al., 1986).

The basal Plinian pumice-fall deposit, the Tsankawi Pumice Bed, consists of four pumice-fall units and two finer-grained ash-fall units, with composite maximum thickness of 3.5 m. Each fall unit has a different dispersal axis, from south to west to north; the most common trend is to the northwest, as shown by an isopach map of fall unit "A" (Fig. 7E). Trends of dispersal axes suggest a central vent for the Plinian eruption within the center of the present Valles caldera.

The Tshirege Member ignimbrite is exposed on nearly all sides of the volcanic field and forms the plateaus flanking these mountains (Fig. 7F). It also forms thick sections of caldera fill, which have been sampled during geothermal drilling. The orangish-tan tuffs of the ignimbrite are nonwelded to densely welded crystal-vitric to vitric-crystal tuff (~32% phenocrysts of mostly sanidine and quartz, with traces of hornblende and magnetite). Thicknesses outside the caldera range from 15 to over 270 m, whereas within the caldera densely welded tuffs range from 400 to over 1100 m. Proximal breccias within the Tshirege Member are rare, with a few thin deposits exposed along the caldera rim.

Within distal parts of the Tshirege Member of the Bandelier Tuff, flow units can be separated visually by thin surge deposits and "sandy partings" and by pumice swarms (Fisher, 1979). Four to five flow units are visible in the well-exposed section along NM-501, east of Los Alamos (Day 3, Stop 1). Overprinting these textural features in the nonwelded, distal sections are vapor-phase alteration and columnar jointing of the upper half of the ignimbrite.

The Valles Rhyolite; intracaldera domes, lava flows, pyroclastic deposits, and sedimentary rocks—After the dust settled from formation of the Valles caldera, less explosive activity continued within the caldera until about 130 Ka. Rhyolitic domes and lava flows were erupted from the caldera ring-fracture system, from the massive Cerro del Medio in the eastern moat to the very small Cerro La Jara dome on the southern margin (Fig. 7G) (Spell, 1987). Some domes are up to 700 m thick. Several extensive pumice-fall deposits and small ignimbrites are associated with dome growth. Coarse breccias, gravels, and lacustrine mudstones are interbedded with tuffs and rhyolite lavas.

The youngest (130 Ka) intracaldera eruption is that of the Banco Bonito obsidian flow (Marvin and Dobson, 1979), which erupted along the southwest caldera ring fracture. The Battleship Rock ignimbrite (well-exposed in San Diego Canyon) and the widespread El Cajete pumice-fall bed are both thought to be explosive precursors to formation of the Banco Bonito lava flow (Self et al., 1988). The pyroclastic sequence is overlain by 30–70 m thick Banco Bonito obsidian lava flow (12% phenocrysts; plagioclase, hornblende, biotite, and traces of clinopyroxene, orthopyroxene, and Fe–Ti oxides). Recently obtained ages for the three eruptions are: Banco Bonito 130–180 Ka (Self et al., 1988); El Cajete 170–151 Ka (Self et al., 1988); and Battleship Rock 278 Ka (F. Goff, unpubl. data). Additional postcaldera rhyolites that have chemical similarities to the youngest moat volcanic rocks were cored in VC-1 (Gardner et al., 1986).

Within the caldera, in the resurgent dome, is a sequence of nonwelded to densely welded silicic ignimbrites with an aggregate thickness of 460 m overlying the Tshirege Member of the Bandelier Tuff ("Upper tuffs" of Nielson and Hulen, 1984). Little is known about this tuff sequence, mainly because of the intensity of hydrothermal alteration, but it is separated from the Tshirege Member by a volcaniclastic sandstone (Nielson and Hulen, 1984) and underlies tephra deposits believed to be associated with the Redondo Creek Rhyolite in CSDP core hole VC-2A; thus, its age is estimated at between 1.12 and 1.0 Ma (Hulen et al., 1987).

Subsurface structure and resurgence of Valles caldera

The structural framework of the Valles caldera is dominated by high-angle normal faulting (including ring faulting) and resurgent, domal uplift of the subsided cauldron block. Location of the caldera, and the entire Jemez volcanic field, is controlled by the intersection of northeast-trending faults of the Jemez volcanic lineament (JVL) with north-trending faults at the western edge of the RGR (Fig. 1) (Aldrich and Laughlin, 1984; Gardner and Goff, 1984). Reactivation of these earlier structures during and following caldera formation and resurgent doming is responsible for much of the complex fault pattern presently observed in caldera-fill rocks. For example, the northeast-trending apical graben of the caldera's resurgent Redondo dome clearly is directly on strike with the Jemez fault zone (the local expression of the JVL) to the southwest (Fig. 1). Ring-fracture and apical graben high-angle normal faults are believed to be the principal permeable conduits for circulation of the active, high-temperature Valles hydrothermal system.

The subsurface structure of Valles caldera has been discussed by Goff (1983), Nielson and Hulen (1984), Heiken et al. (1986), and Wilt and Vonder Haar (1986). Many of these interpretations rely on gravity data acquired by UNOCAL during geothermal exploration and on the drilling results of several organizations. The gravity data of Segar (1974), based on measurements at nearly 700 stations, show a pronounced circular gravity low of as much as 35 mgal that coincides with the location of the caldera depression (Fig. 9A). Modeling of these data by Segar (Fig. 9B) indicates that subsurface fault patterns trend northeast parallel to the trend of the JVL and the trend of nearby faults associated with the RGR. The gravity low, however, is asymmetric and is greatest in the eastern caldera, coincident with Valle Grande. In general, zones of steep gravity gradients

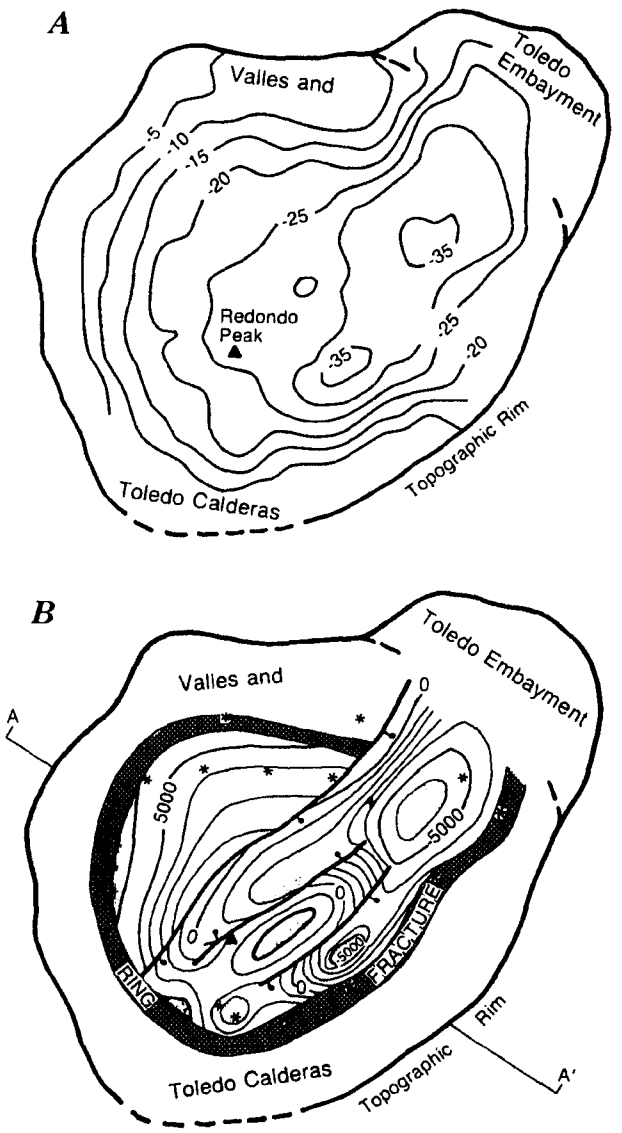

FIGURE 9—**A,** First-order residual Bouguer gravity map of Valles caldera produced from Enclosure IV of Segar (1974); values in mgal. **B,** Gravity interpretation of Segar (1974) using residual map in (A) and a density contrast of 0.35 g/cm^3. No effort was made to map features such as slump along caldera ring fracture, jagged nature of caldera rim, etc. Contour interval is 1000 ft. Checkered pattern shows approximate position of caldera ring-fracture zone in relation to moat rhyolite vents shown by stars. Dot pattern shows relative gravity lows (basins) and gray pattern shows relative gravity highs. Note apparent horst beneath Redondo Peak and northeast trend of major fault zones. Also note large gravity low extending into the Toledo embayment. The near-coaxial relationship of earlier Toledo caldera to Valles caldera was not known at the time of this interpretation. Line A–A' approximates the location of the cross section shown in Fig. 46 (Day 3).

are interpreted to be fault zones with down-to-the-southeast displacements suggesting that rift-related faulting controls the subsurface structure of Valles caldera. An exception to this down-to-the-southeast fault pattern is the northeast-trending horst coincident with the Redondo Peak segment of the Valles resurgent dome.

The model of Fig. 9B is constrained by drilling results in the southwestern quadrant of the caldera. Contours in Fig. 9B represent the approximate elevation in feet of Precambrian basement rocks relative to sea level. For example, basement beneath the western caldera can be as shallow as 6000 ft (1830 m) above sea level or only 2500 ft (760 m) below ground surface, as verified in the WC 23-4 well (Goff et al., 1987; Hulen et al., 1987). Depth to basement increases eastward across faults, being at 5100 ft (1555 m) beneath Sulphur Springs in core hole VC-2B (J. N. Gardner and J. B. Hulen, unpubl. data 1988) and at 10,200 ft (3110 m) in well Baca-12 in the Redondo Creek graben (Nielson and Hulen, 1984). According to the gravity model, depth to basement is approximately 15,000 ft (4570 m), or about 5000 ft (1525 m) below sea level in the vicinity of Valle Grande. Such gross asymmetry prompted Nielson and Hulen (1984) and Heiken et al. (1986) to propose that the Valles caldera is a "trap-door" caldera.

Based on drilling results and gravity modeling, the negative gravity anomaly was interpreted by Segar (1974) to be caused primarily by low-density tuffs and sedimentary rocks filling an asymmetric depression. Segar used a value of 2.45 g/cm^3 for both his Bouguer and topographic corrections. Density measurements on eight samples of intracaldera tuffs and sedimentary rocks from core hole VC-2A range from 2.49 to 2.11 g/cm^3 (Musgrave et al., 1989). Segar's interpretation does not identify a deep circular intrusive or plutonic body beneath the caldera, but it is unlikely that a significant density contrast exists between Precambrian basement and recently crystallized plutonic rocks.

Formation and resurgence of the Valles caldera is well documented (Smith and Bailey, 1968). At 1.12 Ma, eruption of about 300 km^3 (minimum) of rhyolitic ash-flow tuff led to collapse of the caldera simultaneously with emplacement of the Tshirege Member of the Bandelier Tuff (Doell et al., 1968; Izett et al., 1981; Smith and Bailey, 1968; Self et al., 1986). The intracaldera Tshirege Member is therefore much thicker than corresponding outflow sheets. The intracaldera Tshirege Member, as thick as 1156 m in Baca 5 (Nielson and Hulen, 1984), was structurally uplifted during the 100,000-year interval following caldera collapse by more than 1000 m near the caldera center. During uplift, the upper portion of the resurgent dome was subjected to extension, resulting in widespread normal faulting (Fig. 10). Some of this faulting took place along and within the dome's northeast-trending apical graben and through reactivation of older basement structures. A subordinate fault set orthogonal to the apical graben apparently lacks deep-seated control (Behrman and Knapp, 1980).

Nielson and Hulen (1984) suggested a domed plate as a model for deformation of the Redondo dome. The model has two important implications. First, on the basis of the amplitude and diameter of the dome, the top of the presumed causative magma body is at depth of about 5 km. Secondly, the widespread normal faulting presently observed at the crest of the dome is predicted by the model to have formed during extension above a neutral plane situated about halfway down from the dome crest to the top of the magma body; compression prevails beneath this neutral plane. This relation, in turn, implies that fracture-controlled hydrothermal circulation is confined principally to the upper half of the domed sequence, a conclusion supported by the limited downhole data available (Hulen and Nielson, 1986a).

This general model of resurgent doming and fracture permeability would be complicated somewhat if the Valles caldera's precursor, the comparably sized and coincident Toledo caldera (1.45 Ma) (Smith and Bailey, 1968; Izett et al., 1981; Self et al., 1986; Heiken et al., 1986) had undergone a similar volcanotectonic history. However, structural evidence in core from CSDP core hole VC-2A suggests that the Toledo caldera did *not* undergo resurgence. Compaction foliation attitudes in the Tshirege and Otowi Members of the Bandelier Tuff are essentially identical in the VC-2A core (Goff et al., 1987); had the Toledo caldera experienced resurgence, attitudes measured in the Otowi Member presumably would be steeper than those in the overlying Tshirege. However, on the basis of a single intercept, this hypothesis must remain tentative until tested by further scientific drilling.

Petrogenesis of Bandelier magma chamber and associated rhyolites

A comprehensive interpretation of the petrogenesis of the Bandelier magma system (and indeed, the entire Jemez volcanic field) has not been published, but much is hidden in theses (e.g., Loeffler, 1984; Gardner, 1985; Kuentz, 1986; Spell, 1987). Smith and Bailey (1966) proposed from looking at chemical and petrologic variations in the outflow sheets of the ignimbrites (primarily the Tshirege Member) that the Bandelier magma chamber was compositionally zoned. Smith (1979) discussed chemical variations as functions of time with respect to both the Toledo and Valles cycles and suggested that the Bandelier pluton evolved from a (Tschicoma) dacitic parent magma. This concept was substantiated by Gardner (1985) using trace-element and REE data for all Jemez volcanic rocks. Chemical variations with respect to time were elegantly investigated for the Cerro Toledo Rhyolite by Stix et al. (1988), who found that these post-Toledo caldera rhyolites were generated by fractional crystallization of Bandelier magma and not by diffusive processes or wall-rock assimilation.

The first, post-Valles caldera moat rhyolites also appear to have a close genetic relationship to Bandelier magma (Spell, 1987), but the latest moat rhyolites, in the southwestern ring-fracture zone, do not (Gardner et al., 1986; Self et al., 1988). This latest package (VC-1 Tuffs, VC-1 Rhyolite, Battleship Rock Tuff, El Cajete Pumice, Banco Bonito Rhyolite) is more "mafic" in composition, has $^{87}Sr/^{86}Sr$ of about 0.705 (versus about 0.710 for Bandelier Tuff), and could be derived from a mixture of high-silica rhyolite (Bandelier) and dacite magmas (J. N. Gardner and F. Goff, unpubl. data 1989). Unfortunately, a systematic investigation of Sr and Nd isotope ratios of Jemez volcanic rocks does not exist, although the available Sr data have been compiled by Vuataz et al. (1988). Where both ratios have been determined on Jemez rhyolites (El Rechuelos Rhyolite), the results indicate derivation primarily by fractional crystallization from a basaltic parent (Loeffler et al., 1988).

Sommer (1977) analyzed the volatile contents of silicate melt inclusions in quartz phenocrysts of the Tshirege Member of the Bandelier Tuff and concluded that the depth of burial to the top of the chamber was about 5 km (~1.5

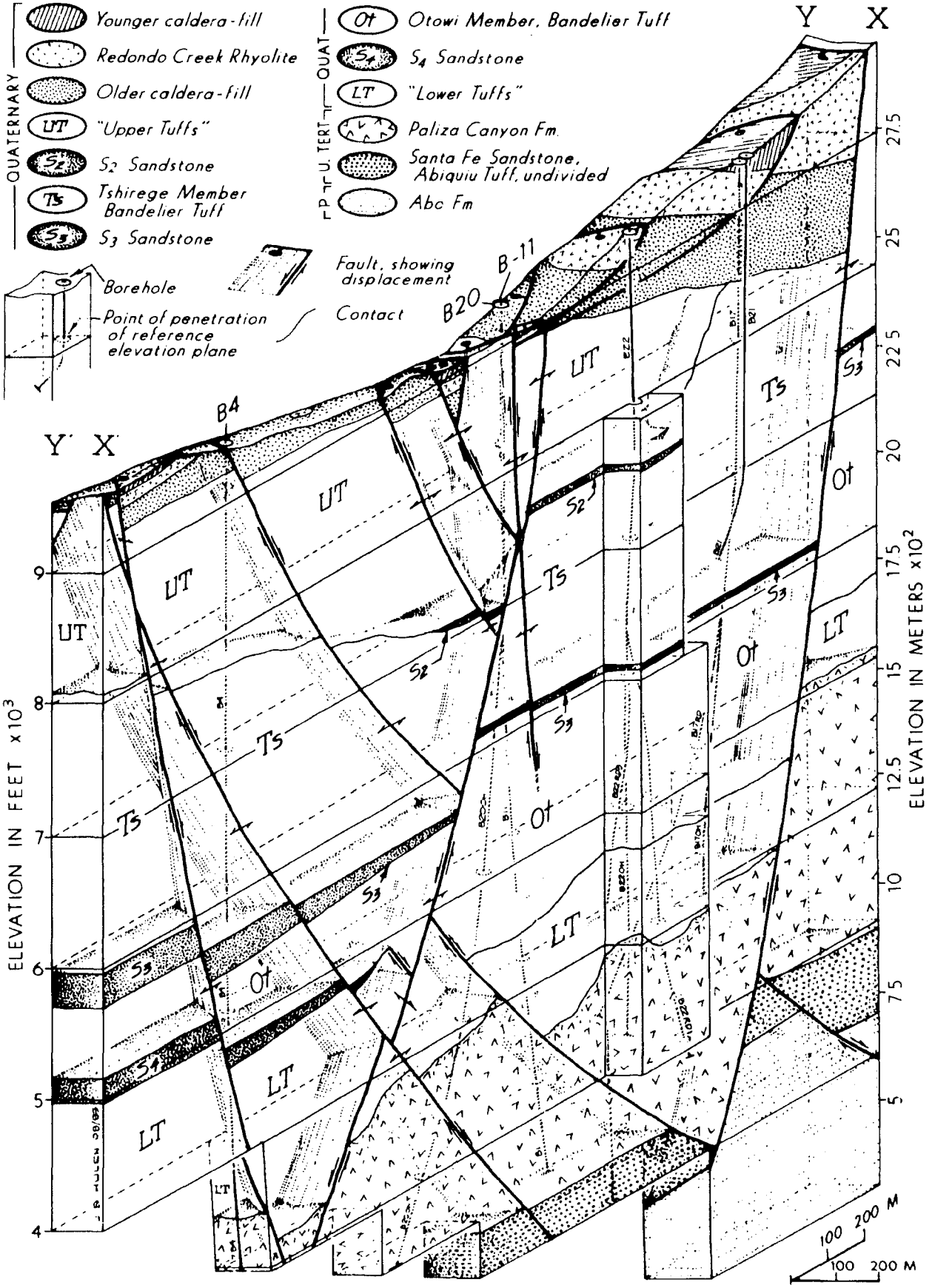

FIGURE 10—Three-dimensional geologic cross section of the Redondo Dome (from Nielson and Hulen, 1984); position Y–X is northwest and position Y'–X' is southeast.

kbar). Warshaw and Smith (1988) investigated the compositions of pyroxenes, fayalites, and iron–titanium oxides in both members and reported that the basal ash fall of the Tshirege (Tsankawi Pumice Bed) formed at a pre-eruption temperature of about 700°C, while the uppermost Tshirege ignimbrite formed close to 850°C. Depths of formation were estimated between 5 and 7 km (1.5 to 2.0 kbar). Nielson and Hulen (1984) used a structural model (mentioned above) to estimate the depth to the present top of the (crystallized) Bandelier pluton at about 4.7 km. Because this estimate accounts for post-eruption resurgence, the depth to the magma chamber before ignimbrite effusion would be between 5 and 6 km.

Precambrian geology

Precambrian rocks occur as small, tectonically disturbed lenses of granite gneiss at Soda Dam and Guadelupe Box on the Jemez fault zone southwest of Valles caldera, as granitic and metamorphic rocks in the core of the Nacimiento uplift (Laramide age) west of the caldera, and as granitic and metamorphic rocks in the San Pedro Park area northwest of the caldera. Precambrian rocks have been encountered in geothermal wells JS-1 (Goff et al., 1981), AET-4, WC 23-4 (Shevenell et al., 1988), Baca-2 (Dondanville, 1971), Baca-7 (Lambert and Epstein, 1980), Baca-12 (Nielson and Hulen, 1984), VC-1 (Hulen and Nielson, 1988a), and VC-2B (J. B. Hulen and J. N. Gardner, unpubl. data 1988), in addition to the wells drilled for the Hot Dry Rock program (Laughlin et al., 1983) (Fig. 3). Precambrian lithologies in all non-HDR wells are variously described as "fresh" to hydrothermally altered granitic rocks, gneisses and schists (Table 2), and no detailed work has been performed on them except for samples from VC-1. If the rock descriptions in non-HDR wells are accurate, it appears that metamorphic rocks dominate the upper Precambrian section outside the caldera, while plutonic rocks dominate the upper section inside the caldera. Depth to Precambrian basement increases dramatically from outside the caldera on the west to inside on the east and from west to east across the grain of precaldera RGR faults.

The thick Precambrian section penetrated by HDR wells at Fenton Hill, located a scant 0.5 km west of the topographic rim of Valles caldera (Fig. 11), has been studied extensively (Laughlin, 1981). The section is very complex in detail and the orientations of contacts are not well known. Gneissic rocks interlayered with many schist intervals dominate the section. Various types of granitoid rocks occur as dikes and as small and large intrusive bodies. A very large body of biotite granodiorite was observed in the interval 2590–3000 m and the first HDR circulating system was engineered in this rock mass. Laughlin et al. (1983) discussed the petrography, chemistry, fracturing, and secondary minerals of the various Precambrian rocks.

Brookins and Laughlin (1983) performed a Rb–Sr geochronologic investigation on 76 Precambrian samples from the HDR wells. They concluded that major metamorphism occurred at 1.62 ± 0.04 Ga, which is in agreement with radiometric ages reported for similar rocks elsewhere in

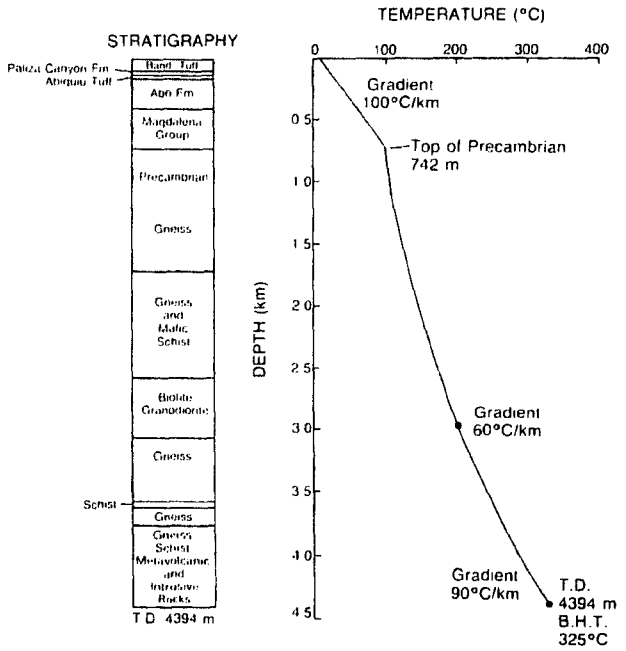

FIGURE 11—Stratigraphic column and temperature profile, Fenton Hill (modified from Laughlin et al., 1983).

TABLE 2—Wells penetrating Precambrian basement rocks in the Valles caldera region, New Mexico. [a]See Fig. 3 for well locations; all wells also penetrate Permian Abo Formation and Pennsylvanian Madera Limestone except well JS-1 (Pennsylvanian only).

Well[a] name	Total depth (m)	Top of Precambrian (m)	Rock types	Reference
Wells drilled for Hot Dry Rock program				
GT-1	785	642	Amphibolite and granite–gneiss	Perkins, 1973
GT-2	2930	730	Gneiss, schist, granite, granodiorite; minor amphibolite and metavolcanic rock	Laughlin et al., 1983
EE-1	3060	730		
EE-2	4390	730		
EE-3	3980	730		
PC-1	664	655	Granite	Shevenell et al., 1988
Wells drilled for other projects				
JS-1	253	235	Granite–gneiss	Goff et al., 1981
AET-4	1221	997	Gneiss; minor schist and amphibolite	Shevenell et al., 1988
WC23-4	2101	737	Granite	Shevenell et al., 1988
Baca-2	1725	1524	Granite	Dondanville, 1971
Baca-7	1687	1650	Granite	Lambert and Epstein, 1980
Baca-12	3211	3101	Altered granite	Nielson and Hulen, 1984
VC-1	856	843	Gneiss; brecciated, altered granite–gneiss	Hulen and Nielson, 1988a
VC-2B	1762	1558	Altered biotite quartz monzonite	This report

north-central New Mexico. The same authors reported an age of 1.50 ± 0.12 Ga for the large biotite granodiorite intrusive which agrees with the U–Th–Pb age of 1.50 ± 0.02 Ga obtained by Zartman (1979). Brookins and Laughlin (1983) also indicated that minor dike emplacement continued to 1.44 ± 0.03 Ga. Harrison et al. (1986) used $^{40}Ar/^{39}Ar$ analyses on microcline to suggest that additional Precambrian metamorphic events occurred at 1.03 and 0.87 Ga.

Thermal history—Much attention has been paid to the Quaternary thermal regime beneath Fenton Hill and the southwestern caldera margin (Heiken and Goff, 1983). Kolstad and McGetchin (1978) used heat-flow data and dates on major events in the history of the caldera to derive a model of conductive thermal cooling of the Bandelier pluton after formation of Valles caldera. Heat flow beneath Fenton Hill averages about 4 HFU but, as can be seen in Fig. 11, the thermal gradient increases from 60 to 90°C/km with depth in the Precambrian section. Although most estimates on the age of most recent thermal heating at the Fenton Hill site vary from 1 to 4 Ma, Harrison et al. (1986) use transient analyses on the thermal gradients to suggest that the heating event may be as young as 10 Ka. Sasada (1988a) also recognized a young (postcaldera) heating event from detailed examination of fluid inclusions in Fenton Hill core samples. The source of this heating is not entirely clear (the youngest volcanism in the Valles region is 130 Ka), but it must be related to magmatic/hydrothermal activity associated with the southwestern caldera (see also Sass and Morgan, 1988). Thus, two "magmatic" episodes are recognized in the Precambrian rocks of the caldera region: a series of Precambrian events at 1.62–0.87 Ga and much more recent events, or a series of closely related events, associated with the Jemez volcanic field and Valles caldera.

Geophysical surveys other than gravity

The thermal regime of Valles caldera was investigated by UNOCAL during their geothermal endeavors and later interpreted by Swanberg (1983) and Sass and Morgan (1988). A map of thermal-gradient data (Fig. 12) shows a broad area in the southwestern caldera where shallow gradients exceed 450°C/km. This area includes the Redondo Creek reservoir and the Sulphur Springs reservoir. These areas are known upflow zones for thermal fluids and hot-water production. Shallow heat flow in the caldera locally exceeds 10 HFU, caused by convective processes (Reiter et al., 1975; Sass and Morgan, 1988), whereas heat flow along the western RGR averages about 2.8 HFU (Reiter et al., 1976). Deep magnetotelluric investigations of the Valles caldera and adjacent RGR (Hermance and Pedersen, 1980) recognized a widespread electrical conductor at 15 km depth, but were not able to discriminate unique (magmatic?) sources beneath the caldera or the rift. A combination of shallower electrical and telluric techniques was integrated by Wilt and Vonder Haar (1986) to define a broad conductive anomaly beneath the southwestern caldera region at 1–3 km depth (Fig. 13). Parts of this anomaly correlate with known fluid production in the Redondo Creek and Sulphur Springs areas. Depending on interpretation, the areal extent of the geothermal reservoir(s) in the caldera varies from 10 to 30 km^2.

The most recent compilation of natural seismic activity for the Valles caldera region has been presented by Gardner and House (1987) for their investigation of seismic hazards in the Los Alamos region. Fig. 14 shows a cumulative plot of all earthquakes located by the Los Alamos Seismic Network from September 1973 to December 1984. A band of seismicity extending south of Chama, New Mexico, to a point about 70 km west of Los Alamos coincides with the Nacimiento uplift (originally a Laramide age structure), which is bounded by a zone of oblique-slip faults on its western edge. The cluster of seismic events northwest of Española lies near the intersection of the Pajarito and Embudo fault zones on the western side of the RGR. Additional seismicity

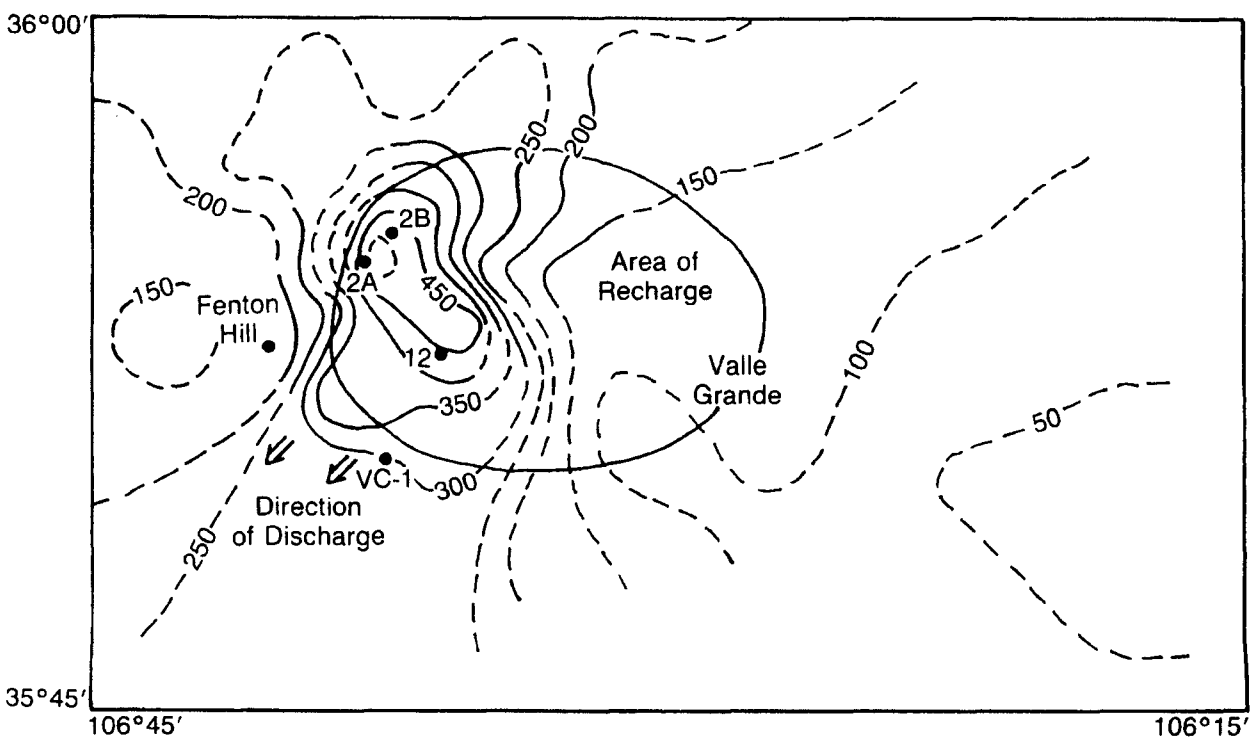

FIGURE 12—Thermal-gradient contours (°C/km) of Valles caldera area (modified from Sass and Morgan, 1988).

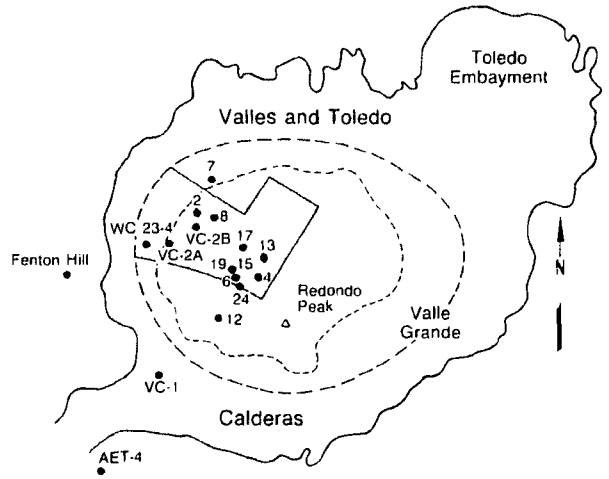

FIGURE 13—Map showing maximum area of geothermal reservoir(s) as defined from electrical surveys (modified from Wilt and Vonder Haar, 1986).

is evident associated with faults of the Pajarito fault system in the Los Alamos area and south. A belt of seismicity generally follows the trend of the northeast-trending JVL from a point west of Albuquerque to a point northeast of Taos. The seismically quiet area west of Los Alamos corresponds with the Valles caldera and is attributed to the presence of high subsurface temperatures and/or relict zones of partial melt that exist beneath the caldera.

Attenuation of seismic waves beneath the caldera complex was first recognized by Suhr (1981). Olsen et al. (1986) studied the complex, shallow crustal structure beneath the Jemez volcanic field using a time-term technique to process first-arrival-time data from a network of temporary seismic stations of the Caldera and Rift Deep Seismic Experiment (CARDEX). Station time terms are highly correlated to

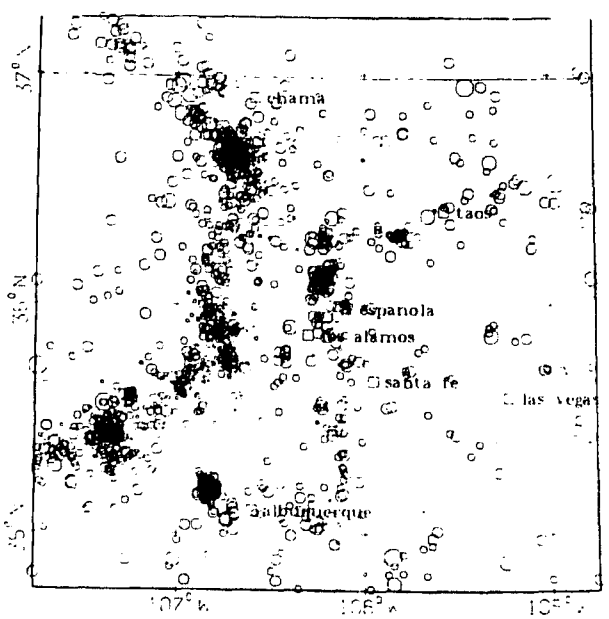

FIGURE 14—Cumulative plot of all earthquakes located by the Los Alamos Seismic Network from September 1973 to December 1984. The size of circle indicates magnitude scale (M_L) with the largest indicating >3 and the smallest indicating a range of −1 to 0. The seismically quiet area west of Los Alamos coincides with the Valles caldera. See text for discussion. From Gardner and House (1987).

gravity anomalies and generally support models for which crystalline basement drops eastward to depths of 600 m below sea level beneath the axial basins of the RGR. Although Olsen et al. (1986) implied that the large gravity low of the caldera and associated time-term delays are caused by residual melt in the silicic Bandelier pluton, other workers have suggested that the gravity low can be modeled solely as a deep asymmetric hole filled with low-density caldera fill (Segar, 1974; Nielson and Hulen, 1984; Wilt and Vonder Haar, 1986). This ambiguity may result because the density contrast between Precambrian basement and nearly crystallized silicic melt is small, as mentioned above.

Ankeny et al. (1986) applied a simultaneous inversion of earthquake and travel-time data to derive a velocity model of the upper 10 km of crust beneath the Jemez volcanic field. The model displays a prominent, low-velocity, cylindrically shaped body beneath the caldera that is 15 km in diameter and 12–15 km thick. This low-velocity body is interpreted to result from the combined effects of a silicic magma body and associated high temperatures, and is centered beneath the southwestern sector of the caldera complex. A possible model incorporating the seismic data is shown in Fig. 15.

Configuration of hydrothermal system

Valles caldera possesses a diverse suite of thermal waters that are typical of those existing at many geothermal areas around the world (Trainer, 1975; Goff and Grigsby, 1982). Table 3 gives selected chemical data for these types of fluids and Fig. 16 compares water types on a plot of δD versus $\delta^{18}O$. Acid-sulfate waters with associated mud pots and fumaroles discharge in the central and western resurgent dome areas, particularly at Sulphur Springs (Goff et al., 1985). These springs result from condensation of steam and oxidation of H_2S to form natural sulfuric acid that mixes with near-surface ground waters. Thermal meteoric waters occur at isolated spots throughout the western ring-fracture zone of the caldera. They appear to be mostly dilute ground water heated by the relatively high subsurface temperatures present at shallow depths. They are not the classic, steam-heated, $NaHCO_3$ waters of Mahon et al. (1980). Deep reservoir waters are those encountered by wells in the Redondo Creek and Sulphur Springs areas beneath the acid-sulfate/vapor zone capping the liquid-dominated part of the hydrothermal system. They are neutral-chloride in character, with anomalous concentrations of As, B, Br, Cs, Li, Rb, and other trace elements. Hot springs derived in part from deep reservoir water are encountered outside the southwest caldera margin in San Diego Canyon (along the Jemez fault zone) and in wells drilled in the flanking plateaus. They appear to be mixtures of reservoir water and various types of ground water (Goff et al., 1981, 1988). Yet another type of thermal water is encountered in Precambrian basement rocks at the Fenton Hill HDR site and at the WC23-4 well in the ring-fracture zone just west of Sulphur Springs (Grigsby et al., 1984; Meeker and Goff, 1988). These waters are more concentrated than reservoir waters and their origin is still not resolved (pore-fluid brine?; magmatic emanations?). The origin and relation of these fluids in Precambrian rocks to overlying reservoir waters is one of the objectives of core hole VC-2B in Sulphur Springs.

Vuataz and Goff (1986) presented stable-isotope and tritium data on over 100 thermal and non-thermal waters in the Valles caldera region. They concluded that recharge to

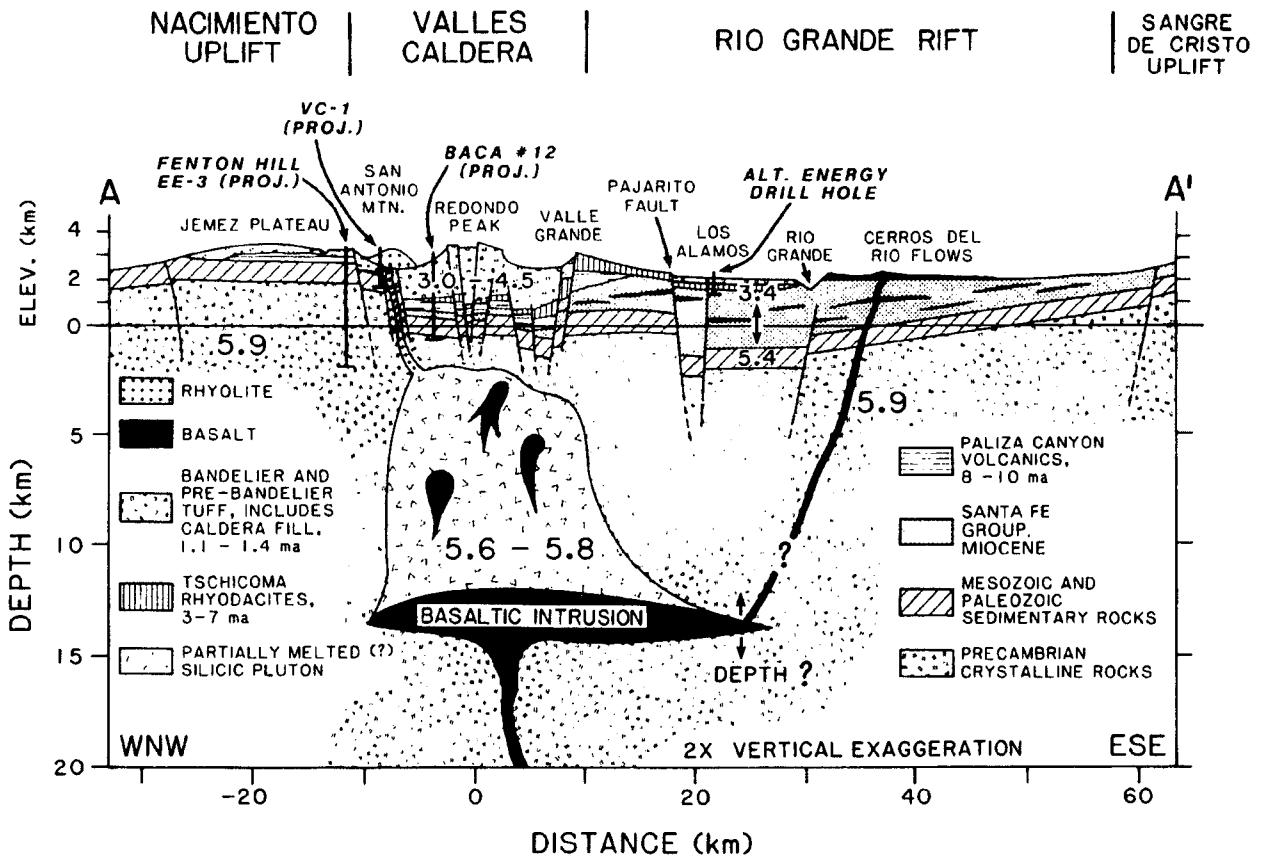

FIGURE 15—A schematic cross section through the Valles caldera and Rio Grande rift based on the three-dimensional inversion interpretation of Ankeny et al. (1986). Velocity values (large numbers) in km/sec are averages determined from the inversion technique. The presence and depth of a tabular basaltic intrusion in the crust are unknown, but, if present, the most likely location would be at the base of the upper crust. For list of references on surface and subsurface control see Ankeny et al. (1986).

TABLE 3—Selected geochemical data for hot springs and geothermal wells, Valles caldera, New Mexico (values in mg/kg except where noted. Locations shown in Fig. 3; data from Goff et al. (1985), Goff et al. (1988), Grigsby et al. (1984), Shevenell et al. (1987), Vuataz et al. (1988), and White (1986); VC-2A data previously unpublished. [a]Acid-sulfate springs occur at Sulphur Springs (Fig. 3). [b]VC-2A data are average of five analyses.

	Hot springs						Geothermal wells						
	Acid-sulfate springs[a]		Thermal meteoric springs		Derivative hot springs		Pore fluid(?) Precambrian rocks		Sulphur Springs	Redondo Creek		Outflow plume	
	Women's Bathhouse Spring	Footbath Spring	Spence Hot Spring	San Antonio Hot Spring	Soda Dam Spring	Main Jemez Spring	EE-3 Fenton Hill	WC23-4 Thompson Ridge	VC-2A[b]	Baca-13	Baca-15	VC-1	JS-1
Sample	S-6-80	S-4-80	VA-120	VA-128	VA-140	VA-216	V56	VA-116	—	BA-1	BA-8	VA-209	VA-15
Date	9/80	9/80	1/83	3/83	2/1/84	10/4/85	5/3/83	1/4/83	8/27/87	6/4/82	9/8/82	9/5/85	1/79
Depth, m							>3000	1921	490	>1000	>1000	483.2	152
Temperature, °C	90	33	42.3	41.3	46.8	73.7	>200	233	210	278	267	111	60.5
pH (field)	1.40	1.10	7.60	7.88	6.71	6.90	6.67	7.10	6.20	7.30	7.12	7.06	6.69
SiO_2	168	214	66	74	47	91	156	450	315	546	441	74	24
Ca	131	56	5.9	3	342	137	140	46.0	5.9	3.35	12.4	49	120
Mg	50.0	26.5	1.6	0.5	21.9	5.1	9.8	0.45	0.14	0.04	0.02	17.8	9.31
Sr	0.14	0.10	0.08	0.06	2.84	0.64	—	1.98	0.76	0.14	0.13	1.33	0.40
Na	18.9	10.8	50	23	960	638	4830	5890	1842	1146	1196	883	185
K	72	94	1.4	1.8	160	68	730	1020	308	244	261	85	29.9
Li	0.17	0.10	0.58	0.06	13.8	8.90	106	68.0	26.5	17.0	15.0	8.00	2.27
Rb	0.1	—	<0.1	—	1.8	0.7	—	—	4.3	2.7	3.1	0.4	—
HCO_3	0	0	140	57.3	1488	745	1100	382	273	168	48	942	479
SO_4	6400	7900	17.1	9.5	34	40.8	51	95	55	42	29	56.8	38.0
Cl	<1	<1	8.2	7.0	1480	917	10500	9960	2943	1897	2093	964	243
F	5.2	10.6	0.76	0.79	3.33	4.99	2.3	13.8	5.68	7.2	5.5	3.94	3.30
Br	<0.4	<0.4	0.10	<0.02	4.60	2.40	71	27.0	5.9	5.3	5.9	2.80	—
B	0.2	0.2	0.12	<0.01	12.1	7.34	272	96.2	25.6	17.0	17.0	8.55	2.20
As	0.04	—	0.05	—	1.5	0.7	18.3	7.8	1.92	1.6	2.3	<0.1	—
δD,‰	−60.8	−82.1	−86.5	−91.6	−84.9	−81.9	—	−71.5	−74.4	−86.0	−84.0	−88.0	−85.9
$\delta^{18}O$,‰	−8.45	−20.4	−12.25	−12.70	−10.56	−10.46	—	−5.05	−7.1	−10.0	−8.7	−11.35	−11.8
$(^{87}Sr/^{86}Sr)m$	0.710614	—	0.708453	—	0.721932	0.721742	—	—	0.718670	0.708423	0.709412	0.715220	—

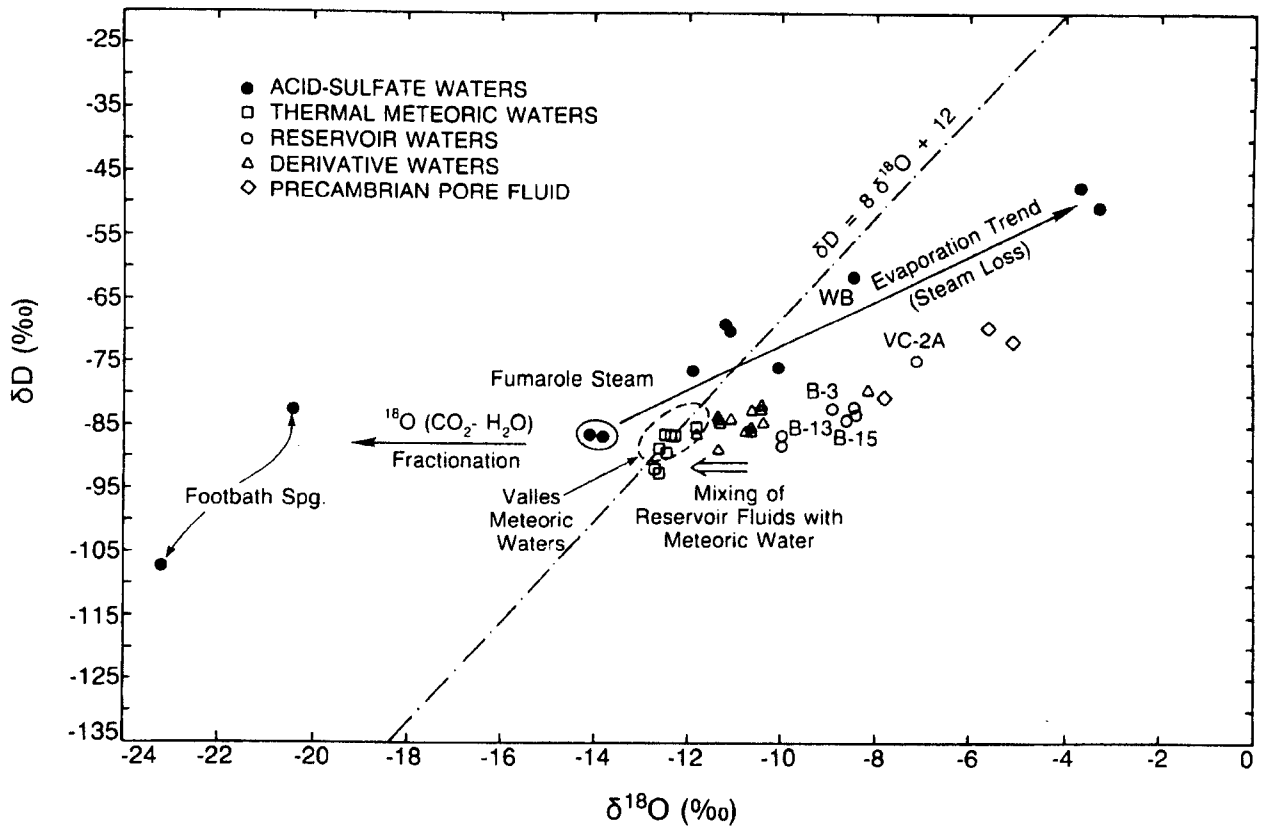

FIGURE 16—Plot of δD versus $\delta^{18}O$ for all thermal water types in the Valles caldera region (data from Vuataz and Goff, 1986; Goff et al., 1988; and unpubl.).

the geothermal reservoir comes from meteoric precipitation and slow infiltration of cool ground water to depth, particularly from the basins of the northern and eastern caldera moat. They also concluded that derivative thermal waters in San Diego Canyon and beneath the southwestern plateaus were mixtures of reservoir water and various cooler ground waters (Fig. 16). Tritium data could only bracket the mean age of reservoir water between 60 and 10,000 years, but an appropriate analytical model has not been applied to the data (e.g., Pearson and Truesdell, 1978). A ^{36}Cl investigation of a limited number of hydrothermal fluids in the caldera (Phillips et al., 1984) concluded that the chloride of the deep Valles hydrothermal fluid was in secular equilibrium with tuffaceous reservoir rocks (half-life of $^{36}Cl = 3 \times 10^5$ yrs).

From examination of thermal-water hydrogeology and hydrogeochemistry in the many geothermal wells drilled inside and outside the caldera (including CSDP corehole VC-1), a reasonably accurate model of the configuration of the present hydrothermal system in the Redondo Creek area can be depicted (Fig. 17) (Faust et al., 1984; Goff et al., 1988). Meteoric precipitation recharges the hydrothermal system, which equilibrates at depths of 2–3 km and at temperatures of about 300°C in caldera-fill tuffs and precaldera volcanic rocks. Thermal waters rise convectively to depths of roughly 500–600 m before flowing laterally to the southwest toward the caldera wall. A vapor zone that contains steam, CO_2, H_2S, and other volatile components has formed above a boiling interface at about 200°C. This interface is the upper surface of a convecting liquid-dominated system. Acid springs, mudpots, and fumaroles occur in a surface condensation zone only a few meters thick (Goff et al., 1987). The lateral flow system crosses the southwestern caldera wall above Precambrian basement through the Jemez fault zone and semipermeable Paleozoic strata. Mixing of reservoir water and other ground waters occurs along the lateral flow path to form derivative waters that issue as hot springs or flow in subsurface aquifers southwest of the caldera. An extremely good correlation is found in the $^{87}Sr/^{86}Sr$ ratio between hydrothermal fluids and coexisting rocks in the geothermal reservoir and its lateral flow system (Vuataz et al. 1988).

The model in Fig. 17 is relatively simple in concept and resembles general models of hydrothermal systems presented by Henly and Ellis (1983). However, we know the hydrothermal system is more complex when examined in detail. Smith and Kennedy (1985) and Truesdell and Janik (1986) demonstrated that the Redondo Creek area contains two somewhat discrete reservoir fluids with subtle differences in chemical and stable-isotopic composition and $^3He/^4He$. A reservoir fluid (separate from Redondo Creek) or set of superimposed reservoirs exists beneath the Sulphur Springs area that is being investigated in CSDP coreholes VC-2A and VC-2B. Inverse variations between temperature and chloride content and stable-isotope variations in the derivative waters southwest of the caldera demand that different reservoir waters and different ground waters produce the mixed waters that are observed (Goff et al., 1988).

Chronology of the hydrothermal system(s)

Hydrothermally altered rocks occur in precaldera volcanic rocks throughout the central and southeastern Valles caldera region (Fig. 18). Based on surface mapping, crosscutting

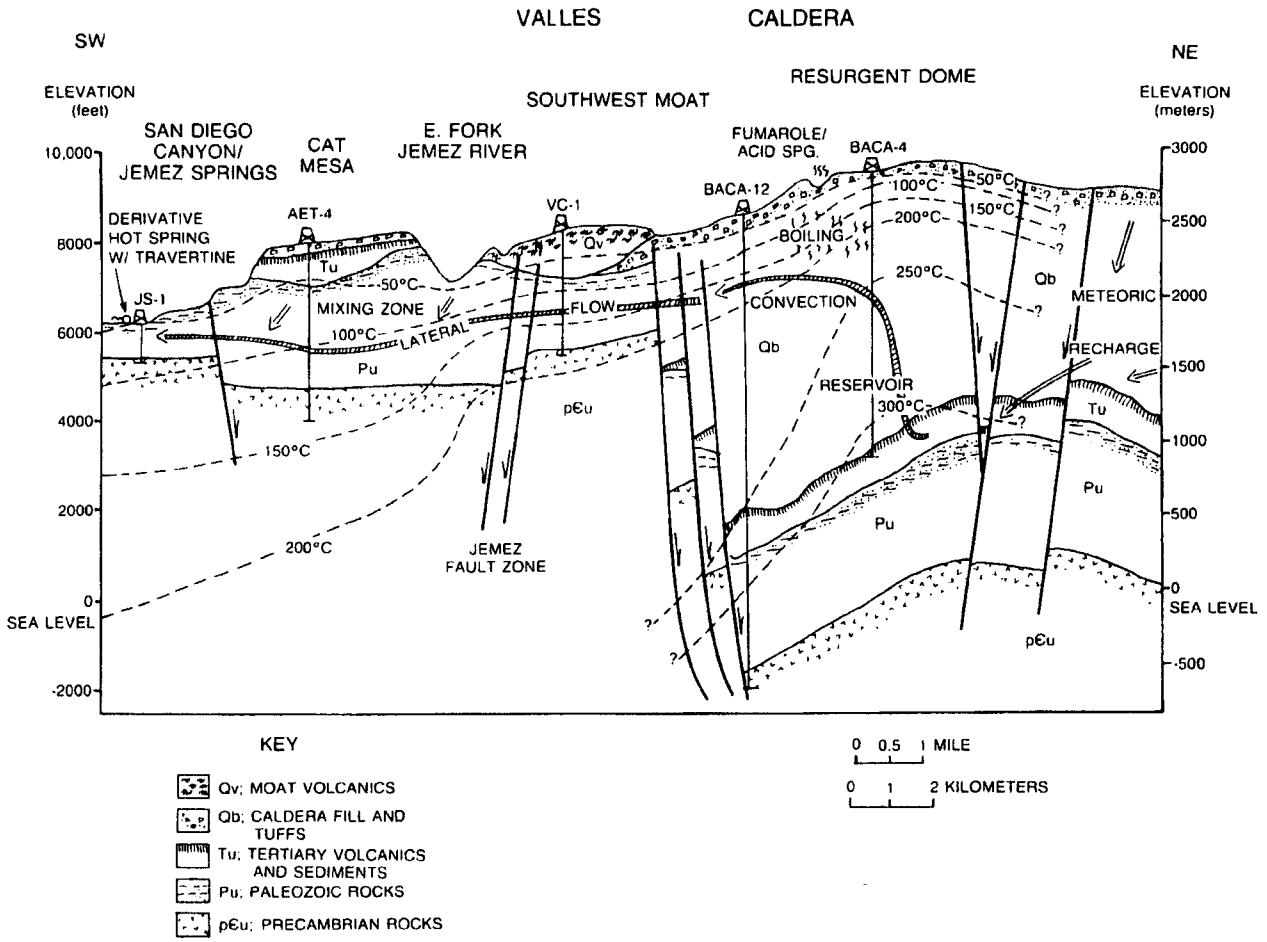

FIGURE 17—Cross section of southwest margin Valles caldera showing general configuration of the active hydrothermal system (modified from Goff et al., 1988). Well locations are shown in Fig. 3.

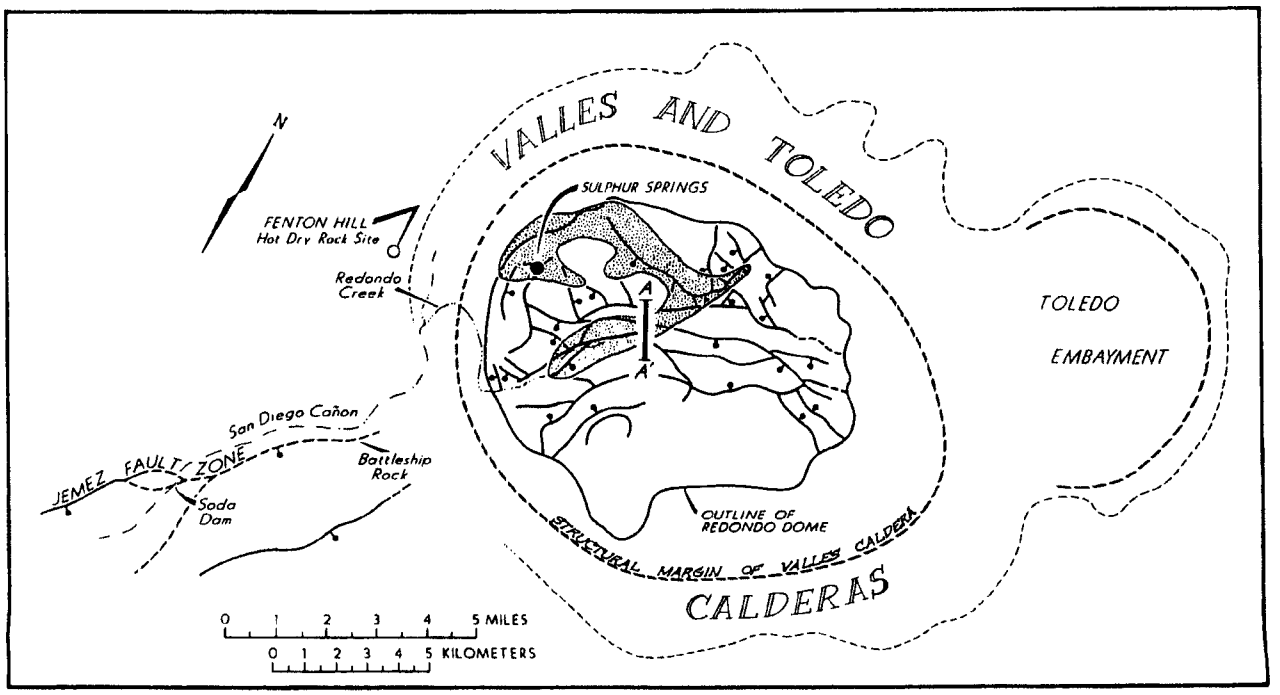

FIGURE 18—Structural map of the interior of Valles caldera showing the extent of active or recent surficial alteration (stippled pattern). Note location of alteration cross section A–A' (Fig. 19) through the apical graben of the Valles resurgent dome. Sulphur Springs is the location of core hole VC-2A (Fig. 20).

relationships of veins and intrusive rocks, and K–Ar dates on volcanic units, Wronkiewicz et al. (1984) and Gardner et al. (1986) concluded that the gold-bearing quartz veins and hydrothermally altered rocks of the Cochiti mining district in the southeast Jemez Mountains were formed about 6 Ma, considerably more recently than postulated by previous workers. Recent K–Ar dates by WoldeGabriel and Goff (1989) on hydrothermal illites pinpoint this event at 6.5–5.6 Ma. The latter authors have used stable-isotopic evidence to argue that the epithermal deposit was formed from a hydrothermal system composed predominantly of meteoric water. Wronkiewicz et al. (1984) have demonstrated from fluid-inclusion studies that the Cochiti veins were formed at temperatures of about 195–375°C and that the fluids had salinities of about 0–4.9 wt% equivalent NaCl. Gardner et al. (1986) also suggested that other hydrothermal events occurred in the time frame 10–7 Ma in Keres Group mafic to intermediate rocks of the southern Jemez volcanic field, but these altered rocks have been barely studied.

Hydrothermally altered, precaldera volcanic rocks along the northern and western Valles caldera wall (Gardner et al., 1986) and K–Ar dates on hydrothermal illites from altered Paleozoic rocks in CSDP corehole VC-1 (Ghazi and Wampler, 1987) suggest that other hydrothermal events may have occurred between 6 and 1.12 Ma, associated with volcanism of the Polvadera Group or with formation of the Toledo caldera. The absolute ages of these events have not been verified.

Much more is known about the evolution of the hydrothermal system created after formation of Valles caldera. Goff and Shevenell (1987) applied U–Th disequilibrium and U–U dating techniques to the present and ancient travertine deposits at Soda Dam hot springs to show that the hydrothermal system was initiated at about 1 Ma. Ghazi and Wampler (1987) obtained a K–Ar date of 1.0 ± 0.1 Ma on hydrothermal illite from Paleozoic limestone at about 500 m depth in corehole VC-1. Geissman (1988) obtained a reverse magnetic polarity of unique magnetic character on hydrothermally altered Paleozoic rocks in VC-1 and concluded that high-temperature (300°C) fluids permeated the rocks ≥ 0.98 Ma. WoldeGabriel and Goff (1989) dated hydrothermal illite throughout the VC-2A core by K–Ar and obtained ages of 0.83 to 0.66 Ma. Because temperatures in VC-2A are still 200°C at only 400 m depth, these dates may have been slightly reset and could reflect the minimum age of initial hydrothermal activity.

Lateral flow has been a characteristic feature of the hydrothermal system during the last 1 Ma. Dates on the travertine deposits of Soda Dam (Goff and Shevenell, 1987) and U–Th dates on calcite veins in VC-1 core (Sturchio and Binz, 1988) indicate that hydrothermal fluids have discharged continuously from the caldera along the Jemez fault zone throughout this period.

The age of the vapor cap above the liquid-dominated reservoir is less constrained. Goff and Shevenell (1987) suggested that the vapor cap began to form about 0.5 Ma. This age corresponds to cessation of travertine deposition of the oldest, large travertine deposit at Soda Dam and coincides with the age of breaching of the southwest caldera wall and draining of intracaldera lakes (Doell et al., 1968; Nielson and Hulen, 1984). It is postulated that draining of the lakes and resulting loss of hydraulic head on the hydrothermal system caused the maximum elevation of the hydrothermal fluids in the geothermal reservoir to drop (Trainer, 1984). If so, this is a completely different hypothesis for formation of vapor zones above liquid-dominated systems than the "hydrothermal sealing and boiling-down" theory proposed by White et al. (1971). Table 4 summarizes related volcanic, hydrothermal, and geomorphic events of the Valles caldera.

Intracaldera hydrothermal alteration

Well-zoned hydrothermal alteration and metallic mineral assemblages recognized in deep geothermal wells have proven useful not only for locating permeable fluid channels in the Valles hydrothermal system, but also for understanding how that system has evolved with time. For example, we know from detailed alteration studies based on drill cuttings (Hulen and Nielson, 1986a, b) that phyllic (quartz–sericite–pyrite) alteration in the Redondo Creek area is commonly associated with widely spaced but active thermal-fluid entries, and that similar but impermeable phyllic zones represent analogous channels now hydrothermally sealed. We also know that the Redondo Creek sector of the active Valles system (the "Baca" geothermal system) and its alteration are similar in many respects to fossil systems that formed certain epithermal precious-metal ores.

Known areas of intracaldera hydrothermal alteration and mineralization are concentrated at Redondo Creek and in the Sulphur Springs area, site of CSDP coreholes VC-2A and VC-2B (Fig. 18). The two areas differ considerably in alteration mineralogy, texture, zoning, paragenesis, and intensity. At Redondo Creek, for example, only widely scattered fumaroles, gas seeps, and small patches of acid-sulfate alteration indicate the liquid-dominated reservoir boiling at depth (Dondanville, 1978). At Sulphur Springs, by contrast, these thermal phenomena are much more concentrated, and occur within a bleached wasteland devoid of vegetation (Goff and Gardner, 1980; Charles et al., 1986).

Alteration in the Redondo Creek sector of the Valles geothermal system, from the surface through the base of the Miocene Paliza Canyon Formation, is of three principal types: argillic, phyllic, and propylitic (Fig. 19; Hulen and Nielson, 1986a). Argillic alteration forms a weak to moderate intensity, high-level blanket, mostly within the system's present vapor cap, and developed within formerly permeable, non-welded tuffs and tuffaceous sediments. The argillic zone is dominated by Ca-smectite, but includes subordinate, R1-ordered, mixed-layer illite/smectite and kaolin. All but kaolin were probably deposited under water-dominated conditions, even though the present water table is now at a nominal depth of 500 m. Beneath the argillic zone, pervasive propylitic alteration is dominant. Comprising the assemblage chlorite–calcite–epidote–albite–sericite–pyrite–hematite–sphene (in various combinations), this propylitic alteration is weakly developed in the thick, intracaldera rhyolite ash-flow-tuff sequence, but is moderately to strongly developed in the intermediate-composition volcanic rocks of the Paliza Canyon Formation; the deeper, more intense propylitic alteration may be inherited in part from a precaldera (Miocene, as in the Cochiti district?) hydrothermal system. Phyllic alteration, as noted above, is tightly confined to present and past thermal-fluid channels, including fault and fracture zones as well as discrete stratigraphic aquifers.

The deepest well in the Redondo Creek area (B-12; 3424 m) may have penetrated the base of the active Valles geothermal system. Below a depth of 2440 m in B-12, the rocks

TABLE 4—Geochronology of volcanic, hydrothermal, and geomorphic events associated with Valles caldera, New Mexico.

Event	Age	Method	Reference
1. Eruption of Tshirege Member, Bandelier Tuff; formation of Valles caldera.	1.12 Ma	K/Ar	Doell et al., 1968; Izett et al., 1981
2. Uplift of resurgent dome; eruption of early rhyolites.	~1.0 Ma	Inference	Smith and Bailey, 1968
3. Eruption of northern arc of postcaldera moat rhyolites.	1.04–0.45 Ma	K/Ar	Doell et al., 1968
4. Initial formation of Valles hydrothermal system and voluminous travertine deposit at Soda Dam.	~1.0 Ma 1.0 Ma >0.97 Ma	U/U K/Ar Paleomag.	Goff and Shevenell, 1987 Ghazi and Wampler, 1987 Geissman, 1988
5. Formation of Sulphur Springs subsystem of Valles hydrothermal system.	≥0.83 Ma	K/Ar	WoldeGabriel and Goff, 1989
6. Formation of Sulphur Springs molybdenite deposit.	≥0.66 Ma	K/Ar	WoldeGabriel and Goff, 1989
7. Breaching of SW caldera wall; deep erosion of SW caldera moat zone.	~0.5 Ma ~0.5 Ma	Inference K/Ar	Doell et al., 1968; Nielson and Hulen, 1984 Hulen and Nielson, 1988a
8. Cessation of voluminous travertine deposition at Soda Dam.	0.48 Ma	U/U	Goff and Shevenell, 1987
9. Initial formation of vapor zone above liquid-dominated hydrothermal system.	≤0.5 Ma	Inference	Goff and Shevenell, 1987
10. Eruption of southern cluster of postcaldera moat rhyolites.	0.49–0.13 Ma	K/Ar; FT; U/Th	Doell et al., 1968; Marvin and Dobson, 1979; Gardner et al., 1986; Self et al., 1988
11. Partial filling of SW caldera breach.	≤0.65 Ma <0.5 Ma	Paleomag. K/Ar	Geissman, 1988 Hulen and Nielson, 1988a
12. Formation of hydrothermal calcite veins along Jemez fault zone beneath SW caldera moat.	>400–95 Ka	U/Th	Sturchio and Binz, 1988
13. Late hydrothermal fluorite vug in Sulphur Springs subsystem.	~150 Ka?	U/Th	N. Sturchio, unpubl. data
14. Second period of travertine deposition at Soda Dam.	110–60 Ka	U/Th	Goff and Shevenell, 1987
15. Last pulse of thermal activity at Fenton Hill.	40–10 Ka	Transient analysis	Harrison et al., 1986
16. Final period of travertine deposition at Soda Dam.	5 Ka–Present	U/Th	Goff and Shevenell, 1987

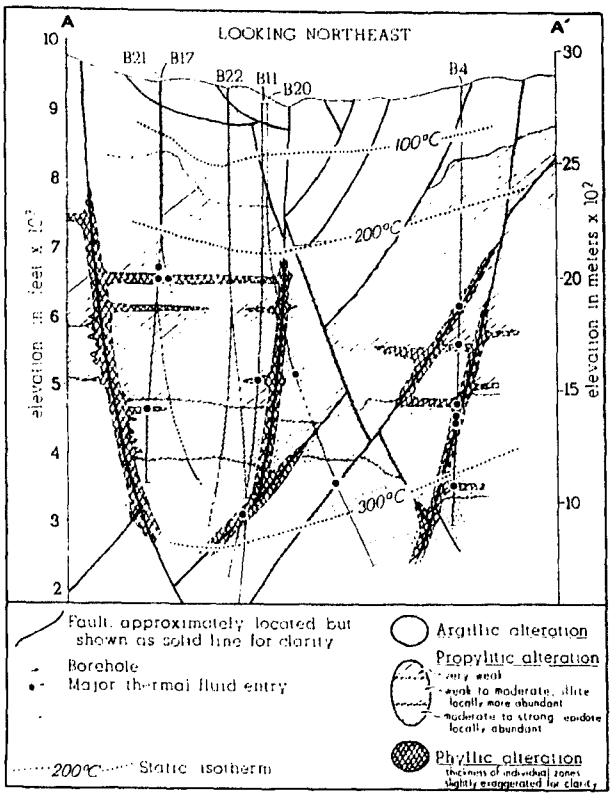

FIGURE 19—Northwest–southeast alteration cross section through the apical graben of the Valles caldera's resurgent dome (from Hulen and Nielson, 1986). Control provided by deep geothermal wells completed by UNOCAL. For location of cross section refer to Fig. 18.

are essentially devoid of veinlets and appear more metamorphic than hydrothermal; they contain high-temperature phases such as diopside and actinolite (Hulen and Nielson, 1986a), possibly formed by isochemical thermal metamorphism. The appearance of these phases and the simultaneous disappearance of veinlets coincide with a prominent change in the downhole temperature profile from an upper, near-isothermal convective signature to one characterized by a steep conductive gradient of about 75°C/km.

The Redondo Creek sector of the Valles geothermal system is similar in many respects to fossil systems which produced Creede-type (or adularia–sericite, or low-sulphur type; Barton et al., 1982; Hayba et al., 1985) epithermal silver/base-metal ores. The Valles and Creede-type systems are similar in terms of tectonic setting, host rocks, alteration mineralogy and zoning, temperature range, fluid type, and geochemical zoning (Hulen and Nielson, 1986a; White and Heropoulous, 1983). The Creede-type systems, however, are generally more saline than the relatively dilute Valles fluids (40,000–120,000 vs. 5000–8000 ppm total dissolved solids), and no Valles borehole has intersected ore-grade silver concentrations. However, argentiferous (up to 71 ppm) pyrite is locally present in well B-17 (Fig. 19) and minor amounts of pyrargyrite (Ag_3SbS_3) were discovered in the upper levels of CSDP corehole VC-2B. It is entirely possible that the relatively widely spaced Valles geothermal wells have missed intervening Creede-type deposits, or that such ores may remain concealed in another part of the Valles caldera complex.

Fluids circulating in the Valles hydrothermal system just southwest of the Valles caldera may have intermittently sealed portions of the Jemez fault zone through deposition of quartz

and other hydrothermal phases. This "self-sealing" appears to have led to frequent hydraulic rupture of the Paleozoic and Precambrian rocks penetrated by CSDP corehole VC-1 (Fig. 18; Hulen and Nielson, 1988b). The rupture is recorded by fluid inclusions with homogenization temperatures exceeding those appropriate for a hydrostatic boiling-point curve at the assumed depth of brecciation (see also Sasada, 1988b). The overpressurized fluid responsible for the brecciation apparently also led to intense quartz–illite–phengite alteration and sparse molybdenite mineralization in the resulting hydrothermal breccias.

Alteration and metallic mineralization in the Sulphur Springs area of the Valles caldera complex (Fig. 18) differ considerably from their Redondo Creek counterparts. The Sulphur Springs alteration is much more pervasive and intense, and generally of higher grade than at corresponding levels in the Redondo Creek area. Surficial alteration at Sulphur Springs, mapped by Goff and Gardner (1980), has been studied in detail by Charles et al. (1986), who note that typical acid-sulfate alteration (kaolin–opal–pyrite–alunite–miscellaneous sulfates) is concentrated around active thermal phenomena. Although this acid-sulfate alteration is the surface expression of an underlying vapor cap on a deep, liquid-dominated geothermal system (Goff et al., 1985, 1987), it is superimposed on an older, higher-temperature, liquid-dominated assemblage. Subsurface alteration in Sulphur Springs area geothermal wells and scientific coreholes has been characterized by Hulen and Nielson (1986b), Hulen et al. (1987), Sasada (1987), Gonzalez and McKibben (1987), Bayhurst and Janecky (1987), and Janecky et al. (1987). In the northern part of the Sulphur Springs area, as exemplifed by borehole B-8, a high-level, mixed-layer illite/smectite zone overlies an intermediate-depth phyllic interval which in turn overlies an unusual adularia–illite–quartz–epidote zone (Hulen and Nielson, 1986b). The illite in this zone is late-stage, replaces adularia, and is believed to indicate a shift toward more acidic conditions after adularia deposition.

Hydrothermal alteration of the rocks penetrated by CSDP corehole VC-2A is the most intense and pervasive yet encountered in any Valles borehole. The alteration is separable into an intense, upper phyllic zone (0–163 m depth) and a subjacent, mostly moderate-intensity chlorite–sericite zone (163–528 m; Fig. 20; Hulen et al., 1987). The high-level phyllic zone is notable in containing a unique occurrence of poorly crystalline molybdenite, locally reaching concentrations of 0.56 wt% in scattered breccia zones. The molybdenite occurs in veinlets and vugs intergrown with quartz, sericite, fluorite, and pyrite, and locally with traces of rhodochrosite, sphalerite, and chalcopyrite. Fluid-inclusion homogenization temperatures obtained for quartz and fluorite intergrown with the molybdenite suggest that it was deposited from dilute liquid at temperatures averaging about 200°C (Hulen et la., 1987; Sasada, 1987; Gonzalez and McKibben, 1987).

Clay mineralogy and zoning in VC-2A support fluid-inclusion data in suggesting that a high-temperature, liquid-dominated reservoir once extended up to, and probably above, the level of the present ground surface in the Sulphur Springs area (Hulen and Nielson, 1988b), even though the system is now vapor-dominated to a depth of at least 240 m. Textural evidence from VC-2A core suggests that the high-temperature alteration postdated or accompanied the waning stages of resurgent doming. Baca-8, located north of VC-2A, has shown a similar cooling and drop in the water table (Hulen and Nielson, 1986b). Wells in the Redondo Creek area also show cooling of 50–100°C relative to past activity; this temperature decline has been attributed to draining of an intracaldera lake (Hulen and Nielson, 1988b).

Intense sericitization affects the uppermost in-place rocks penetrated by the VC-2A corehole. This high-level sericite is principally R3-ordered, illite-rich, mixed-layer illite/smectite (I/S), which, according to the methods of Srodon (1980) and Srodon and Eberl (1984), contains an average 5–10% interlayer smectite. Numerous clay studies (e.g., McDowell and Elders, 1980; Steiner, 1968; Muffler and White, 1969) in active geothermal systems worldwide have shown that illitic I/S of this type forms under water-dominated conditions at temperatures near 200°C. This is also the approximate average homogenization temperature for primary fluid inclusions in quartz and fluorite intergrown with the sericite at high levels in VC-2A. Thus, both fluid-inclusion and sericite geothermometer data indicate that the present vapor-zone evolved from a much higher-temperature, liquid-dominated precursor.

Conclusions

The major conclusions that we would like to stress are as follows:

1. The Jemez volcanic field has been continuously active for more than 13 Ma and volcanic rocks are predominantly calc-alkaline in composition. Although basaltic to rhyolitic rocks have been produced, the most voluminous pulses of activity consisted of two-pyroxene andesite erupted from about 10 to 7 Ma and high-silica rhyolite erupted from 1.45 to 0.13 Ma. Petrogenesis of the older volcanic sequences involved mostly fractional crystallization, although magma mixing and melting of lower crust were involved in some of the more silicic rocks. Volcanism is intimately related to tectonic activity associated with the RGR and the JVL.

2. High-silica rhyolite ignimbrites erupted from the evolving "Bandelier" magma chamber were first produced as early as 3.64 Ma from the approximate center of the volcanic field. It is now known that the Valles caldera complex contains at least two small and two large calderas, but the earlier collapse features have been nearly obliterated by Valles caldera (1.12 Ma). Several petrologic studies indicate that the Bandelier magma chamber is compositionally zoned, but the petrogenesis of the chamber (estimated volume at least 3000 km^3) is still not resolved.

3. The subsurface structure of the caldera complex is controlled by northeast-trending structures associated with the earlier RGR and JVL. Drill holes throughout the southwestern sector of the caldera and gravity modeling over the entire caldera indicate that the caldera-fill sequence is three or more times thicker than originally proposed and that the depth of the caldera floor is asymmetric, relatively shallow on the west and deep on the east. As a result, the interior structure of the resurgent dome is much more complex than previously thought. Drilling results have not verified that resurgence occurred after the comparably sized and coincident Toledo caldera (1.45 Ma). Structural models and petrologic studies indicate that the roof of the Bandelier magma chamber was at a depth of 5–6 km when the Tshirege Member was vented and that the eruption temperature varied from 700 to 850°C.

4. The highest convective heat flow and subsurface seismic attenuation in the caldera complex occur in the south-

western sector coincident with the main zones of hydrothermal upflow and the youngest moat rhyolite eruptions (<0.5 to 0.13 Ma). Two different investigations in the thick Precambrian section on the west caldera margin indicate that subsurface temperatures beneath the caldera may be increasing. If so, the "reheating" must be caused by evolution of the new batch of "mafic" rhyolite in the southwestern moat.

5. The Valles hydrothermal system is configured like most volcanic-hydrothermal systems the world over. The basic hydrologic elements consist of local meteoric recharge, equilibration at temperatures approaching 300°C, convective upflow along faults and fractures, and lateral flow along structures that cut the southwestern caldera wall (Jemez fault zone). A vapor zone and acid-sulfate condensation zone

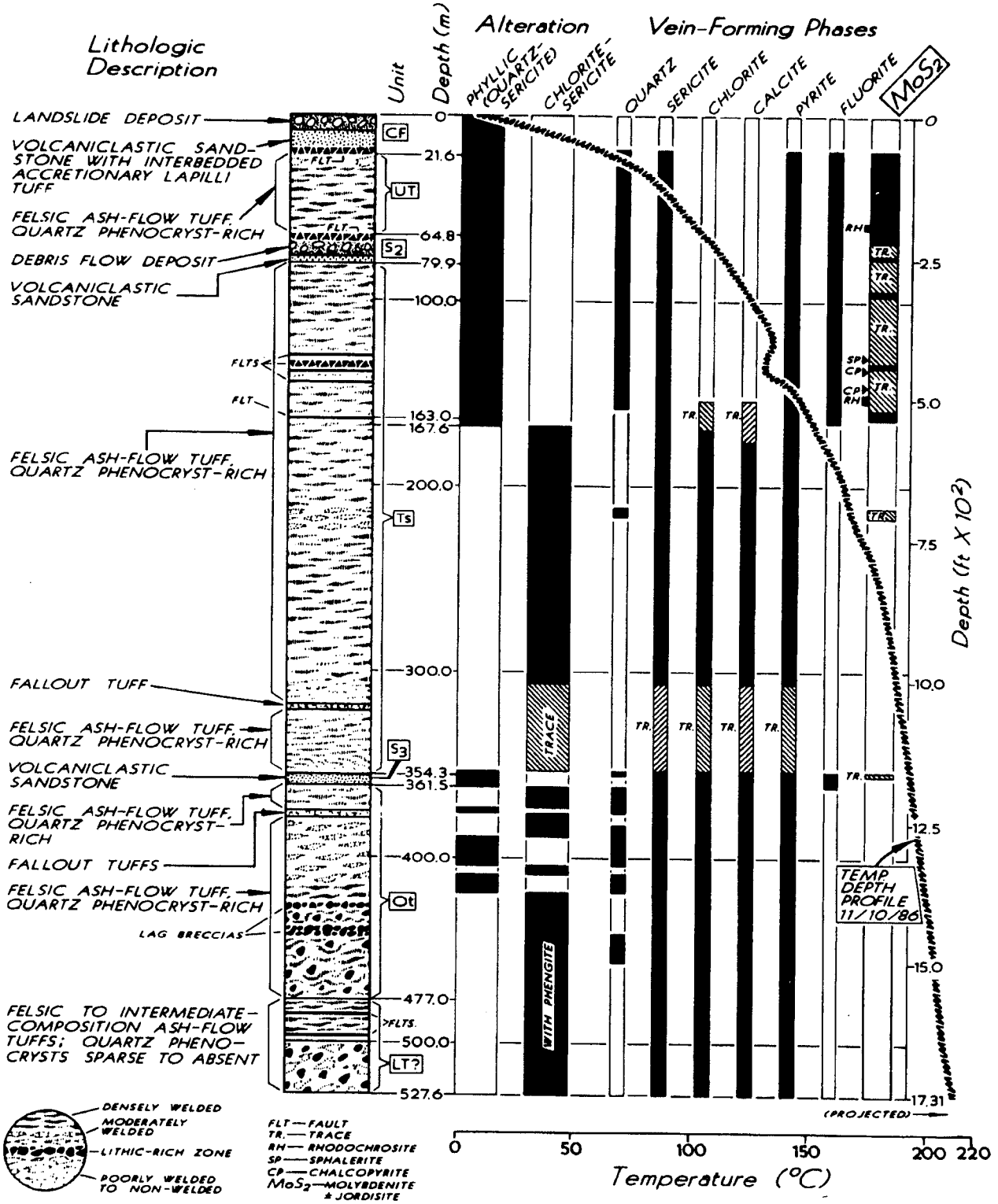

FIGURE 20—Generalized lithologic, structural, alteration, and vein-mineralization log for CSDP corehole VC-2A, Sulphur Springs, Valles caldera (modified from Hulen et al., 1987).

originate from subsurface boiling (200°C) above the liquid-dominated reservoir inside the caldera. The lateral flow system produces a subsurface tongue of mixed reservoir water and cooler ground waters in Paleozoic rocks around the southwestern caldera margin. The areal extent of the geothermal reservoir inside the caldera is 10 to 30 km^2, but permeability is extremely localized. About 20 MW(e) was proven by UNOCAL before they terminated their lease in 1984.

6. Episodic hydrothermal events have occurred in the Jemez volcanic field for about the last 8 Ma (e.g., the Cochiti gold–silver district at 6.5–5.6 Ma). The Valles hydrothermal system has been continuously active for the last 1 m.y., but the vapor zone first formed about 0.5 Ma. Creation of the vapor zone is apparently linked to breaching of the southwestern caldera wall by the ancestral Jemez River, draining of intracaldera lakes, and resulting loss of hydraulic head on the liquid-dominated hydrothermal reservoir.

7. Hydrothermal alteration and ore mineralization in Valles caldera resemble those found at many fossil calderas hosting economic ore deposits. Alteration style ranges from advanced argillic to anhydrous calc-silicate, depending on depth and location. Secondary mineral assemblages and fluid-inclusion studies indicate temperatures of formation and salinities similar to those presently occurring in the hydrothermal system, although a complex evolutionary history can be unraveled. Sub-ore-grade molybdenite (up to 0.56 wt% MoS_2) is the primary ore mineral found so far, but Cu, Pb, Zn, Mn, and Ag minerals have also been recently identified.

First-day road log: Tectonic and magmatic development of the southern Jemez volcanic field

Summary—The route of the first day takes us across the southern Jemez Mountains where we will see representatives of most precaldera magma types described by Gardner (1985) and Gardner et al. (1986). Although most of the rocks we will look at today are of the Keres Group, the group also contains rocks petrologically analogous to rocks of the Polvadera Group. We will also view the Pajarito fault zone, which is a major active fault along the Rio Grande rift, and deposits of the Cochiti Formation. Much of the early tectonic activity in the volcanic field's history can be interpreted by analysis of the Cochiti deposits.

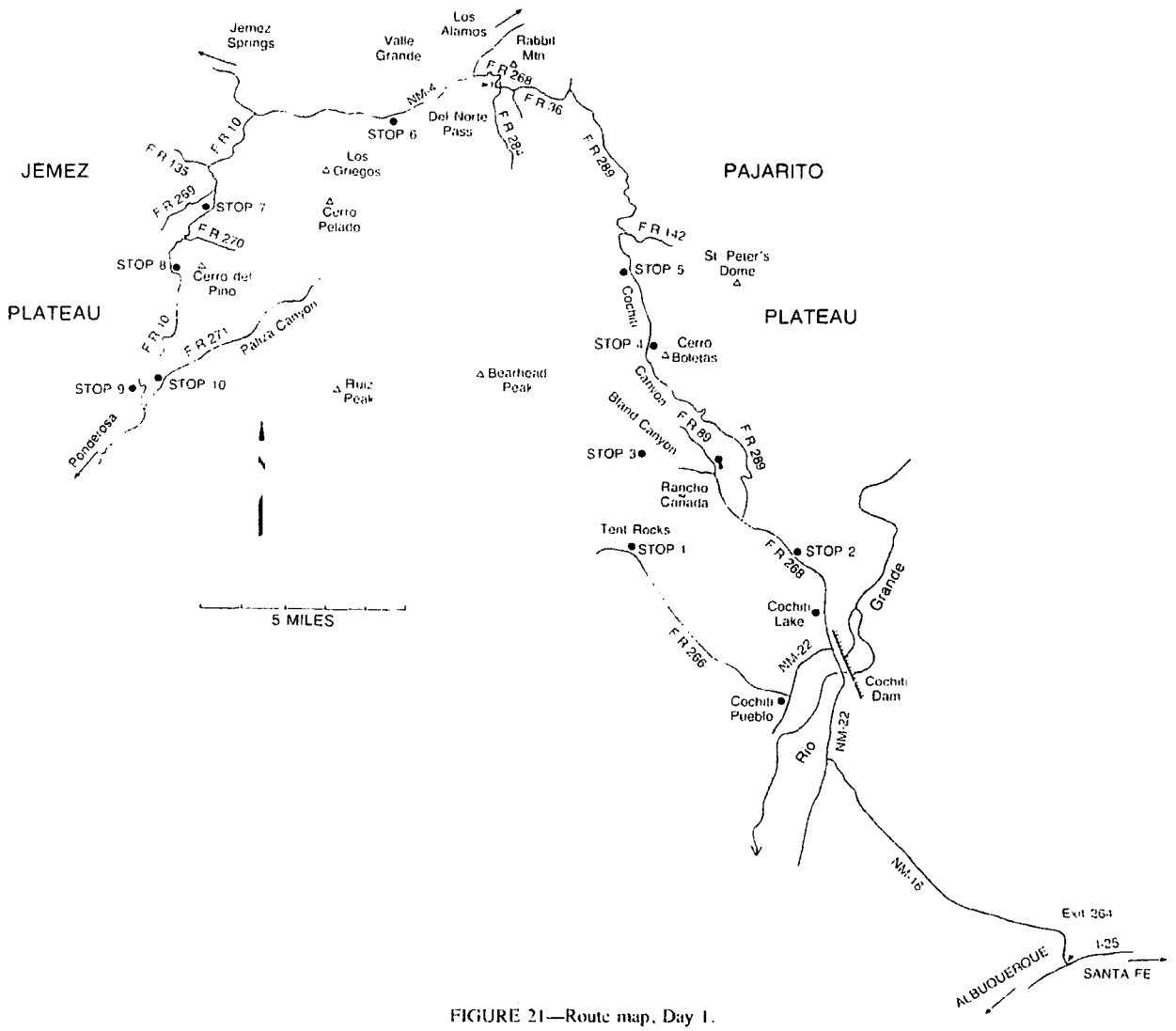

FIGURE 21—Route map, Day 1.

Mileage

0.0 Overpass at junction I-25 and US-285 on south side of Santa Fe. Head south on I-25 into the southern Española Basin of the Rio Grande rift. Between 1:00 and 3:00 in distance are the Jemez Mountains. In middle distance are the low hills of the Cerros del Rio. At 10:00 are the Ortiz Mountains; the white scar marks the Ortiz gold mine. **10.6**

10.6 On left are the Cerrillos Hills, consisting of Oligocene volcanic rocks and plutons known for their turquoise mines. On right, roadcuts of Santa Fe Group and basalts of Cerros del Rio. **3.8**

14.4 Santo Domingo Basin of the Rio Grande rift comes into view with Sandia Mountains on skyline. **1.4**

15.8 Head of La Bajada grade, a fault scarp separating the Santo Domingo and Española Basins. **1.3**

17.1 **Exit** on turnoff #264 toward Cochiti Pueblo. **0.2**

17.3 **Turn right** on NM-16. **0.9**

18.2 Zia Sandstone of Oligocene age (white outcrops) at base of La Bajada fault on right. **5.1**

23.3 Junction with road to Cochiti Lake; continue on NM-16. **2.0**

25.3 Junction with NM-22. **Turn right** toward Cochiti Pueblo. **2.6**

27.9 **Turn left** toward Cochiti Pueblo on NM-22. **1.7**

29.6 **Turn right** on Forest Road (FR) 266 (dirt road) toward Bear Springs. **1.2**

30.8 Rift-fill gravels on hills at right. **1.3**

32.1 Bandelier Tuff overlies rift sedimentary rocks on right. **2.3**

34.4 **Turn right** on dirt road toward white cliffs. **0.1**

34.5 **STOP 1. Peralta Tuff Member of the Bearhead Rhyolite.** Park anywhere on dirt road. This is the type area for the Peralta Tuff Member of the Bearhead Rhyolite (Bailey et al., 1969). Here the bedded, high-silica rhyolitic pyroclastic rocks are mainly reworked or water-lain tuffs with subordinant fallout and flow units (Fig. 22). The tuff was apparently vented from within a dome and flow complex of high-silica Bearhead Rhyolite about 10 km northwest of here. Sanidine from pumice lumps, collected about 200 m north of here, yielded a K–Ar age of 6.85 ± 0.15 Ma (Gardner et al., 1986). The Peralta Tuff forms a prominent stratigraphic marker in the southern Jemez Mountains, and as such approximates the somewhat arbitrary boundary, at about 7 Ma, between the Canovas Canyon and Bearhead rhyolites (Gardner et al., 1986). These two rhyolite formations are the products of a continuum of high-silica rhyolite volcanism from 13 to about 6 Ma. The Bearhead Rhyolite represents an apparent volumetric pulse that postdated most of the voluminous andesitic activity of the southern Jemez Mountains. Working within the rift basin to the south, Kelley et al. (1976) included the tuffs at this locality as a facies of the Santa Fe Group rift-fill sequence. These are also some of the most photographed "tent rocks" in New Mexico.

Turn vehicles around and retrace route to Cochiti Pueblo. **4.9**

39.4 **Turn left** on NM-22 toward Cochiti Dam. **1.6**

41.0 Junction, **turn left** on FR-268 toward town of Cochiti Lake. **2.1**

43.1 **STOP 2. Vista of the southeastern Jemez Mountains.** Park on right side of road just beyond summit of hill. From this vantage point we can look west-northwest and see Tertiary to Quaternary domes and ignimbrites of the southeastern Jemez volcanic field (Fig. 23). The rounded hills are primarily andesitic and rhyolitic domes of the Keres Group (>13–6 Ma). Bearhead Peak is the type locality of the Bearhead Rhyolite. Cerro Boletas is a sequence of bedded rhyolite tuffs of the Bearhead Rhyolite. Cerro Picacho is yet another Bearhead dome and St. Peter's Dome is a complicated pile of andesitic lavas and interstratified volcaniclastic rocks (both to right of photo). Low places in volcanic rocks of the Keres Group were subsequently filled by the mesa-forming Otowi and Tshirege Members of the Bandelier Tuff (1.45–1.12 Ma) erupted from the Toledo and Valles calderas. The visible scarp is the Pajarito fault, which has been periodically active in this area over the last 16 Ma. In the foreground are various sedimentary units that are mostly Quaternary in age and have been shed from the Jemez Mountains toward the Rio Grande.

Continue straight ahead (FR-268). **1.2**

44.3 Golf course on right; begin dirt road. **0.8**

45.1 Junction FR-289 on right; continue straight ahead on FR-268. **1.4**

FIGURE 22—Peralta Tuff type section; lower Peralta Canyon, Jemez Mountains. View to north.

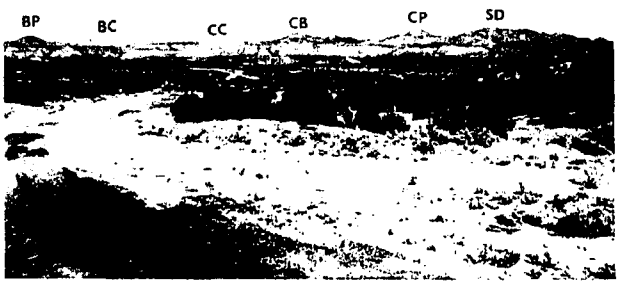

FIGURE 23—View to west-northwest of southeastern margin of the Jemez volcanic field; BP = Bearhead Peak, BC = Bland Canyon, CC = Cochiti Canyon, CB = Cerro Boletas, CP = Cerro Picacho, and SD = St. Peter's Dome.

of the Bandelier Tuff, we can see ridges of Paliza Canyon andesite cut by faults of the Cañada de Cochiti fault zone (east to southeast); Borrego Mesa, basalt capped with andesite (9 Ma; Luedke and Smith, 1979) (south-southeast); the transition from the Albuquerque Basin of the Rio Grande rift to the Colorado Plateau (south to southwest); a distant Mount Taylor, the next volcanic field of the Jemez lineament to the southwest; and the Nacimiento Mountains, a Laramide structure (southwestern to western skyline).

Continue ahead on FR-10. **2.1**

87.0 Poorly exposed Triassic red shales of Chinle Formation. **0.1**

87.1 **Turn left** on FR-271 toward Paliza Canyon. **0.5**

87.6 Gravels of Cochiti Formation on left. **0.4**

88.0 **STOP 10. Dacitic plug and Cochiti Formation deposits.** Pull off along side of road beyond cattleguard. This volcanic plug is one of several in the southern Jemez Mountains that show geochemical similarities to dacite of the Tschicoma Formation. Petrologically, these dacites appear to have been generated by mixing of andesite and high-silica rhyolite magmas. This plug probably intruded surrounding Cochiti Formation gravels, which are well exposed about 100 m farther up the canyon. This is close to the western limit of the Cochiti Formation. Here the maximum thickness of the immature basin-fill sequence is about 30 m, but the formation thickens to over 300 m eastward into the rift.

Turn around and retrace route toward south. **0.9**

88.9 Junction with FR-10; **turn right** and retrace route (about 12 mi) back to NM-4; **turn right** and drive about 22 mi to Los Alamos.

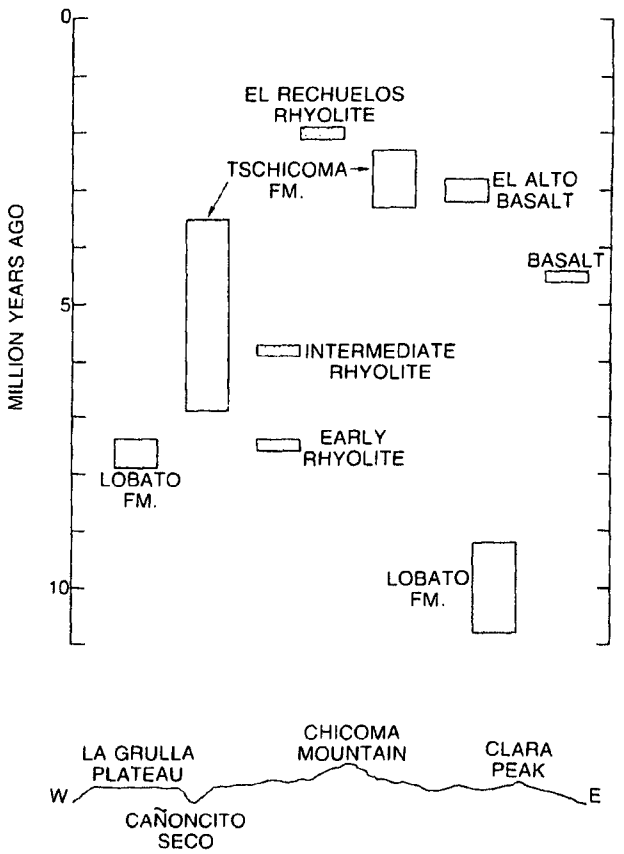

FIGURE 27—Generalized stratigraphic relations of volcanic units in the northern Jemez volcanic field. Units are arranged schematically from west (left) to east (right). Note, however, that distribution of Tschicoma Formation is portrayed simplistically; much overlap of older and younger dacites actually occurs. A schematic topographic profile is shown across the bottom of the figure.

Second-day road log: Tectonic and magmatic development of the northern Jemez volcanic field

Summary—This day's field trip focuses on rock types and stratigraphic relationships of the northern Jemez volcanic field. The basic stratigraphy for the area was established by Bailey et al. (1969) and Smith et al. (1970). Volcanic rocks range in age from 10.8 to 2.0 Ma and in composition from basalt to rhyolite. The earliest rocks are predominantly basalts (but include minor volumes of dacite) erupted in the eastern part of the area 10.8–9.2 Ma ago (Fig. 27). The sources for the basalts included several broad shield cones. These basalts were followed (7.9–7.4 Ma ago) by a suite of rocks ranging from basalt to dacite erupted in the western part of the area. Evolved rocks of this suite were probably derived from the basaltic endmember by a combination of fractional crystallization and assimilation of granitic crust (Singer and Kudo, 1986). Rocks from both of these areas were defined as Lobato Basalt by Bailey et al. (1969) and Smith et al. (1970). Because of the range of compositions (basalt to dacite), Baldridge and Vaniman propose to rename this unit Lobato Formation. In addition, a single dome of rhyolite ("Early Rhyolite" of Loeffler et al., 1988) was erupted 7.5 Ma ago.

Large volumes of andesites, dacites, and rhyodacites were erupted 6.9–2.3 Ma ago. K–Ar dates define two main periods of activity: 6.9–3.5 and 3.3–2.3 Ma ago. Rocks of the older phase of activity, which consist mainly of hornblende- and biotite-bearing dacites, many containing mafic clots, are exposed predominantly in the western part of the area. Flows on the northern flank of the Valles/Toledo calderas were erupted from highlands (named by us the "precaldera highlands"; Baldridge et al., 1987) that existed in the area presently occupied by the calderas. These highlands subsequently collapsed and were buried during caldera formation, leaving only the flows on the lower slopes exposed. Fewer dacitic lavas from the highlands are recognized after the first rhyolitic ignimbrites were erupted from the developing Bandelier magma chamber at 3.6 Ma.

Rocks of the younger phase consist both of hornblende- and biotite-bearing dacites and of relatively anhydrous dacites, many of which are clot-free. These younger dacites erupted both from the precaldera highlands and from a group of domes and flows in the eastern part of the area. Flows from the precaldera highlands were erupted as recently as 2.18 Ma (Heiken et al., 1986). This timing overlaps with early rhyolitic ignimbrites from the Bandelier system (San Diego Canyon ignimbrites of Turbeville and Self, 1988), indicating that multiple magma chambers still existed beneath the central volcanic field at that time. Small quantities of basalts were erupted 4.6–4.4 Ma ago. The areal and temporal extent of this phase of basaltic activity is poorly

characterized at present. A single dome of rhyolite ("intermediate rhyolite" of Loeffler et al., 1988) was erupted at 5.8 Ma. Both the early and intermediate rhyolites are probably related to the Keres Group rhyolites (Canovas Canyon and Bearhead Rhyolites) south of the Toledo/Valles calderas.

In the northern part of the area, basaltic lavas (El Alto Basalt) were erupted between 3.2 and 2.8 Ma (Baldridge et al., 1980; Manley, 1982), contemporaneously with nearby dacite domes of the Tschicoma Formation. The close spatial and temporal association suggests a close petrological relationship. In addition, three rhyolite domes (El Rechuelos Rhyolite) were erupted 2.0 Ma ago. Although extrusion of these domes occurred while precursor rhyolitic ignimbrites were being erupted from the Bandelier magma chamber, Sr- and Nd-isotopic data suggest that the El Rechuelos was not derived from the upper-crustal Bandelier chamber, but rather from lower-crustal magma chambers. The origin of this rhyolite is compatible with fractional crystallization from a basaltic parent with concomitant assimilation of small amounts (<6%) of lower crust (Loeffler et al., 1988).

Note: The following trip is divided into three main and two optional segments. If it is desired to complete the trip in one day, only segments A, C, and E should be followed. Two days are required to complete all segments. All segments are on poorly to non-maintained dirt roads; four-wheel-drive vehicles are strongly recommended!

Segment 2A: US-84/285 to Forest Road 427

Mileage

0.0 Junction of US-84/285 and Forest Road (FR) 144 (District 7 Headquarters of New Mexico State Police), 0.1 mi (160 m) north of stop light at junction of US-84/285 and NM-584, Española. Drive west on FR-144. **0.3**

0.3 For the next 4 mi (6.6 km) the road ascends onto a series of successively older geomorphic surfaces, labeled (from lowest to highest) Q4 to Q1. These surfaces formed over the periods 130 to >80, 240 to 150, 350 to 240, and 1100 to >350 ka, respectively, in response to climatic variations and downcutting during the Pleistocene (Dethier et al., 1988). **9.0**

9.3 Sharp curve to left; begin steep ascent. You are crossing the trace of the northeast–southwest-trending Santa Clara fault zone, part of a transfer fault connecting the Española graben with the San Luis graben to the northeast (Aldrich, 1986). Eight kilometers to the southwest, this fault zone merges with the north–south-trending Pajarito fault zone. Cerro Roman, the ridge to the east, is the remnant of a Lobato shield cone. **1.7**

11.0 Basalts of Clara Peak. The basalt here, part of the

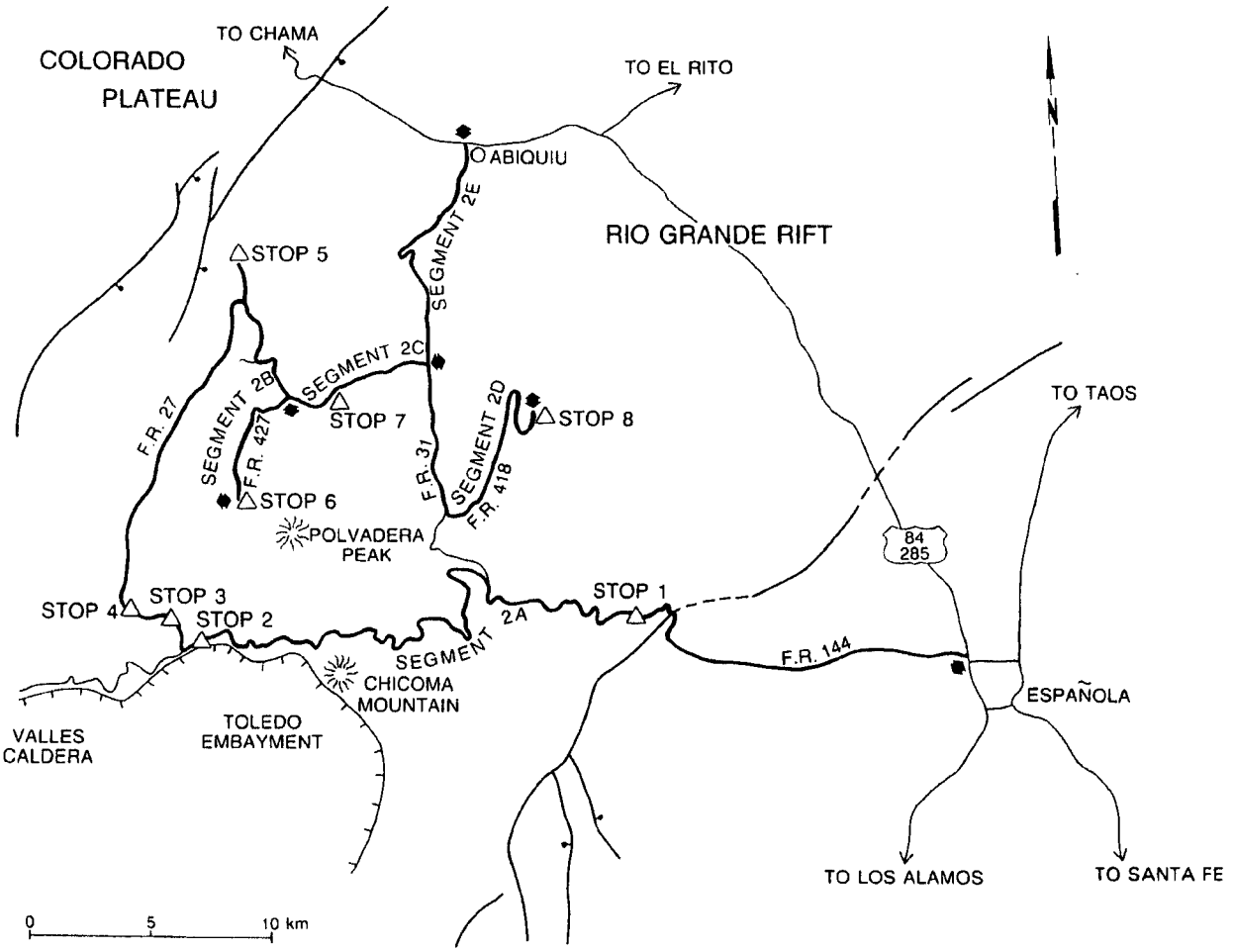

FIGURE 28—Route map, Day 2.

Lobato "Formation," is olivine-phyric and hypersthene-normative (P533 and P534, Table 5), with a K–Ar age of 9.99 ± 0.27 Ma (P533). It was erupted from a shield cone on the mesa directly above (one of several shield vents from which basalts of the Lobato "Formation" were erupted). For the next 1.4 mi (2.2 km) you will be driving through the subsurface conduit of this vent. **0.2**

11.2 Subvolcanic plug underlying the Clara Peak shield cone. This basalt (P551, Table 5) is the intrusive equivalent of the flows on the mesa above. **0.6**

11.8 Cinders, inferred to be an interior part of the Clara Peak shield cone, intruded by the basaltic plug. **0.6**

12.4 **STOP 1. Lobato Basalt.** This stack of thin flow units separated by scoriaceous rubble (Fig. 29) represents a cross section through Clara Peak shield cone. The basalt is an olivine-phyric, hypersthene-normative tholeiite (P552, Table 5), equivalent to other basalts associated with the Clara Peak center. Here the basalt contains resorbed crystals of quartz. Low hills in the foreground to the west (Los Cerritos, Fig. 30) are underlain by dacite (of the Lobato "Formation") dated at 9.6 ± 0.2 Ma (P75, Table 5). The peaks in the background (including Polvadera Peak and Tschicoma Mountain) are younger (<4 Ma) dacites of the Tschicoma Formation. Gallina Mesa is underlain by a dacite flow, dated at 3.90 ± 0.15 Ma (P68), which was vented from near the top of Tschicoma Mountain. **2.1**

14.5 Lobato dacite is exposed in low outcrops along the south side of the road (P74, Table 5). This dacite contains phenocrysts of hastingsitic hornblende (with cores of orthopyroxene) and of plagioclase (Fig. 31). **2.3**

16.8 Canyon at bottom of Gallina Mesa flow. For the next 7 mi (11.2 km) you will drive along the surface of the Gallina Mesa flow. This dacite is characterized by phenocrysts of hastingsitic hornblende, plagioclase, and in some samples biotite; and microphenocrysts of bronzite, augite, magnetite, and occasionally apatite (Fig. 31). **14.8**

31.6 **STOP 2A. Overview of the northern Jemez volcanic field and Rio Grande rift/Colorado Plateau margin.** The high peaks to the northeast (Fig. 32), including Polvadera Peak (3.13 ± 0.07 Ma) and Cerro Pelon (2.96 ± 0.27 Ma), are younger dacitic domes of the Tschicoma Formation. The low hills in the foreground are remnants of older (up to 6.6 Ma) domes(?) and flows of dacitic lava. The low terrain to the west is formed on Tschicoma andesitic lavas (approximately 5 Ma) that flowed to the north along paleovalleys.

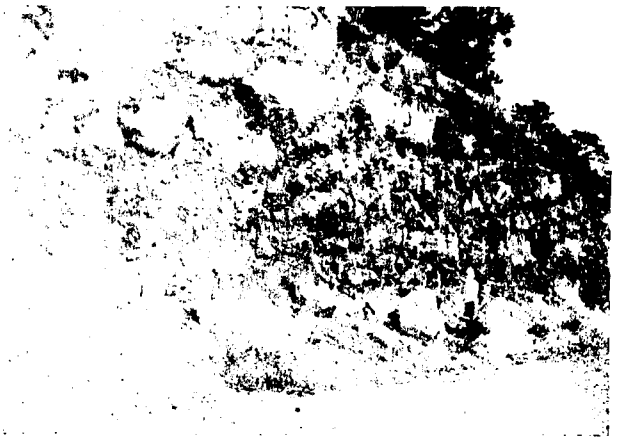

FIGURE 29—Thin flow units of olivine-phyric, hypersthene-normative basalt, probably representing a cross section through the Clara Peak shield cone.

The paleovalleys followed a set of major faults along the western margin of the Rio Grande rift. Channels along these faults persisted after Tschicoma time and provided the major northern route for Bandelier ignimbrites (erupted at 1.45 and 1.12 Ma), which form the buff-colored columnar-jointed plateau in the middle ground to the north. In the middle distance to the northwest is a 7.5 Ma rhyolite dome, the oldest rhyolite in the northern volcanic field (Stop 4). Beyond and to the north is Cerro Pedernal, capped by 7.8 Ma basalt flows of the Lobato "Formation" (Manley, 1982), and thick strata of the Colorado Plateau above Abiquiu Reservoir. In the far distance to the north are the Tusas and San Juan Mountains.

Walk 160 m farther west to a small dirt road, then 160 m south to the rim of the Toledo embayment.

STOP 2B. Panorama of the Toledo embayment and Valles caldera. Due south is the large Cerro Toledo rhyolite dome (1.38 Ma; Heiken et al., 1986). In the distance to the southwest is the far rim of the Valles caldera, 24 km away. The Redondo resurgent

TABLE 5—Major-element compositions of selected volcanic rocks from the northern Jemez volcanic field.

	Early Rhyolite	North Rim	Tschicoma Mt.	Cerro Pelon	Lobato Dacite		North Rim	Cerrito Chato				Clara Peak Shield			
	P8	P52	P69	P71	P74	P75	P79	P99	F212	P430	P487	P533	P534	P551	P552
SiO_2	73.68	58.40	65.94	65.68	64.32	65.63	60.94	64.85	52.25	51.03	51.31	48.59	51.03	51.74	51.32
TiO_2	0.25	0.88	0.56	0.57	0.57	0.56	0.86	0.60	1.48	1.30	1.20	1.40	1.25	1.19	1.20
Al_2O_3	13.91	15.86	15.29	15.71	16.40	16.51	16.48	15.03	16.80	17.06	16.50	15.88	16.02	16.53	15.97
Fe_2O_3	1.79	6.21	3.93	4.04	4.09	4.01	5.47	4.52	9.26	10.37	8.47	10.86	9.98	10.14	9.68
MnO	0.07	0.12	0.07	0.07	0.07	0.07	0.09	0.08	—	0.16	0.13	0.17	0.16	0.15	0.14
MgO	0.26	3.62	1.72	1.95	1.99	2.05	2.59	2.29	5.84	7.34	5.39	7.33	7.01	7.12	6.84
CaO	1.29	6.25	3.67	3.98	4.17	4.27	4.89	4.22	8.45	9.39	8.75	10.08	8.68	8.84	9.38
Na_2O	3.98	3.63	2.78	3.11	3.32	3.33	2.97	3.66	4.46	3.29	3.92	2.49	2.53	3.17	3.17
K_2O	3.88	2.18	3.18	2.93	2.04	1.98	2.71	2.76	1.53	0.64	1.98	0.74	0.89	0.86	0.99
P_2O_5	0.05	0.48	0.22	0.25	0.26	0.26	0.43	0.25	0.64	0.24	0.61	0.29	0.24	0.25	0.24
Total	99.16	97.63	97.36	98.29	97.23	98.67	97.43	98.26	100.71	100.82	98.26	97.83	97.79	99.99	98.93

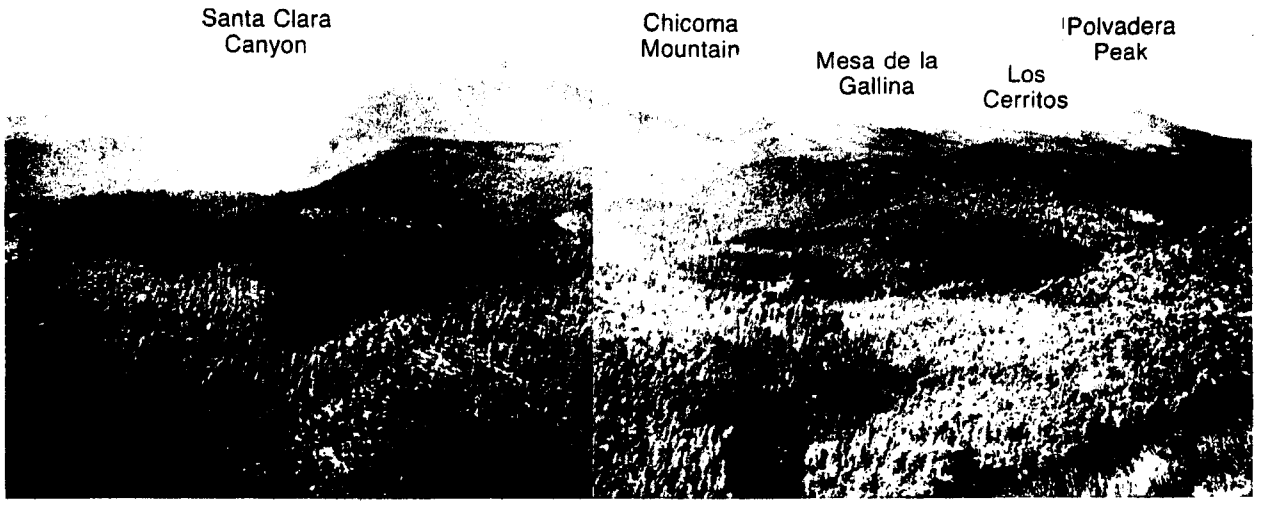

FIGURE 30—Panorama of Tschicoma terrain from Stop 1.

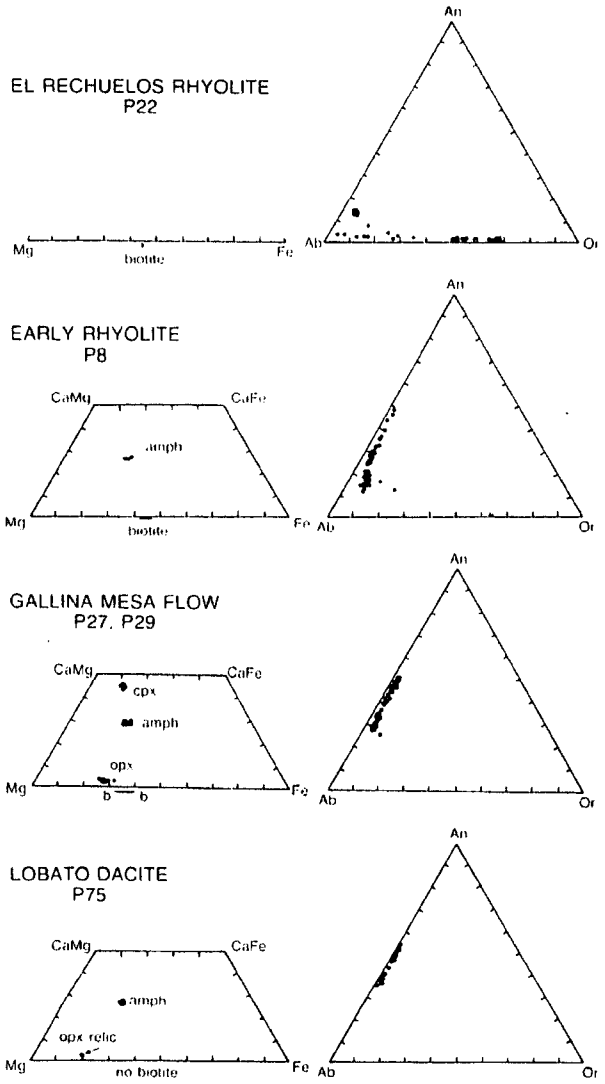

dome dominates the middle of the caldera; from this observation point you are looking along the southwest-trending axial graben which cuts the resurgent dome. The rhyolitic domes of Cerro Santa Rosa (0.88 Ma), Cerro San Luis (0.69, 0.82 Ma), and Cerro Seco (0.73 Ma; Doell et al., 1968) lie within the northern moat of the caldera. To the east, the dacites of Tschicoma Mountain (3.2 ± 0.1 to 3.7 ± 0.2 Ma; P47 and P69, respectively, Table 5) are high on the rim of the Toledo embayment.

The origin of the Toledo embayment is still uncertain. It may be partly tectonic, partly erosional, and partly the result of Tschicoma pyroclastic eruptions which deposited dacite pumices (2.5 ± 0.1 Ma) in the Puye Formation to the east. The Otowi Member of the Bandelier Tuff may lie buried within the embayment, but the major deposits within the embayment are the Cerro Toledo Rhyolite domes, onlapped by a thick sequence of the Tshirege Member of the Bandelier Tuff (1.12 Ma). The Tshirege partly filled the Santa Clara paleocanyon but has since been deeply eroded. The ridge on which this stop is located is underlain by flows from the precaldera highlands, which once occupied the region of the Toledo embayment. These flows, which form the northern rim of the Toledo embayment, range in age from 2.3 to 4.2 Ma. The flow which caps this ridge (P52, Table 5) is a distinctive dacite with remnants of olivine crystals (Fo_{82}), probably inherited from a basaltic magma which was petrographically similar to the Lobato and El Alto basalts. A small remnant of the precaldera highlands may be preserved within the embayment as Cerro Rubio dacite (2.2–3.6 Ma), a pair of dacite plugs at the far eastern end of the embayment (Table 1; Gardner

FIGURE 31—Mineral compositions for Lobato dacite, Gallina Mesa flow, and Early and El Rechuelos Rhyolites.

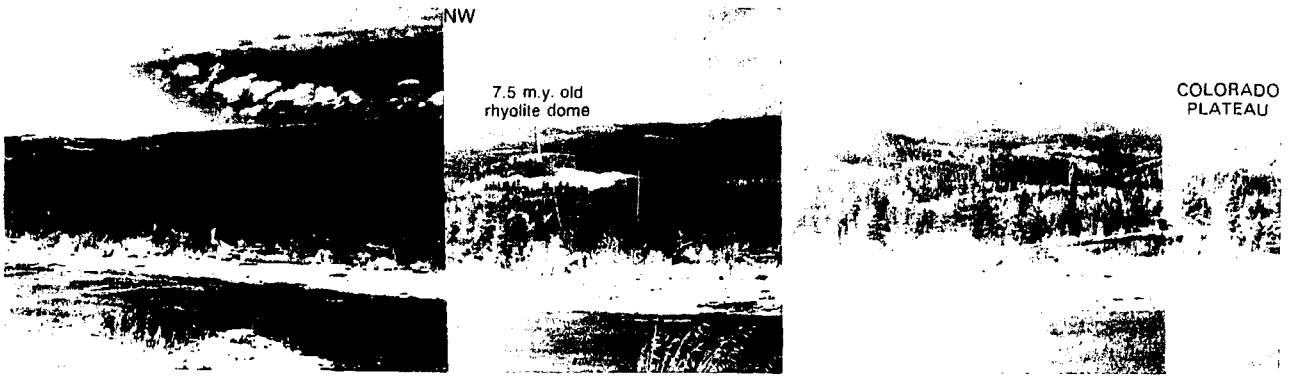

FIGURE 32—Panorama from Stop 2A of the northern Jemez

et al., 1986; Heiken et al., 1986), which are hidden behind the Cerro Toledo Rhyolite domes and the Bandelier Tuff. **0.4**

32.0 **Turn right** onto FR-27. Clot-rich Tschicoma dacite extends for the next 1.9 mi. **0.7**

32.7 **STOP 3. Clot-rich dacite.** Park at junction with minor road to right. Mafic clots are common in dacites of the Tschicoma Formation, but they are rarely as large or as abundant as they are in this unit (P79, Table 5). These clots have generally been interpreted as remnants of quenched mafic magma that was mixed into a more silicic host (Eichelberger, 1980). This clot-rich unit, dated at 4.2 Ma, is one of the major dacite flows from the precaldera highlands.

Continue to left (northwest). **1.8**

34.5 **STOP 4. Dome of early rhyolite** (7.5 Ma; Loeffler et al., 1988). This rhyolite (P8, Table 5) is unusual in that it contains phenocrysts of plagioclase, biotite, and edenitic amphibole, but not quartz or alkali feldspar. The compositions of these phenocrysts (Fig. 30) are similar to those of Tschicoma dacites. Another rhyolite plug (Intermediate Rhyolite, 5.8 Ma old) occurs 2 km to the southeast, and the El Rechuelos Rhyolite domes (2.0 Ma) lie a few kilometers to the east and northeast (Stop 6). Each of these three rhyolites is chemically and petrographically distinctive, but all three appear to have originated from mafic magmas with little crustal assimilation (Loeffler et al., 1988). **0.8**

35.3 Road crosses onto the Tshirege Member of the Bandelier Tuff, which extends for the next several miles. **8.5**

43.8 **Turn left** onto small track. **0.8**

44.6 **STOP 5. Overview of western margin of Rio Grande rift** (Fig. 33). The broad valley in the distance is underlain by continental red beds of the Chinle Formation (Triassic). Above it, the Entrada Sandstone and overlying gypsum of the Todilto Formation (Jurassic) form a very prominent white marker unit over wide areas of the Colorado Plateau. The Morrison Formation (Jurassic) forms the slopes and benches above the Todilto. Above the Morrison is the Dakota Sandstone (Cretaceous), which crops out as a cliff-forming unit capping the mesas.

The Entrada and Todilto Formations are visible in the cliffs northeast of Cañones, the small village lying in the valley (foreground). The white rocks cropping out in the canyon walls to the east (right) of Cañones at the same elevation are Abiquiu Formation of late Oligocene to early Miocene age, deposited in broad basins during an early phase of rifting. The bounding faults along which the Abiquiu was displaced downward underlie Cañones. The Bandelier Tuff, capping the mesa to your left, flowed down paleovalleys excavated along these rift-bounding faults. The nearest mesa to the right consists of Tschicoma dacite, with internal structure that indicates flow from the southeast. The farther mesa behind it is capped by El Alto Basalt dated at 2.8 Ma (Manley, 1982).

The ruin of Tsiping, a prehistoric Tewa pueblo, is visible on the mesa capped by Bandelier Tuff to the left. Occupied during the 13th and 14th centuries A.D., Tsiping had over a hundred ground-floor masonry rooms constructed of cut blocks of Bandelier Tuff. A line of "caveate" rooms hollowed out of the soft tuff is visible at the base of the escarpment immediately below the main pueblo. Fifteen or more "kivas" (subterranean ceremonial chambers) were also excavated into the tuff bedrock along the western edge of the pueblo. Tsiping was a fortified village. Protected on the north, east, and west by a vertical escarpment, a high masonry wall protects the site on the south.

Return to FR-27. **0.8**

FIGURE 33—View from Stop 5 of western margin of Rio Grande rift.

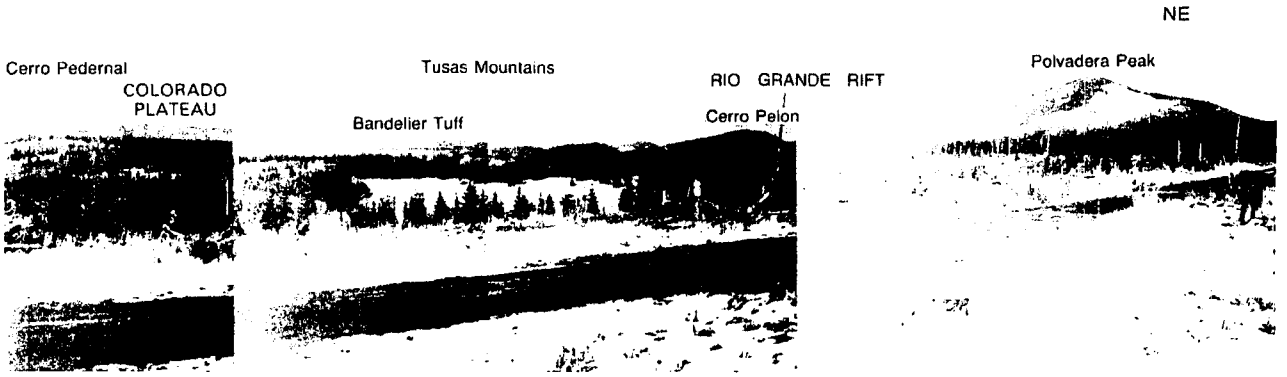

volcanic field and Rio Grande rift/Colorado Plateau margin.

45.4 **Junction** with FR-27. Turn left. **2.1**

47.5 **Junction** with FR-422. Bear left and continue on FR-27. **1.7**

49.2 **Junction** of FR-27 and 427. Bear left on FR-27 for continuation of one-day trip; refer to Segment 2C of road log. Turn right onto FR-427 for Optional Segment 2B.

Optional Segment 2B: El Rechuelos Rhyolite dome

Mileage

0.0 **Junction** of FR-27 and 427. Follow FR-427 (main track) to south (see map, Fig. 34). **4.3**

4.3 **STOP 6. Middle dome of the El Rechuelos Rhyolite (2.0 Ma).** End of road. This is a very fine-grained biotite rhyolite (Fig. 31), which is distinctive from the Early Rhyolite of Stop 4. The El Rechuelos Rhyolite is higher in SiO_2 and K_2O (P22, Table 5) and has lower overall REE contents. Nd- and Sr-isotopic data indicate that the El Rechuelos Rhyolite is derived from fractional crystallization of basalt similar to that of the Lobato "Formation," combined with assimilation of a small amount of lower crust (Loeffler et al., 1988).

Obsidian remnants within the banded perlite are visible along the flanks of the rhyolite dome. Obsidian–perlite associations in the El Rechuelos Rhyolite were used by Friedman and Smith (1958) to study deuterium–hydrogen relations. They deduced that the water in obsidian is largely magmatic, whereas the additional water in perlite is meteoric.

The dacites (3.7–6.6 Ma) across the canyon to the west form an older and lower terrain. The younger dacite flanks of Polvadera Peak (3.1 Ma) lie beneath the El Rechuelos Rhyolite to the east.

Return to FR-27.

Segment 2C: Forest Road 427 to Forest Road 31

Mileage

0.0 **Junction** of FR-27 and 427. Bear left on FR-27. **1.4**

1.4 **STOP 7. Cerrito Chato.** This is a dome, dated at 3.81 ± 0.19 Ma, of hornblende–biotite dacite with minor pyroxene (P99, Table 5). To the north is Cerro Pelon, a younger (2.96 ± 0.27 Ma) dacite vent with

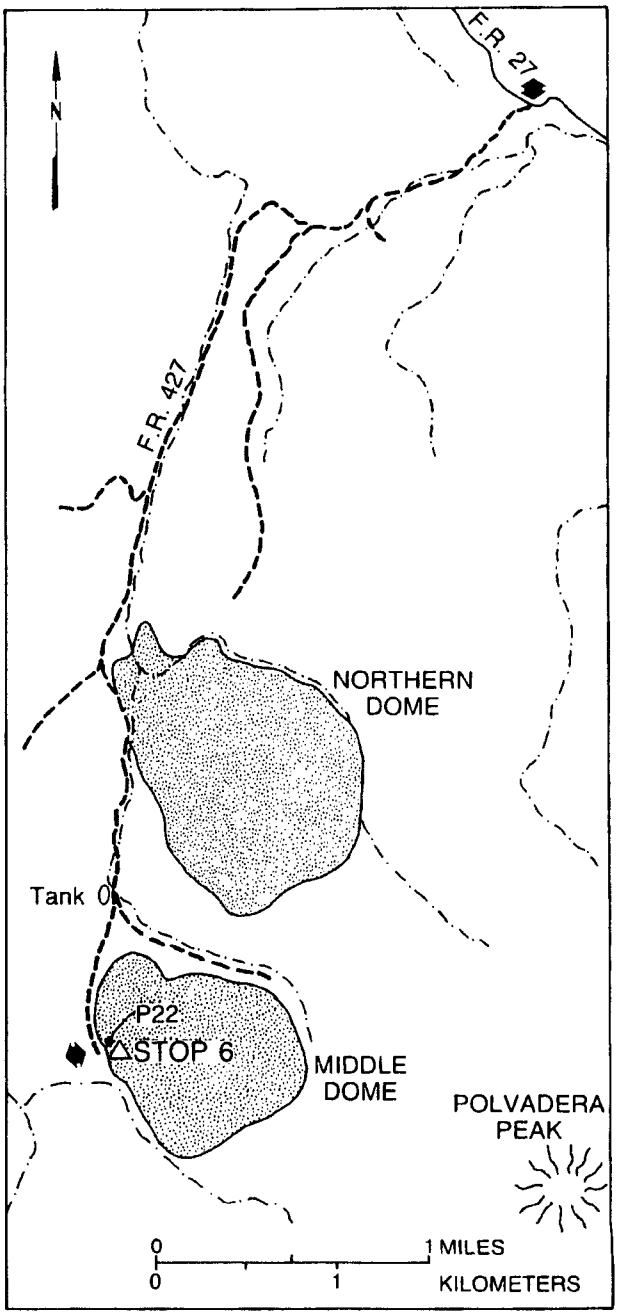

FIGURE 34—Map of Segment 2B of road log.

a well-preserved steep flow lobe emanating from the central crater, which breached to the south. The dacite from Cerro Pelon is similar in composition to that of Cerrito Chato, but contains augite and orthopyroxene with minor hydrous minerals (P71, Table 5). A similar petrographic relationship occurs throughout the younger (3.3–3.2 Ma) Tschicoma Formation: the hydrous mafic minerals which are abundant in the earlier dacites are largely absent from the later. Absence of hydrous minerals from the youngest dacites probably reflects decreasing P_{H_2O} in these magmas. If this difference in water pressure results from evolution of the youngest dacites at the shallowest depths, then the younger eruptions came from chambers at <2 kb (<7 km, assuming $P_{H_2O} = P_{total}$). **2.7**

4.1 Flow of the El Alto Basalt. The El Alto basalts, which include both hypersthene- and nepheline-normative types, were erupted approximately concurrently (3.2–2.8 Ma; Baldridge et al., 1980; Manley, 1982) with young dacite domes of the Tschicoma Formation, such as Cerro Pelon (Stop 7).

Junction of FR-27 and FR-31 (Vallecitos Road). Turn left for continuation of one-day trip; refer to Segment 2E of road log. Turn right for Optional Segment 2D.

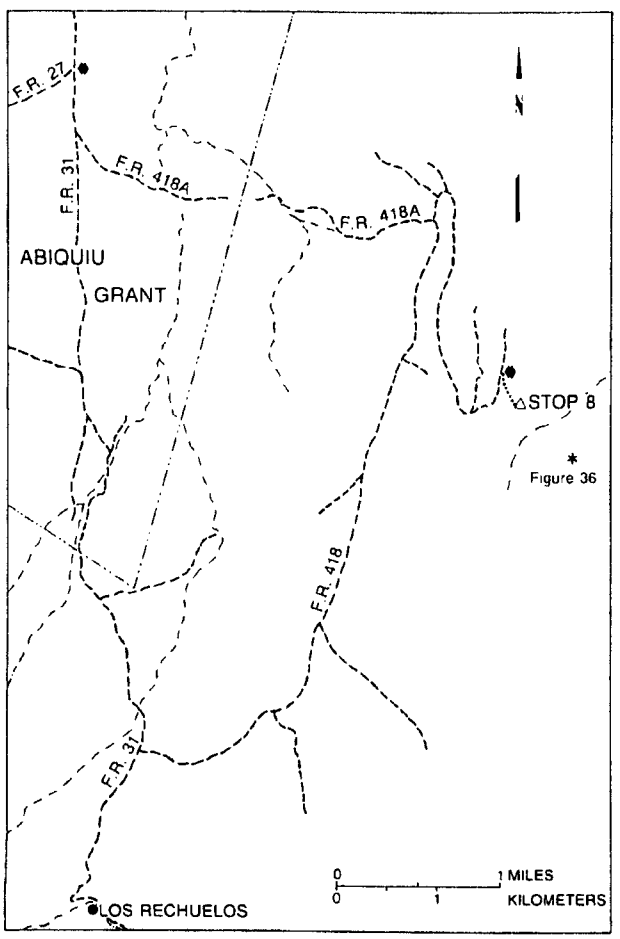

FIGURE 35—Map of Segment 2D of road log.

Optional Segment 2D: Lobato Mesa

Mileage

0.0 **Junction** of FR-27 and 31 (Vallecitos Road). Proceed south (see map, Fig. 35). **4.1**

4.1 **Junction** of FR-31 and FR-418. Turn left. **4.3**

8.4 **Junction** with FR-418A. Turn right and continue bearing to right (south). Road ascends fault scarp. **2.1**

10.5 **STOP 8. Lobato basalt and overview of the Rio Grande rift.** Park along edge of meadow. Walk 0.3 mi to the south-southeast along ridge crest and descend approximately 100 ft to view point. The flow exposed along this ridge is hawaiite, dated at 9.2 ± 0.2 Ma (P487, Table 5). It is typical of the youngest flows on Lobato Mesa, which in general are slightly more evolved than most of the Lobato "Formation" on Lobato Mesa. The source of this flow was a broad vent 3.3 km to the north-northwest, which was subsequently downfaulted some 130 m relative to the block on which this stop is located. The platy structure which characterizes this flow and other hawaiites of the Lobato "Formation" probably resulted from alignment of plagioclase microlites during flow.

Across the canyon to the south, a section of more than 30 flows is exposed (Fig. 36). These flows consist of fine-grained, olivine-phyric tholeiitic basalt of fairly uniform composition. The lowermost flow (P430) is dated at 10.8 ± 0.3 Ma and an upper flow (P465) at 10.1 ± 0.3 Ma. We interpret these flows to be part of a shield cone (La Sotella shield), the central vent of which was located on the ridge crest 1 km west of the exposure. Evidence for a shield structure comes mainly from topography and from the uniformity of basalt compositions, both vertically and areally. Subsequent faulting displaced these flows 120 m upward relative to the vent. The central vent was bisected by a normal fault. The western half was displaced at least 190 m downward and is now buried beneath the alluvium in the small valley west of the fault scarp. The La Sotella shield cone is one of a small number of shield vents from which basalts of the Lobato "Formation" were erupted.

To the east is an excellent overview of the Española Basin. The Sangre de Cristo Mountains in the far distance mark the eastern side of the Rio Grande rift. The rift is filled dominantly with continental sediments of the Miocene Santa Fe Group, which in the foreground consist mainly of aeolian sands (Ojo Caliente Sandstone Member of the Tesuque Formation; Galusha and Blick, 1971; Dethier and Manley, 1985). In the middle distance is Black Mesa, capped by a 2.8 ± 0.4 Ma (Manley, 1976) basalt flow that was erupted from the Taos volcanic field and flowed down the channel of the ancestral Rio Grande.

Return along same route to FR-31.

Segment 2E: Forest Road 27 to US-84

Mileage

0.0 **Junction** of FR-27 and FR-31 (Vallecitos Road). Proceed north. **3.1**

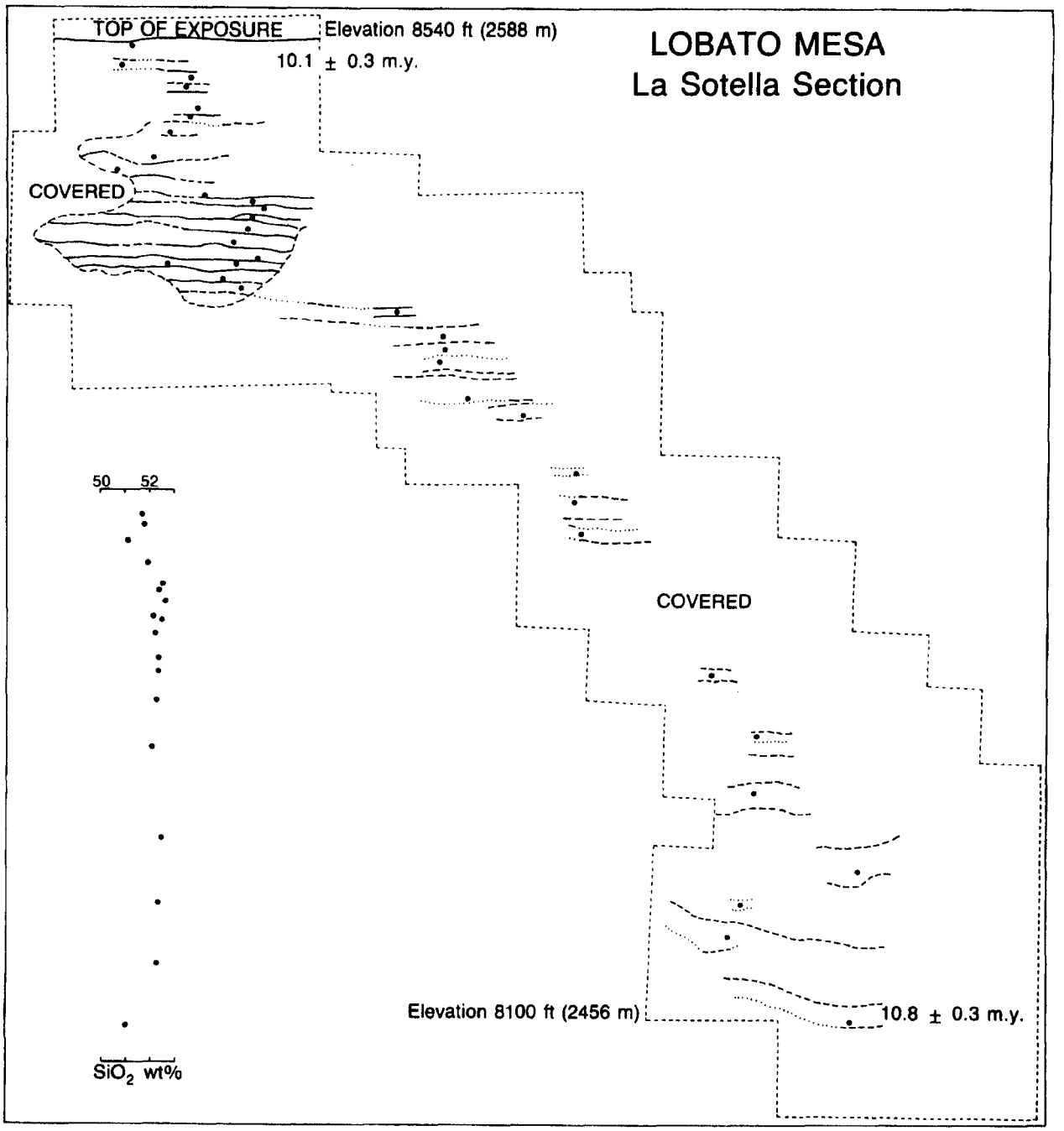

FIGURE 36—Section through La Sotella basaltic shield cone as seen from Stop 8, showing individual lava flows (where discernible). Fault somewhere near base of section duplicates lower part of section. Dots show sample location. Dashed line is limit of photomap base. Inset: SiO_2 composition of flows (only alternate flows analyzed). Location of Fig. 36 is shown in Fig. 35.

3.1 Flow of El Alto basalt. This hawaiite flow (F212, Table 5), which extends 6 km to the northeast, flowed down the ancestral channel of Abiquiu Creek. It now caps Mesa de Abiquiu, which at its northern end is 224 m above Abiquiu Creek and the Rio Chama. This flow, K–Ar dated at 3.2 Ma (Baldridge et al., 1980), contains xenoliths of pyroxenite and megacrysts of plagioclase and orthopyroxene (Baldridge, 1979). **0.6**

3.7 **Ford** Abiquiu Creek and turn right. Sediments of the Santa Fe Group are exposed along the sides of this canyon. Lobato basalts cap the mesa to the left; the Mesa de Abiquiu flow (El Alto) is on the right. **3.1**

6.8 **Bear left. 0.8**

7.6 **Junction** with US-84. Turn right and drive about 36 mi to Los Alamos.

Third-day road log: Bandelier Tuff, Valles caldera, and resurgent dome

Summary—The route of the third day will begin with a distal view of the Bandelier Tuff (Smith and Bailey, 1966) and will progress toward the rim and center of Valles cal-

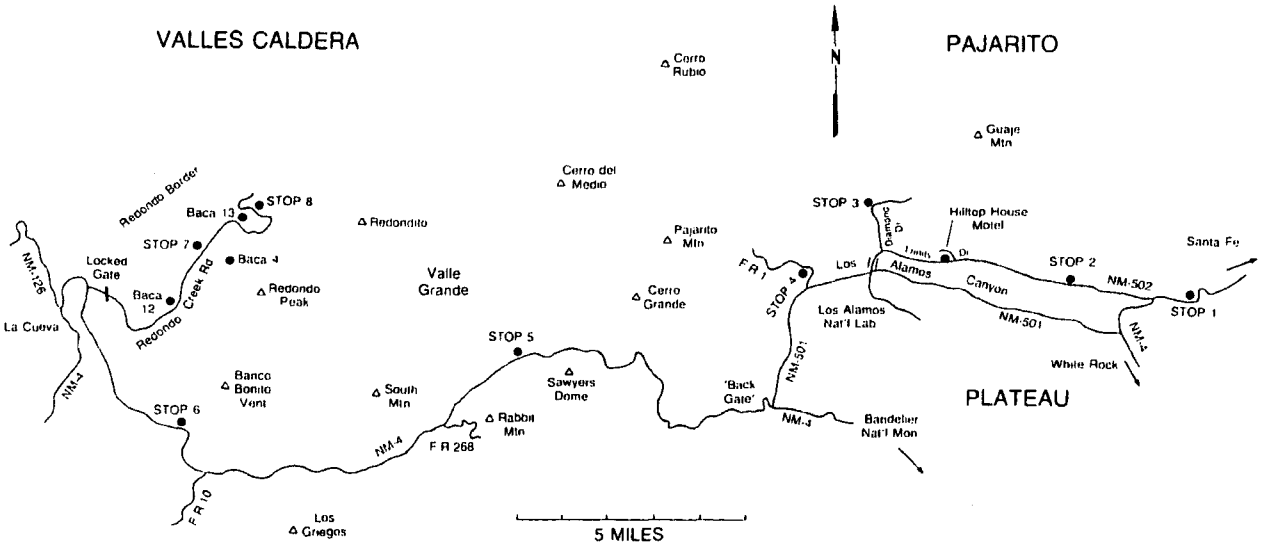

FIGURE 37—Route map, Day 3.

dera. The ignimbrites will appear more welded with each stop and we will have an opportunity to look at some base-surge deposits. Within the caldera we will discuss early and present models of caldera development and structure, look at the youngest moat rhyolites, and wander into the Redondo Peak resurgent dome. From within the Redondo Creek graben we will begin our detailed discussion of the intracaldera stratigraphy, structure, hydrothermal system, and alteration.

Mileage

0.0 Hilltop House parking lot at the junction of NM-502 (Trinity Drive) and Central Avenue, Los Alamos. Drive east on NM-502. In the distance (east) are the Sangre de Cristo Mountains forming the east flank of the Rio Grande rift. **3.3**

3.3 Clinton P. Anderson Memorial Overlook. The cliffs are composed of the Tshirege Member of the Bandelier Tuff. Cerro Toledo Rhyolite tuffs and the Otowi Member of the Bandelier Tuff are mostly buried by talus. Pink, sculptured sediments of the Rio Grande rift can be seen in the middle distance between the mesas. These sediments are part of the Santa Fe Group of Miocene age. **1.1**

4.4 Junction with NM-4; continue straight ahead (east). **0.9**

5.3 **STOP 1. Guaje Pumice and late Tertiary stratigraphy.** Park in large turn-out, right side of highway. Guaje Pumice Bed of the Otowi Member of the Bandelier Tuff overlies 2.4 Ma basalt in roadcut on left (Fig. 38). Note soil developed on top of basalt. In the slopes and cliffs above the basalt, about 100 m of Bandelier Tuff is exposed. The Guaje Pumice Bed is about 7 m thick here, but the bed is commonly as much as 10 m thick on the east side of the mountains. Underlying the slopes and exposed in gullies to the base of the cliffs are about 50 m of nonwelded Otowi ash flows. At the base of the cliffs is 1 m of fine-grained ash fallout of the Tsankawi Pumice Bed of the Tshirege Member, and above are 50 m of partly welded Tshirege ash flows. In the upper 30 m of columnar-jointed tuff, at least eight distinct flow units separated by sandy partings and pumice concentrations are discernible.

Rocks exposed in lower Los Alamos Canyon are typical of sequences along the length of White Rock Canyon. They record interfingering stratigraphic re-

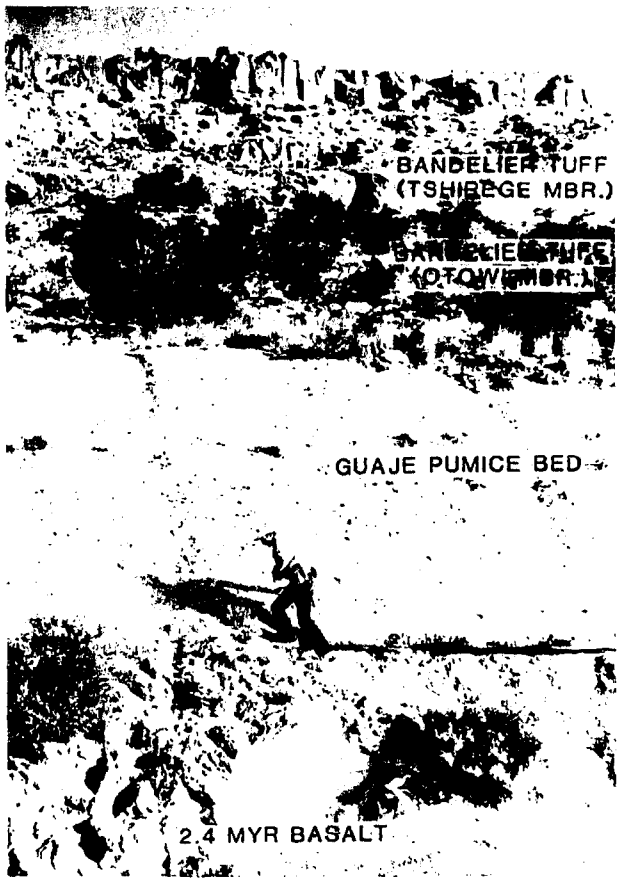

FIGURE 38—Photo of the Guaje Pumice (1.45 Ma), the ash-fall unit at the base of the Otowi Member, Bandelier Tuff. The pumice bed overlies, a thin soil horizon, lake deposits and olivine basalt and pillow breccia (2.4 Ma) of the Cerros del Rio volcanic field.

lations between lavas and tuffs of the Cerros del Rio volcanic field with rift-basin sedimentary units (especially those derived from the Jemez volcanic field), regional tilting, uplift, and erosion of the Española Basin in the late Cenozoic, and the Quaternary pyroclastic deposits erupted from the Valles and Toledo calderas. Locally, there were interactions between magma and meteoric/surface waters resulting in phreatomagmatic tuff rings; lava flows erupted within the course of the ancestral Rio Grande repeatedly dammed it to produce lakes in which lacustrine-deltaic sedimentary sequences were deposited. The geology of the small area included in Fig. 39 illustrates this complex history.

Sedimentary units of the lower Puye Formation (Waresback, 1986) comprise a volcaniclastic apron shed from the northeastern margin of the Jemez volcanic field. The roadcuts along NM-502 expose coarse debris-flow and fluvial facies (plus minor tuff and lacustrine facies) containing a high proportion of Tschicoma andesite to dacite clasts. The Totavi Formation, which underlies the Puye Formation, is similar but also contains a significant fraction of Precambrian clasts, carried southward by the ancestral Rio Grande. Transport directions of fluvial-sediment systems were dominantly south-southeast. The debris-flow dominated unit (Ts1) is abruptly succeeded in this area by a lacustrine sequence (Ts2) that overlies an erosion surface and grades upward from dark, thinly laminated silts, through lighter colored sandy beds, to fluvial gravels with southerly transport directions and dominantly Precambrian clasts (derived from reworking of the Totavi). This sequence records the damming of the ancestral Rio Grande and filling of the consequent lake basin. The basalt flow that formed the drainage obstruction is exposed to the southeast on the rim of Los Alamos Canyon. The paleotopography of the lake basin is recorded by the geometry of this sediment package, which thins to the east, north, and west from a maximum local thickness of 30 m.

At 2.4 Ma (Baldridge, 1979), a basaltic eruption west of the map area produced a lava flow and associated dark-green, thinly laminated basaltic tuff

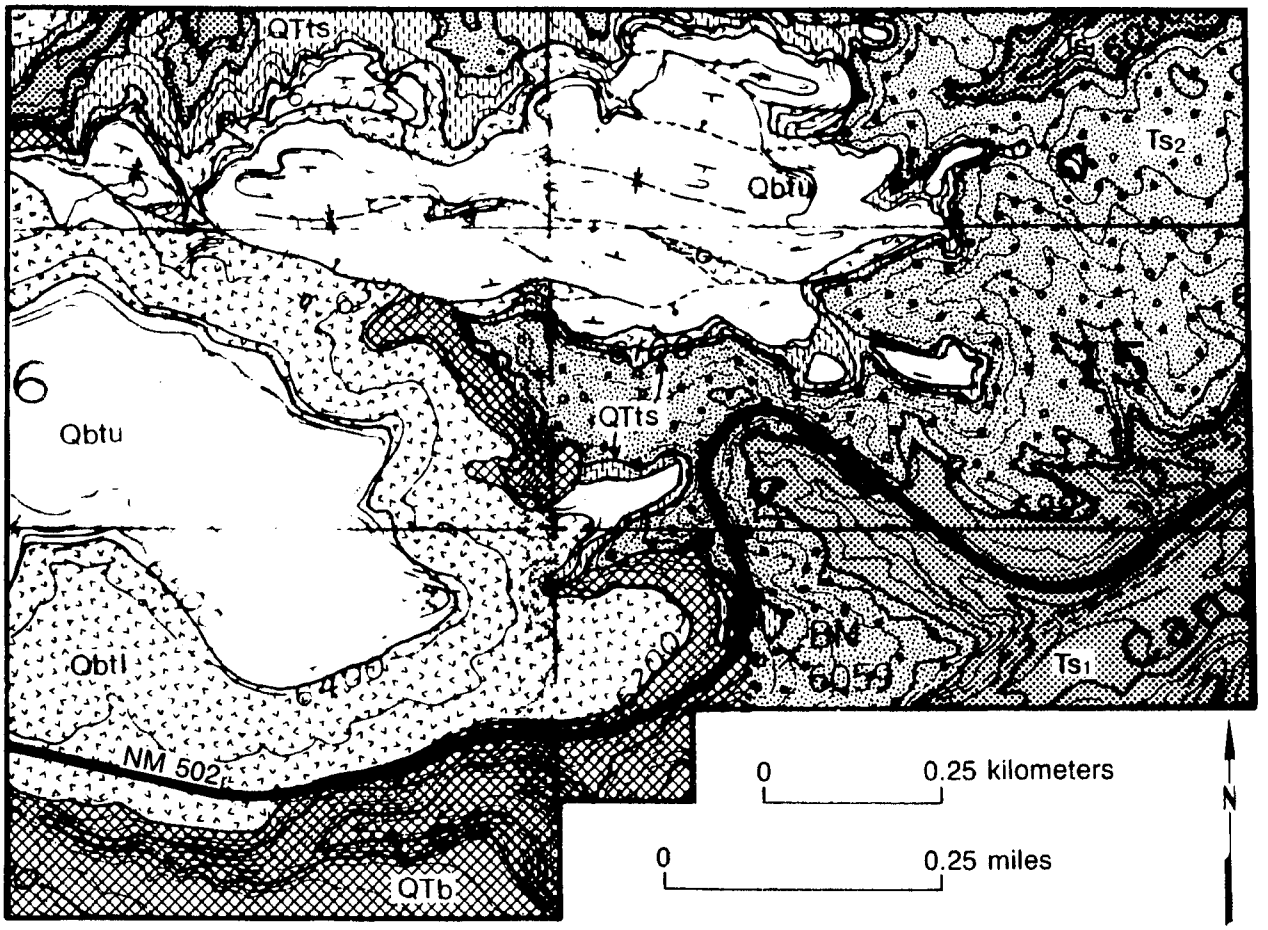

FIGURE 39—Detailed geologic map of northern rim Los Alamos Canyon. Map units: Ts1 and Ts2 = informal units of Puye Formation (volcaniclastic facies of the Tschicoma Formation, Polvadera Group). The lower unit (Ts1) consists of coarse debris flows, tuffs, and fluvial sediments dominated by material derived from contemporaneous Tschicoma andesite and dacite volcanic constructs to the west. The upper unit (Ts2) is an upward-coarsening, lacustrine silt to fluvial pebble-conglomerate sequence deposited in a lake basin. QTb = basalt lava flow and pillow breccia, locally forming well-developed east-dipping foreset beds (vent located 1 mi west). QTts = tuffaceous sedimentary units related to eruption and subaqueous emplacement of basalt QTb. A basaltic tuff (0.2–3 m), locally fluvially reworked, has been overridden by the basalt and associated pillow breccia. Lava and tuff are overlain by green lacustrine silt (gypsum-bearing) deposited in lake basin dammed by the basalt (QTb). Qbtl and Qbtu = Otowi and Tshirege Members of the Bandelier Tuff. Dips in slumped and tilted Bandelier Tuff in northern part of the map area are 15–25°.

(<1 m) that spread across a braided-stream system in the map area. Where the basaltic ash was deposited within channels, it was reworked, mixed with clastic sediment, and filled these paleochannels to thicknesses >3 m. As the basalt flow moved eastward it overrode the tuff, which exhibits both brittle and soft-sediment deformation (see roadcut exposures near water tank). The river became dammed to the south by the lava and the flow front became a pillow-palagonite delta. Eastward-dipping foreset beds of this delta are spectacularly exposed in Los Alamos Canyon south of the water tank. Ashy sediment, forming the green lacustrine shale unit, filled the lake to a level which locally topped the lava flow.

The Bandelier section is in place where it rests on the basalt flow, but northeast of the flow front it is thinned by erosion of the Otowi Member prior to eruption of the Tshirege Member and it is allochthonous, having slumped extensively. The green lacustrine shales have acted as a highly deformable decollement; the underlying basaltic tuff is virtually undeformed by post-Bandelier slumping.

Turn around and go west on NM-502. **0.8**

6.1 Junction with NM-4; return toward Los Alamos on NM-502. **2.0**

8.1 **STOP 2. Pueblo Canyon and Cerro Toledo Rhyolite tuffs.** Park vehicles in turn-out on right side of road where canyon view fades away. Walk right (north) toward canyon rim. From this vantage point we can look into Pueblo Canyon, named for the many Indian ruins that occur here (Fig. 40). The tip of the near mesa displays a beautiful exposure of Tshirege Member of the Bandelier Tuff (1.12 Ma) overlying bedded air-fall and reworked tuffs of the Cerro Toledo Rhyolite (1.45–1.20 Ma). These in turn overlie Otowi Member of the Bandelier Tuff (1.45 Ma). The "Toledo tuffs" are missing to the left of the scene where the Tshirege Member rests directly on the Otowi. The Toledo tuffs were vented from domes erupted within the Toledo caldera and Toledo embayment (Smith et al., 1970; Heiken et al., 1986; Stix et al., 1988).

Continue west on NM-502. **2.6**

10.7 **Keep left** on NM-502 (Trinity Drive). **0.8**

11.5 Ashley Pond on right; one of the old sites of the Manhattan Project. **0.9**

12.4 **Junction** with Diamond Drive, turn right. **1.2**

13.6 **Turn left** into the parking lot of the Church of Christ and park; backtrack along sidewalk south to cliff face exposed on Diamond Drive.

STOP 3. Surge deposits in the Tshirege Member, Bandelier Tuff. The proximal, welded, upper part of the Tshirege Member here contains beds of pyroclastic surge material with prominent cross-bedding (Fig. 41). Thicknesses of these surge units reach 0.5 m. These units occur in the upper cooling unit of the Tshirege Member, which has a gray color because of welding. The crystal-rich surge beds are intimately related to welded flow units. Sparse lithic clasts of rocks from the Jemez volcanic field occur in the ignimbrite. These surges may be either ground surge deposits left by the passage of flow units or surge layer deposits at the edge of the flows channeled down local drainages (Self et al., 1987). Flow direction was roughly eastward, perpendicular to the outcrop face.

Turn right (south) on Diamond Drive and return toward Los Alamos. **1.2**

14.8 **Junction** with NM-502, continue straight ahead over bridge. **0.4**

15.2 **Junction** with NM-501 (West Jemez Road), turn right. **0.2**

15.4 Main entrance to Los Alamos National Laboratory on left. **1.0**

16.4 Surge deposits in Tshirege Member, Bandelier Tuff on right. **0.2**

16.6 **Junction** with FS-1 (Camp May Road); turn right. **0.3**

16.9 **Keep left** on FS-1. **0.3**

17.2 **STOP 4. Pajarito Plateau overlook. Turn left** into parking lot at top of steep grade. The escarpment below our vantage point marks the Pajarito fault, which extends 50 km along the east side of the Jemez Mountains and is one of the main displacements on the west side of the Rio Grande rift. The Pajarito fault in this area has been intermittently active throughout Pleistocene time. It has displaced 5–4 Ma dacites of the Tschicoma Formation as much

FIGURE 40—View northwest into Pueblo Canyon showing Tshirege Member, Bandelier Tuff, overlying bedded pyroclastic rocks and tuffaceous sediments of the Cerro Toledo Rhyolite. Note that Cerro Toledo Rhyolite has been cut out at left of photo and that Tshirege rests on the Otowi Member.

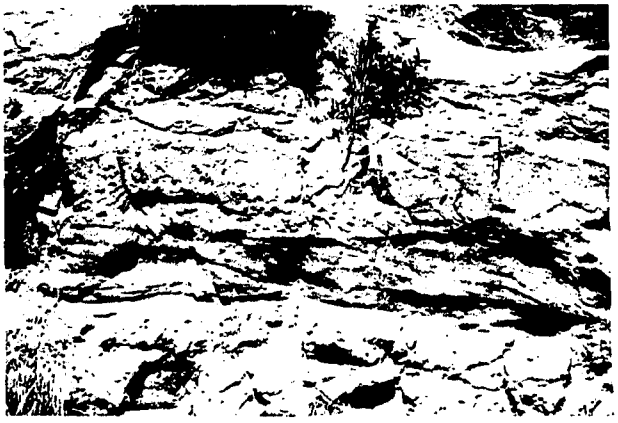

FIGURE 41—Surge beds between flow units of the Tshirege Member, Bandelier Tuff, along Diamond Drive, Los Alamos. Thickness of surge deposit is about 30 cm.

as 300 m and the Bandelier Tuff 100–150 m. Below the escarpment of the Pajarito fault, the Pajarito Plateau stretches eastward. The town of Los Alamos and the Los Alamos National Laboratory sit on the Tshirege Member of Bandelier Tuff on, or adjacent to, several fault strands of the Pajarito fault zone (Gardner and House, 1987). In the near distance is White Rock Canyon, gorge of the Rio Grande, and just beyond are the Cerros del Rio, composed of Pliocene and Pleistocene basaltic rocks that are covered locally by distal Bandelier Tuff. On the skyline are the Sangre de Cristo Mountains which border the east side of the Rio Grande rift.

Ignimbrites blanket the southwest segment of the Española Basin, one of the sedimentary basins of the Rio Grande rift. The Española Basin is asymmetric in configuration; being deepest on the west, next to the Pajarito fault and becoming shallower to the east. Depth to Precambrian basement just east of the escarpment is estimated to be about 3.5 km. A 3–7 ω-m resistivity low between 2 and 3 km depth adjacent to, and east of, the fault suggests that warm and/or saline fluids exist in Paleozoic–Mesozoic rocks, probably Madera Limestone above basement (Goff and Grigsby, 1982). Many seismic reflectors of continuous horizontal extent above the basement interface also suggest as much as 1.5 km of Paleozoic–Mesozoic rocks. Tertiary fill is estimated to be roughly 1400 m thick overlain by 600 + m of Puye Formation and Bandelier Tuff (Budding, 1978; LANL, unpubl. data, 1979; Williston, McNeal and Associates, 1979).

The Tshirege Member of Bandelier Tuff at this location is densely welded because of proximity to its source in Valles caldera. Pumice fragments are flattened and chatoyant blue sanidine and clear quartz phenocrysts are conspicuous.

The mountainous highlands that flank the eastern margin of the Valles caldera are made up of dacitic to rhyolitic volcanic rocks of the Tschicoma Formation. The Tschicoma Formation in this part of the volcanic field consists of coalescing lava domes with little or no pyroclastic rocks. Individual lava flows can often be recognized by their basal flow breccias and/or zones of dark cryptocrystalline devitrification. The interior of the lava flows is devitrified and in some cases has undergone vapor-phase alteration.

The oldest recognized unit is a thick accumulation of low-Si rhyolites (or rhyodacites) in the Rendija Canyon and Guaje Mountain areas. These rhyolites typically contain 72% SiO_2, 2.60% Fe_2O_{TT}, 120 ppm Rb, and 300 ppm Sr. Phenocrysts make up 11–16% of the rock and include quartz, plagioclase, anorthoclase, sanidine, biotite, sphene, and zircon. Quartz is often wormy and feldspar phenocrysts are characterized by disequilibrium textures. Clots of andesite and dacite and xenocrysts(?) of hornblende, clinopyroxene, and orthopyroxene are minor (<1%) contaminants. A K–Ar age of 4.55 ± 0.22 Ma was obtained for sanidine from the rhyolite (date courtesy of F. W. McDowell, University of Texas, Austin).

The low-Si rhyolite is overlain by two-pyroxene dacites at Pajarito Mountain. These dacites increase in SiO_2 content upsection from 66% to 69% and are relatively potassic (~3% K_2O). These dacites have 10–24% phenocrysts consisting of plagioclase, clinopyroxene, and orthopyroxene. Plagioclase crystals have sieve and skeletal textures. The rims of pyroxene phenocrysts are sometimes altered to hornblende. Xenolithic clots made up of subhedral and interlocking clinopyroxene and othopyroxene are common in these rocks. A K–Ar age of 4.81 ± 0.53 Ma was determined for plagioclase. This age overlaps that for the low-Si rhyolite; thus, the two units were probably erupted in close succession.

Hornblende-bearing dacites crop out at Cerro Grande. These hornblende dacites are chemically and petrographically distinct from the two-pyroxene dacites at Pajarito Mountain. The dacites of Cerro Grande are slightly less siliceous (63–66% SiO_2) than those at Pajarito Mountain. They are also less potassic (2.7 vs. 3.0% K_2O) and more iron-rich (4.3 vs. 3.7% Fe_2O_{TT}). The hornblende dacites contain ~20% phenocrysts, consisting of plagioclase, hornblende, and orthopyroxene. Clinopyroxene is found only in trace amounts. The stratigraphic relations between the hornblende-bearing and two-pyroxene dacites are not known, but a published age of 3.67 Ma (Dalrymple et al., 1967) for the dacites of Cerro Grande suggest they are the younger unit.

The southernmost exposures of Tschicoma Formation occur at Sawyers Dome on the southeast rim of the caldera. Sawyers Dome is made up of hornblende-bearing andesite and dacite. SiO_2 contents of lavas range from 62% near the base of the dome to 66% at the top. The rocks of Sawyers Dome are crystal-rich (32–34% phenocrysts) and have a phenocryst assemblage of plagioclase, hornblende, and minor orthopyroxene. The youthful morphology of the dome suggests an age younger than hornblende-bearing dacites of Cerro Grande. Unfortunately, critical contacts between the two units are covered by Bandelier Tuff.

Turn right on Camp May Road and return to NM-501. **0.6**

17.8 **Turn right** on NM-501. **2.9**

20.7 **Junction** of NM-501 with NM-4 ("Back Gate"); turn right toward Jemez Springs. **0.6**

21.3 Small turnout on left in hairpin turn affords another spectacular view of the Pajarito Plateau. **0.7**

22.0 Pumiceous flow top of Tshirege Member, Bandelier Tuff, on right. **1.2**

23.2 Hornblende-bearing dacite flows of Cerro Grande, Tschicoma Formation, on right. **1.0**

24.2 Frijoles Canyon on left. Thick accumulations of the Bandelier Tuff ponded in this area in a low on the pre-Bandelier topography. **2.4**

26.6 Road to St. Peter's Dome on left. Continue straight ahead on NM-4. **0.8**

27.4 East rim of Valles caldera; descend into Valle Grande. **1.3**

28.7 **STOP 5. Valle Grande overlook into Valles caldera.** Park in turnout on right side of road adjacent to yellow sign. Valles caldera formed 1.12 Ma during catastrophic eruption of approximately 300 km^3

FIGURE 42—Panoramic view of Valle Grande looking northwest toward the resurgent dome of Redondo

of ignimbrite of the Tshirege Member, Bandelier Tuff. By comparison, the amount of ash released during the May 1980 eruptions of Mt. St. Helens is estimated at <2 km^3. From this vantage (Fig. 42) we can gaze across Valle Grande, the eastern section of the caldera "moat," toward the broad mountain of Redondo Peak (3460 m) forming the eastern segment of the resurgent dome. This segment is really a northeast-trending ridge that includes the knob of Redondito (see Figs. 7 and 18 for geology and geomorphology). The resurgent dome is composed primarily of densely welded Bandelier Tuff that was uplifted during postcaldera tumescence of the volatile-depleted Bandelier magma chamber (Smith and Bailey, 1968; Smith, 1979). Dips on foliations in the ignimbrite are generally south to southeast on the Redondo Peak segment of the dome. The relations between the tilted ignimbrites of the resurgent dome, overlying volcaniclastic rocks and lacustrine deposits, and postcaldera rhyolites indicate that resurgence probably occurred within 50–100 Ka after caldera formation (Doell et al., 1968; Smith et al., 1970; Hulen et al., 1987).

Visible postcaldera, ring-fracture rhyolites of the Valles Rhyolite that partly surround the resurgent dome are Cerro del Medio (1.04 Ma), Cerro del Abrigo (0.89 Ma), Cerro Santa Rosa (0.88 Ma), Cerro la Jara (0.50 Ma), and South Mountain (0.49 Ma). These rhyolites range from crystal-poor (Cerro del Medio) to coarsely porphyritic (South Mountain), but all are high-silica rhyolites (e.g., San Antonio Mtn. Rhyolite, Table 1). Geochemical data presented by Spell (1987) indicate that they were derived from Bandelier parental magma.

Geothermal development and the cooperative agreement between UNOCAL and the U.S. Department of Energy have provided drill-hole and geophysical data that give us an interesting picture of subsurface caldera structure. The gravity model of Segar (1974) indicates the floor of the caldera is very asymmetrical, being shallow on the west and deep in the east (Fig. 9); this model is verified by drill-hole data in the western and central caldera. The model also indicates a series of steep, northeast-trending gravity gradients that are probably precaldera structures inherited from the Rio Grande rift (Goff, 1983; Nielson and Hulen, 1984; Heiken et al., 1986; Aldrich, 1986). Depth to Precambrian basement west of the ring-fracture zone beneath Valle Grande is estimated at 5000 m.

If you look northwest between the extension of the resurgent dome and Cerro del Medio, you can see the northwest wall of the caldera (about 18 km distant) formed primarily of Tschicoma Formation dacites overlying hydrothermally altered Paliza Canyon Formation andesite and dacite. The caldera wall immediately to our right is formed of Tschicoma Formation, but to our left is formed mostly of Paliza Canyon Formation. The exception is Rabbit Mountain (1.43 Ma), part of the Cerro Toledo Rhyolite that was vented after formation of Toledo caldera (1.45 Ma).

Several lines of evidence indicate that the Toledo caldera, which erupted 300–400 km^3 of the Otowi Member, Bandelier Tuff, is coaxial with the Valles caldera. This evidence includes isopachs on the Guaje Pumice Bed (Self et al., 1986), radial distribution of the Otowi Member around the present Valles caldera (Smith et al., 1970), flow-direction indicators in the Otowi Member (Potter and Oberthal, 1983), an arc of post-Toledo-age rhyolite domes exposed in the northern moat of Valles caldera (Goff et al., 1984), and the thick sequence of Otowi Member beneath the Valles resurgent dome (Nielson and Hulen, 1984). The feature denoted as Toledo caldera on the northeast margin of Valles caldera by Smith et al. (1970) represents some other structural feature (see Self et al., 1986, and Heiken et al., 1986) and has been renamed the Toledo embayment (Goff et al., 1984).

Continue southwest along NM-4. **3.9**

32.6 Sheeted, devitrified core of South Mountain rhyolite flow on right. **1.9**

34.5 Several outcrops of bedded ash-fall tuff (El Cajete Pumice) are exposed for the next 2 mi. They comprise the only extensive postcaldera ash-fall eruption in the Jemez Mountains. **1.5**

36.0 View of Tshirege Member, Bandelier Tuff, along upper west wall of San Diego Canyon in far distance. **2.2**

38.2 **Cross** East Fork of the Jemez River. **0.2**

38.4 **STOP 6. Southern moat-rhyolite stratigraphy.** Park along left side of road near head of short grade. Exposed in downward succession in roadcut (Fig. 43) are three members of the Valles Rhyolite: (1) vitrophyric blocks of colluvium of the Banco Bonito Rhyolite, (2) well-bedded ash-fall tuff and ignimbrite of the El Cajete Pumice, and (3) a coarsely porphyritic flow of South Mountain Rhyolite.

The Banco Bonito Rhyolite is the youngest erup-

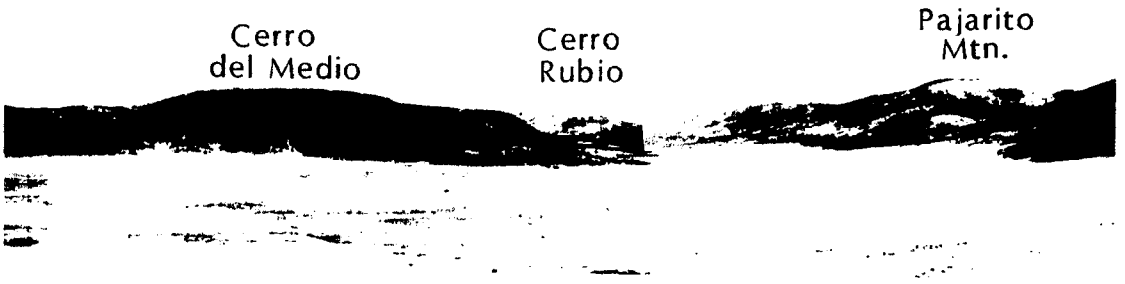

Peak and northward toward the northern moat rhyolites and Cerro Rubio, in the Toledo embayment.

tion in Valles caldera (0.13 Ma; Marvin and Dobson, 1979) and forms a 7 km long sequence of four flow units that filled a paleovalley in the southern moat of the caldera (Manley and Fink, 1987; Goff et al., 1986). The El Cajete Pumice (0.15 Ma) fills in topography on the South Mountain Rhyolite at this location but the main dispersal direction of the pumice and ash was to the southwest (Self et al., 1988). El Cajete Pumice is easily distinguished from Bandelier pumice because the latter does not have obvious, visible biotite phenocrysts but does have chatoyant-blue sanidine phenocrysts. South Mountain Rhyolite (0.49 Ma) is very frothy and perlitic at this locality. The Banco Bonito Rhyolite, El Cajete Pumice, and Battleship Rock Tuff are considered to be one co-magmatic suite of rhyolites according to Self et al. (1988), but see discussion at Stop 5, Day 4.

Two previously unrecognized moat rhyolites were discovered during drilling of CSDP corehole VC-1, located about 4 km west of here (Goff et al., 1986). One is named the VC-1 Rhyolite, a slightly porphyritic obsidian (0.365 Ma), and the other is named the VC-1 Tuffs, which consist of three flow units of lithic-rich ignimbrite (<0.49 but >0.365 Ma). South Mountain Rhyolite, VC-1 Tuffs, VC-1 Rhyolite, Battleship Rock Tuff, and Banco Bonito Rhyolite fill a paleocanyon in the southern caldera moat that was 335 m deep (Goff et al., 1986; Hulen and Nielson, 1988a).

FIGURE 43—The bedded ash-fall and ash-flow deposits of the El Cajete Member of the Valles Rhyolite overlie erosional topography on South Mountain Rhyolite and underlie colluvium of porphyritic obsidian of the Banco Bonito Member.

Compositionally, the youngest moat rhyolites composed of the VC-1 Tuffs, VC-1 Rhyolite, Battleship Rock Tuff, El Cajete Pumice, and Banco Bonito Rhyolite are distinct from other members of the Valles Rhyolite because the former have less SiO_2 but more Fe_2O_3 (total), MgO, CaO, and P_2O_5 (water-free basis, see Table 1) (Gardner et al., 1986). The youngest moat rhyolites also have relatively low $^{87}Sr/^{86}Sr$ compared to other Valles rhyolites (see Vuataz et al., 1988). Thus, the youngest moat rhyolites are probably not derived solely from the Bandelier magma chamber. According to Ankeny et al. (1986), the southern moat zone appears to be the best location for a present (liquid) magma chamber and the geothermal features of the caldera are focused toward the southwest quadrant of the caldera (Sass and Morgan, 1988).

Continue west on NM-4. **1.0**

39.4 Road ascends onto top of Banco Bonito Rhyolite (0.13 Ma). **1.8**

41.2 **Junction** with FR-1850 on left; CSDP corehole VC-1 is 0.8 mi (1.3 km) south from this point on FR-1850. **1.2**

42.4 **Turn right** on Redondo Creek road. **0.7**

43.1 Locked gate to Baca Land and Cattle Co. **NOTE: Access by special permission only; do not trespass.** Continue only if on approved field trip. **0.3**

43.4 Banco Bonito Rhyolite on right. South edge of resurgent dome on left. **0.8**

44.2 Redondo Flats, a valley formed at the mouth of the Redondo Creek graben, on right. **0.7**

44.9 Enter Redondo Creek graben. Redondo Peak on right, Redondo Border on left. **0.9**

45.8 Well pad to Baca-12 on left. This was the deepest well in the old Baca geothermal lease of UNOCAL, reaching a depth of 3211 m and bottoming in hydrothermally altered Precambrian granite. **0.4**

46.2 Old UNOCAL headquarters building on right. **0.9**

47.1 **STOP 7. Redondo Creek graben and Baca-6.** Park along road and walk into clearing bounded by retaining walls on left. This beautiful site was cleared in the early 1980's for construction of a 50 MW(e) geothermal power plant (Fig. 44). UNOCAL intended to sell power to the Public Service Company of New Mexico, but after drilling 24 geothermal wells only 20 MW(e) was proven. The project was terminated in 1984 because of lack of permeability and the threat of lawsuits by various Indian pueblos over water-rights issues (Kerr, 1982; Goldstein and Tsang, 1984). The turbines intended for use at Valles

FIGURE 44—View northeast up the Redondo Creek graben from the former site of Baca-6 well (marked by pole). The gravel embankment and cement retaining wall at the back of the clearing protected the site of the proposed 50 MW(e) geothermal power plant that was never constructed due to permeability problems. Redondo Border, the west segment of the resurgent dome, is at left of photo.

caldera are now in use in the Los Azufries geothermal field, Mexico. In spite of the problems, a few wells in this area are very productive.

The principal zone of geothermal exploration was centered in the Redondo Creek graben that formed in response to stresses developed by uplift of the resurgent dome (Fig. 45). Details of the stratigraphy and structure within this area have been presented by Nielson and Hulen (1984) and are shown in Fig. 10. The steep dips observed to either side of the valley are the result of rotation along listric faults, probably representing a response to topographic instability along the boundary faults of the Redondo Creek graben. Units at depth are nearly horizontal across the crest of the dome.

Drilling results and gravity modeling indicate that the subsurface structure of Valles caldera is considerably different from that postulated by earlier workers (Goff, 1983; Nielson and Hulen, 1984; Heiken et al., 1986) (Fig. 46). The caldera floor is controlled by preexisting structures of the RGR and is much shallower on the west side than on the east side. The thickness of caldera-fill ignimbrites in the Redondo Creek area is approximately three times greater than previously thought based on surface mapping (Smith et al., 1970). Although the caldera is very symmetrical and has a near-perfect ring of moat rhyolites and a central structural uplift, the structural interior of the resurgent dome is more complicated in detail than the model presented in Fig. 45 because of preexisting structures and the presence of the earlier, coaxial Toledo caldera.

Geothermal fluids produced by wells in this area (Table 3) are very typical of volcanic-type geothermal waters the world over (Goff and Grigsby, 1982). They are neutral chloride in character, having about 5000–8000 mg/kg total dissolved solids (TDS) and anomalous concentrations of As, B, Br, Li, etc. Formation temperatures range from about 220 to 300°C depending on depth and location. Both

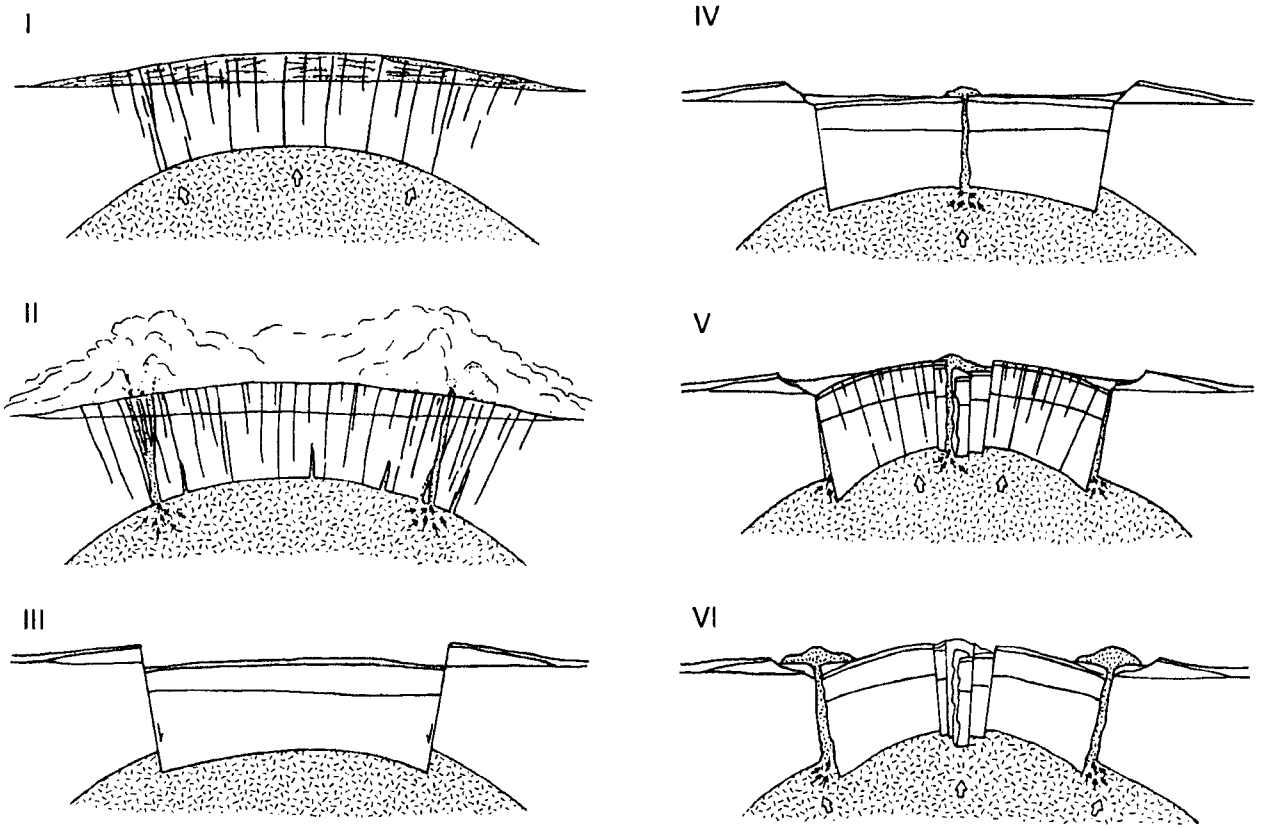

FIGURE 45—The six stages of caldera formation and resurgence according to the model of Smith and Bailey (1968). I. Regional tumescence and generation of ring fractures; II. Caldera-forming eruptions; III. Caldera collapse; IV. Preresurgence volcanism and sedimentation; V. Resurgent doming; VI. Major ring-fracture volcanism.

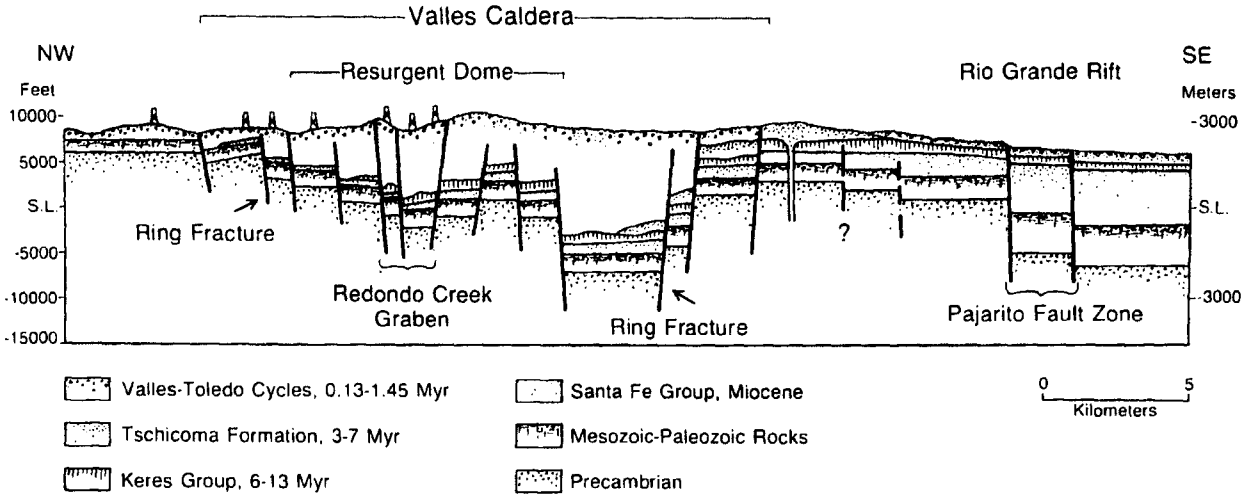

FIGURE 46—Schematic northwest–southeast cross section across Valles caldera based on the stratigraphy of many geothermal wells projected into the plane of the section and the gravity interpretation of Segar (1974); intracaldera volcanic rocks are omitted for clarity. Structure between Valles caldera and Pajarito fault zone is poorly constrained due to paucity of geophysical and drill-hole information. Structure east of Pajarito fault zone is discussed by Goff and Grigsby (1982) and Gardner and Goff (1984). Other interpretations can be seen in the section of Heiken et al. (1986, fig. 7) and in Fig. 17 of this report. See Fig. 10 for a detailed section of the interior of the resurgent dome.

Smith and Kennedy (1985) and Truesdell and Janik (1986) claim that two subtly different fluid types occur in this area. Scaling by calcite and silica was not a problem during any of the flow tests of the wells. A vapor zone about 280 m thick overlies the liquid-dominated system in Baca-6.

Hydrothermal alteration can be observed in the areas excavated for the drill pads and through the woods to either side of the road. Present alteration is acid-sulfate in character and results from small gas seeps along faults of the Redondo Creek graben. The gas seeps and alteration result from subsurface boiling and release of acid gases from the underlying liquid-dominated reservoir. There is no evidence that neutral-chloride hot springs were once present along Redondo Creek.

Rocks exposed along the walls of the graben are primarily Bandelier Tuff with caldera-fill breccias and debris. Redondo Creek Rhyolite, a postcaldera dome, flow, and intrusive complex thought to be about 1.0 Ma, also is found in this area. No intrusive rocks were ever identified in any of the wells drilled in the graben area.

Continue northeast up Redondo Creek. **0.5**

47.6 Altered caldera-fill rocks and fumarole area on left. **0.1**

47.7 **Bear** right. **0.3**

48.0 Road to Baca-13 on left. This well, drilled to a depth of 2472 m, attained a bottom-hole temperature of about 300°C and was one of the best producers in the field. **0.1**

48.1 **Bear** left up hill. **0.2**

48.3 **Bear** left; right fork leads to Baca-4 (280°C, 1915 m), the "discovery well" and also one of the best producers in the field. **0.6**

48.9 Pass at head of Redondo Creek and Jaramillo Creek. Seven dirt roads join here. **Turn left** on main road contouring around hill. **0.4**

49.3 **STOP 8. View of Redondo Peak/Redondo Creek Rhyolite.** Stop along road and be careful of cliff. From this spectacular view point, Redondo Peak and Redondito can be seen to the left (Fig. 47) and

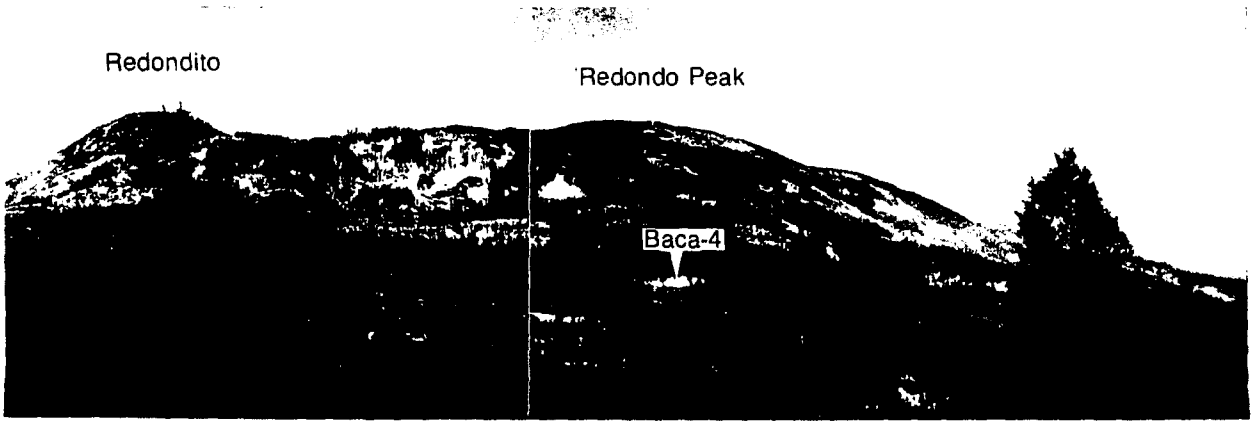

FIGURE 47—Panoramic view looking southeast to south of the east segment of the resurgent dome of Valles caldera; Redondo Peak (3430 m) on right, Redondito on left. The well pad for Baca-4, the "discovery" well of the geothermal system, is shown. The valley in foreground is part of the Redondo Creek graben. Redondo Border, the west segment of the dome, is behind photographer.

Redondo Border to the right. Looking down (southwest) the Redondo Creek graben, we can see the southern moat zone of the caldera, San Diego Canyon, the Jemez Plateau, and the Nacimiento uplift in the far distance.

Although Redondo Creek appears to be the center of resurgent uplift, Redondo Peak is the highest topographic point on the resurgent dome. Stratigraphic work (Nielson and Hulen, 1984) as well as the previously cited gravity study of Segar (1974) demonstrate that the ignimbrite section thickens to the east. It is likely that the higher topography on the eastern portion of the resurgent dome is a manifestation of isostatic uplift of this thicker, low-density tuff section.

Behind us is a small hill of Redondo Creek Rhyolite which has erupted in the graben area between the two creek drainages. Redondo Creek Rhyolite is a formal stratigraphic unit; there are several patches of it mapped in the resurgent dome area that originated from discrete eruptions. It is distinctive in the field because it lacks quartz phenocrysts (all other postcaldera rhyolites have some visible quartz) but has obvious biotite and plagioclase phenocrysts. The unit has been difficult to date by K–Ar because it is usually altered. No dikes or sills of Redondo Creek Rhyolite have been identified in cuttings in the Baca wells.

Continue straight ahead on road. **0.7**

50.0 **Turn around** in junction area of roads and return the way we have come. **1.1**

51.1 **Turn right** and drive down Redondo Creek past Stop 7. **0.6**

51.7 Bear right at junction. **5.3**

57.0 Gate. **0.8**

57.8 **Junction** NM-4; turn left and return to Los Alamos (about 28 mi).

Fourth-day road log: Hydrothermal systems/hot springs

Summary—The fourth day's route returns to Valles caldera to look at some of the hot springs and other geothermal projects besides the earlier Baca geothermal development. These projects include the Continental Scientific Drilling Program, the Hot Dry Rock program, and a small space-heating project at Jemez Springs. Besides providing abundant information on subsurface structure and stratigraphy across the boundary of the caldera, these wells and coreholes have yielded a wealth of information on hydrothermal-fluid compositions, configuration and plumbing of hydrothermal fluids, evolution of the systems with time, and secondary alterations.

Valles caldera contains a variety of hot-spring types (Table 3), although the absolute number of hot-spring sites is relatively small. Included are acid-sulfate hot springs, mud pots, and fumaroles inside the caldera; a ring of dilute, conductively heated hot springs in the caldera moat zone; and neutral-chloride hot springs derived from the deep geothermal reservoirs but located outside the caldera. Recent projects have shown that the Valles hydrothermal system has been active for the last 1 Ma and has deposited molybdenite and other ore minerals.

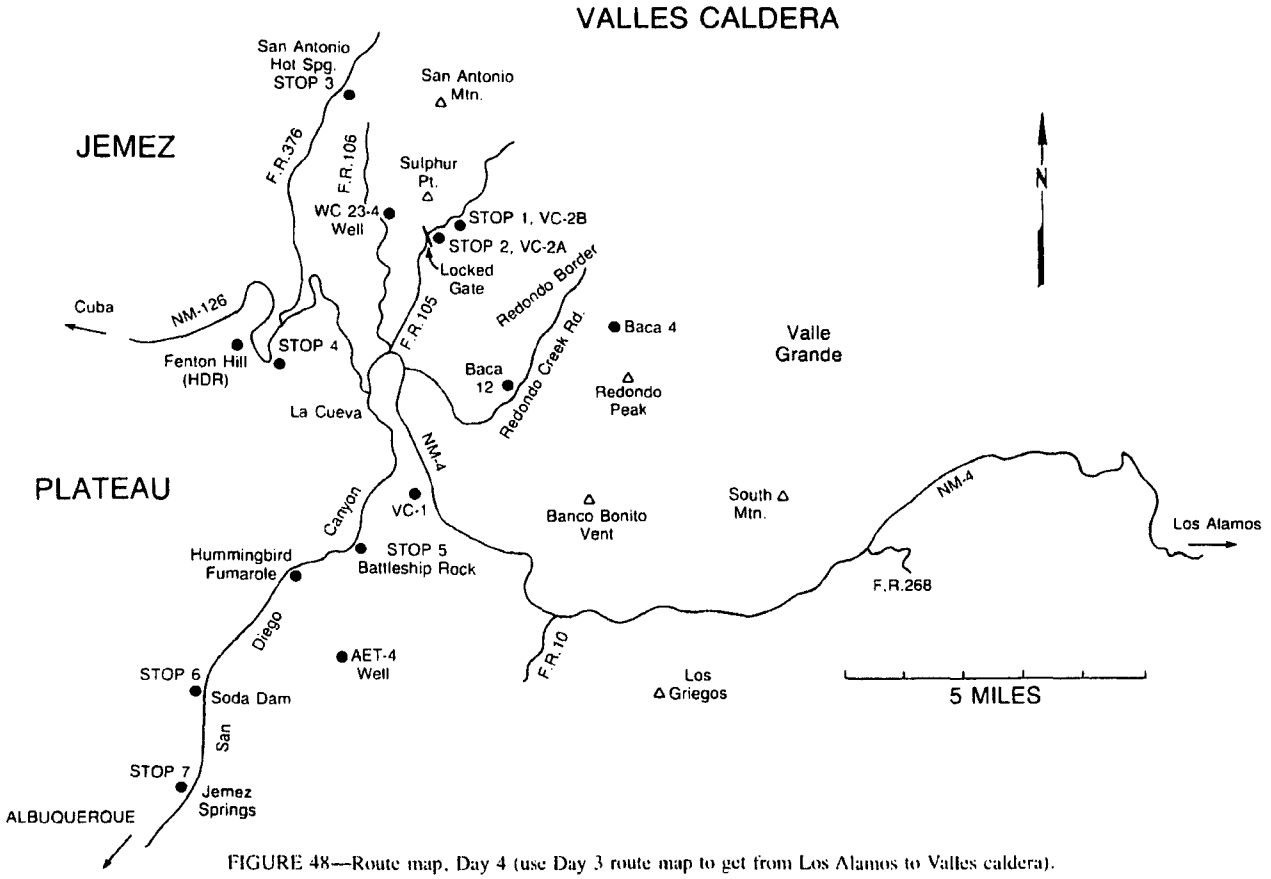

FIGURE 48—Route map, Day 4 (use Day 3 route map to get from Los Alamos to Valles caldera).

Mileage

0.0 Hilltop House parking lot. **Turn right** (west) on NM-502 (Trinity Drive). **1.7**

1.7 **Turn left** on Diamond Drive, cross bridge. **0.4**

2.1 **Turn right** on NM-501. **4.7**

6.8 **Turn right** at the "Back Gate" on NM-4 toward Jemez Springs. Drive into caldera and past the crossings over the East Fork Jemez River. **22.0**

28.8 **Junction** with FR-105. Turn right beyond row of mailboxes toward Sulphur Springs. **0.1**

28.9 Junction with Thompson Ridge Road (FR-106) on left. Continue on FR-105. **1.5**

30.4 Cross bridge over Sulphur Creek, drive past several outcrops of hydrothermally altered rhyolite flows and flow breccias of Redondo Creek Rhyolite. **0.3**

30.7 Locked gate across road to Sulphur Springs. **NOTE: Access by special permission; do not trespass.** Continue only if on approved field trip. **0.7**

31.4 The bleached-out area and the smell of hydrogen sulfide signify the location of Sulphur Springs. Continue straight ahead. **0.4**

31.8 **STOP 1. CSDP corehole VC-2B and Turkey Flats.** Park along the side of road. Walk to right (east) onto grassy meadows. Turkey Flats is a park-like spot in a large landslide complex that occurs on the west side of the resurgent dome of Valles caldera. West of the toe of the slide is the ridge capped by Sulphur Point, which consists of San Antonio Mountain Rhyolite (0.5 Ma) overlying Redondo Creek Rhyolite. The face of the northeast-trending ridge is in part the trace of the Sulphur Creek fault (Goff and Gardner, 1980) along which Sulphur Creek flows. Hydrothermally altered, tectonically brecciated, rhyolite flow breccia is well exposed along Sulphur Creek upstream of our vantage point. Typical alteration minerals are kaolinite, pyrite, silica, iron oxides, and soluble sulfates.

VC-2B is the third continuously cored hole drilled in Valles caldera for the U.S. Continental Scientific Drilling Program (Fig. 49). Objectives of the project were: (1) to penetrate through the main hydrothermal system into a conductive regime between convecting fluids and crystallizing magma, (2) to study structure/stratigraphy near the boundary of the resurgent dome and the western ring-fracture, and (3) to investigate possible ore-deposit mechanisms in a large silicic caldera. VC-2B was cored from July to October 1988 and achieved a total depth of 1762 m (5780 ft) (Fig. 50). Bottom-hole temperature was 295°C as of early November 1988, making this one of the hottest, deepest coreholes in the U.S. VC-2B penetrates a relatively thin caldera-fill sequence at 700 m and then Tertiary Santa Fe Group, Permian Abo–Yeso Formations, Pennsylvanian Magdalena Group, and Precambrian quartz monzonite. Many lost circulation zones indicate that hydrothermal fluids probably exist at all levels. Alteration minerals include quartz, calcite, fluorite, illite, chlorite, epidote, anhydrite, anorthoclase, pyrite, chalcopyrite, sphalerite, pyrargyrite, and rhodochrosite. Scientific investigations have barely begun.

FIGURE 49—Corehole VC-2B during coring operations, July 1988.

The depth to Precambrian basement in VC-2B is 1558 m (5110 ft). Just west of the Sulphur Creek fault, beyond Sulphur Point, the WC23-4 geothermal well hit Precambrian rocks at 737 m (2417 ft); thus, considerable offset occurs along this ring-fracture fault (or fault zone) going east into the caldera depression. Maximum temperature in the WC23-4 well is 233°C at 1890 m (6200 ft); temperature thus decreases noticeably going west out of the caldera depression.

Turn around in wide spots along road and retrace route. **0.4**

32.2 **STOP 2. Sulphur Springs and CSDP corehole VC-2A.** Park along road or on dike to left of road. Do not block traffic. Walk to left (east) toward pond and then walk up road to wellhead. Sulphur Springs was a small resort where people bathed in waters from the springs and mudpots. The resort burned down several years ago and most of the original facilities have fallen to ruin (Fig. 51). The hot springs occur at the intersection of the northeast-trending Sulphur Creek fault and several cross faults (Goff and Gardner, 1980). A variety of thermal features is visible here: fumaroles, hot springs, mud pots, and gaseous cold springs. Temperatures at Sulphur Springs range from background to about 94°C (the boiling point at 2530 m), pH may be less than 1, and SO_4 may be as high as 8000 mg/kg (Table 3). Gases contain 98 mol-% CO_2 and 1.25 mol-% H_2S (dry-gas basis). Empirical gas geothermometry indicates that gases originate from a reservoir at about 215°C, and stable-isotope relations between fumarole steam and meteoric water also suggest about 200°C boiling at depth (Fig. 16) (Goff et al., 1985). Wells drilled in this general area (east of the Sulphur Creek fault) have extremely low formation pressures ($\leq$0.76 MPa) to a depth of about 500 m.

CSDP corehole VC-2A (Fig. 52) was drilled at Sulphur Springs near Footbath Spring in September 1986. Scientific objectives were: (1) to study the vapor zone and its "interface" with the underlying liquid-dominated reservoir, (2) to study structure/stratigraphy, and (3) to study ore-deposit mechanisms (Goff et al., 1987). Technical objectives were to obtain a temperature of at least 200°C and a depth of at least 500 m while obtaining continuous core. VC-2A is 528 m deep and has a BHT of 212°C.

The configuration of the Sulphur Springs hydro-

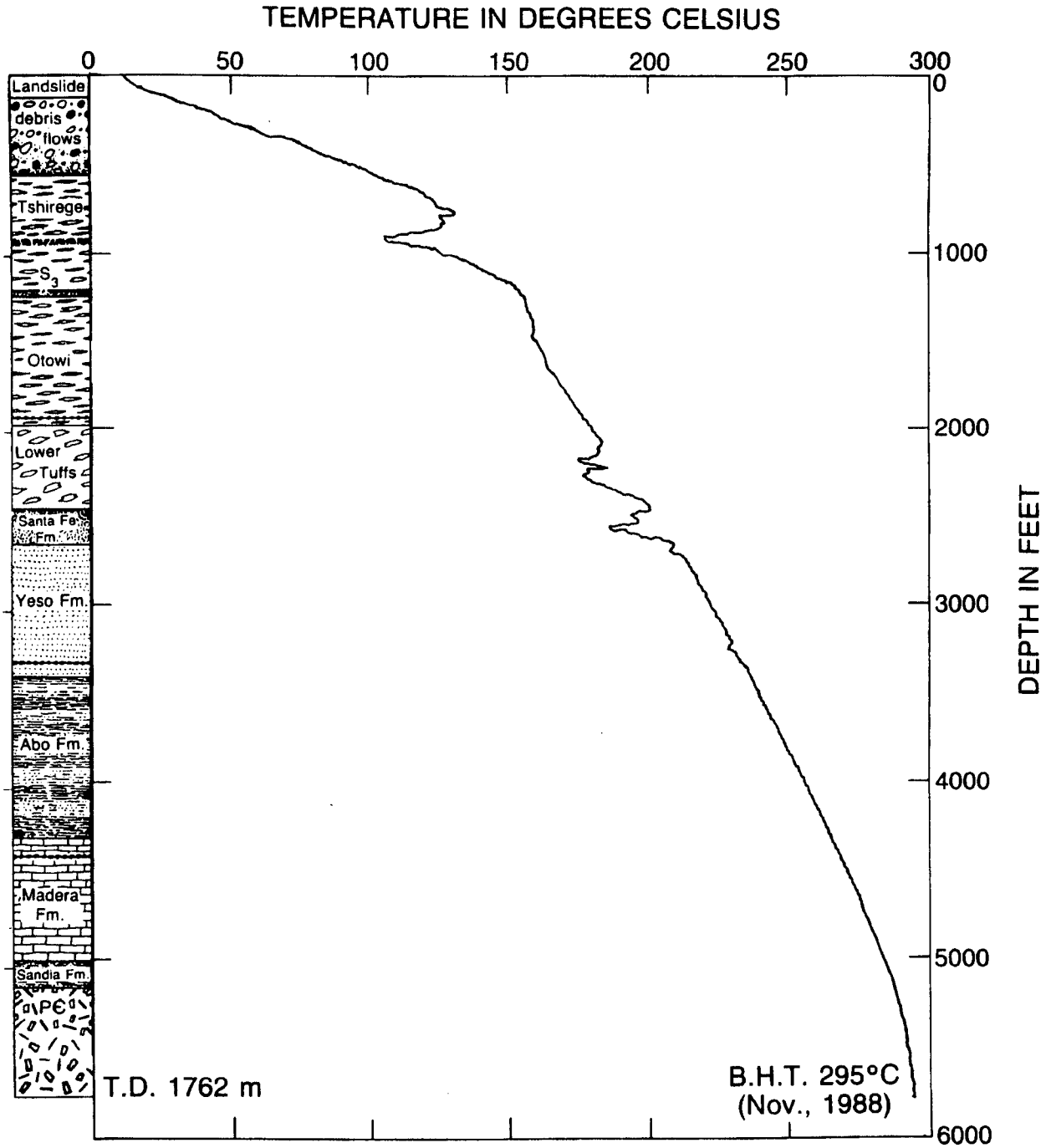

FIGURE 50—Stratigraphy and temperature log of VC-2B.

thermal system consists of an acid-sulfate condensation layer (pH <1.5) no more than 5 m thick, a vapor zone extending to roughly 240 m depth, a "transitional" layer or "cap rock" of fractured but tightly sealed rock that extends from 240 to about 490 m, and a liquid-dominated zone at the bottom. A zone at 490 m and at 210°C was perforated in 1987 and stimulated. After several months of short tests this horizon was purged of drilling fluids. Chemically, the aquifer at 490 m is similar but more concentrated than other "reservoir" fluids in Valles caldera (Table 3). Sr-isotope data indicate more interaction of the fluid with precaldera basement rocks compared with fluids to the east (Meeker and Goff, 1988).

The stratigraphy, alterations, and mineralization in VC-2A appear in Fig. 20 (Hulen et al., 1987, 1988). Shallow, sub-ore-grade molybdenite mineralization was penetrated by VC-2A from 25 to 125 m. The MoS_2 is an unusual, poorly crystalline variety that occurs in vuggy veinlets and breccia cements. Other associated minerals are quartz, fluorite, illite, pyrite, chalcopyrite, sphalerite, and rhodochrosite. Analyses of selected zones grade as high

FIGURE 51—View looking north from Women's Bathhouse Spring (~90°C) toward the main area of Sulphur Springs. Men's Bathhouse Spring (75°C) lies under pile of fallen lumber of old bathhouse. Note bleached appearance of rocks that have been altered by acid-sulfate waters.

FIGURE 52—Corehole VC-2A erupting after perforation and stimulation operations, May 1987. Flashed water and steam flow from 210°C aquifer at 490 m in hydrothermally altered, pre-Toledo caldera ignimbrite.

as 0.56 wt% equivalent MoS_2. Fluid-inclusion data from quartz and fluorite suggest that this assemblage was deposited from dilute fluids (0.2–0.5 equivalent wt% NaCl) at temperatures of 195–215°C. Because the molybdenum mineralization was deposited from liquid water but now occurs in a zone where low-pressure vapor fills fractures, the surface of the liquid-dominated reservoir has descended since the deposit was formed. An illite separate from the molybdenite zone has a K–Ar age of 0.66 Ma (WoldeGabriel and Goff, 1989); thus, the present vapor zone is younger than this age.

Continue straight ahead toward NM-4. **0.5**

32.7 Gate. **2.1**

34.8 **Turn right** on NM-4. **0.8**

35.6 La Cueva and **junction** with NM-126. **Bear right** on NM-126. **2.1**

37.7 Outcrops of Permian Abo Formation on left and then on right. **1.3**

39.0 Outcrops of Miocene Santa Fe Group on right. **0.4**

39.4 **Turn right** on FR-376 toward San Antonio CC Camp. **1.2**

40.6 Outcrops of Tschicoma Dacite and Paliza Canyon Basalt underlie Bandelier Tuff along left side of road for next 2 mi (3.2 km). **2.3**

42.9 Permian Abo Formation on left. **0.9**

43.8 **Turn right** and descend into San Antonio Creek. **0.1**

43.9 **Park** in turnout before crossing bridge. **NOTE: San Antonio Hot Spring cannot be used for bathing; $50 fine.** Walk across bridge to rail fence. Walk uphill on left side of fence to big trees. Cross fence and walk south through forest to cascade from hot spring. Walk uphill to spring.

STOP 3. San Antonio Hot Spring. This spring (Table 3) is one of several dilute hot springs that issue from the western ring-fracture zone of Valles caldera (Fig. 53). Isotopically, the waters are meteoric (Fig. 16) and contain extremely low concentrations of As, B, Br, Cl, and Li that are often enriched in high-temperature geothermal fluids. Water issues at the base of fractured San Antonio Mountain Rhyolite (0.5 Ma), a moat rhyolite of the western caldera (Table 1). The rhyolite resembles South Mountain Rhyolite in appearance (seen at our earlier stops).

If you gaze west across San Antonio Canyon toward the caldera wall, you can see the Otowi Member of Bandelier Tuff overlying red stratified sandstones and shales of the Permian Abo Formation. This unit is the uppermost Paleozoic formation in the immediate vicinity of the caldera. As much as 400 m of Permian rocks have been penetrated by some geothermal wells to the southeast, and 500 m of Permian is present in corehole VC-2B. Because it is well cemented and lithified by eons of

FIGURE 53—View to north of San Antonio Hot Spring (~41°C), which issues from the contact of San Antonio Mountain Rhyolite and Redondo Creek Rhyolite. This spring is a favorite destination of cross-country skiers in winter. Cliff in background is composed of Otowi Member, Bandelier Tuff, overlying Permian red beds of the Abo Formation.

diagenesis, the Abo is fairly impermeable; thus, shallow ground waters are perched above the Abo all over the region.

Return to vehicles, turn around, and retrace route to NM-126. **4.5**

48.4 **Turn right** on NM-126. **0.5**

48.9 **STOP 4. West caldera overlook; corehole VC-1 and Hot Dry Rock project. Turn left** onto paved drive to picnic area. Park at end of drive and walk east toward overlook. From this vantage point (elev. 2615 m) on the southwest topographic rim of Valles caldera, we can gaze across the caldera moat toward Redondo Peak (elev. 3460 m), the resurgent dome occupying the approximate center of the caldera (Fig. 54). The nearer and lower ridge to the left of Redondo Peak is Redondo Border, which forms the western half of the resurgent dome. The valley between the two is the northeast-trending Redondo Peak graben.

To the northeast, in the middle distance, are San Antonio Mountain and Cerro Seco, two post-resurgent moat-rhyolite domes (Valles Rhyolite) dated at 0.54 and 0.73 Ma, respectively. A thick rhyolite flow from San Antonio Mountain overlies Redondo Creek Rhyolite on Thompson Ridge in the caldera moat immediately before us. Another flow of rhyolitic obsidian (Banco Bonito Member, Valles Rhyolite) fills the caldera moat to our right (age 0.13 Ma).

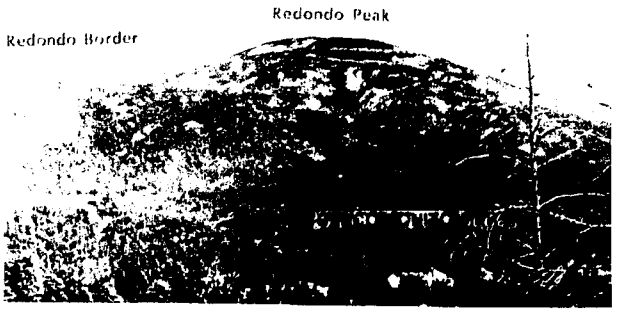

FIGURE 54—View looking east toward Redondo Peak. Redondo Border on left. The linear valley separating these two ridges is the Redondo Creek graben, the medial graben of the resurgent dome. In foreground is the southern moat of the caldera which is filled by postcaldera rhyolites, the Banco Bonito Member on the right and the Redondo Creek Member on the left. Corehole VC-1 was drilled on the south edge of the Banco Bonito rhyolite flow approximately on strike with the southwest extension of the medial graben (just right of photo). Stratigraphy of VC-1 is shown schematically in the cross section of Fig. 17.

On the distant skyline to the northeast, on the northern rim of the caldera, is Cerro de la Garita formed of dacite of the Tschicoma Formation. On the skyline to the southeast is the crest of Los Griegos (on the south rim of the caldera), formed mainly of andesites of the Paliza Canyon Formation.

CSDP corehole VC-1 was drilled in August 1984 on the southern side of the Banco Bonito flow on strike with the southwest projection of the Redondo Creek graben. Objectives were: (1) to intersect a hydrothermal outflow plume from the geothermal reservoir near its source, (2) to study the structure and stratigraphy near the intersection of the ring-fracture zone and the precaldera Jemez fault zone, and (3) to study the petrology of the youngest moat volcanics in the caldera. Total depth is 856 m and the BHT is about 185°C. Fluid chemistry of aquifers at 400–600 m depth in VC-1 resembles, but is more dilute than, reservoir waters in the caldera (Table 3, Fig. 16). A more detailed discussion of the outflow plume will be given at Stop 6.

VC-1 core was found to be altered and structurally disrupted below 335 m, particularly the lowermost interval of brecciated Precambrian rocks and Sandia Formation (Hulen and Nielson, 1988a; Keith, 1988). Molybdenite was also found in this breccia zone along with chalcopyrite, sphalerite, galena, pyrite, and barite. Fluid-inclusion work suggests that the molybdenite was deposited from dilute water at tempertures as high as 280°C (Hulen and Nielson, 1988a; Sasada, 1988). Ghazi and Wampler (1987) obtained a K–Ar age of 1.0 Ma on hydrothermal illite in Madera Limestone, while Sturchio and Binz (1988) obtained ages of 95 to >400 Ka on calcite veins using the U–Th disequilibrium technique. Geissman (1988) found that the paleomagnetic character of Paleozoic rocks in the corehole was overprinted by a reversed magnetic signature and concluded that major hydrothermal activity at about 300°C occurred between 1.4 and 0.97 Ma.

The location of the first Hot Dry Rock (HDR) demonstration project is a scant 0.5 km to the west of this site. In the HDR concept, two wells are drilled into hot, impermeable-rock units and connected by man-made fractures. Cold surface water is pumped down one well, where it is heated by the rock adjacent to the fracture, and removed up the second well. A heat exchanger or turbine is used to extract the heat or energy from this circulation system, after which the water is pumped down the first well for another cycle. The first (research) system (Fig. 11) was constructed at a depth of 3 km where the ambient temperature is 195°C. This system demonstrated technical feasibility (Heiken et al., 1981; Laughlin, 1981; Smith, 1983). The second system,

constructed at depths of 3.7 km and a temperature of about 250°C, is designed to demonstrate commercial feasibility. For a tour of the HDR facilities call (505) 667-7900.

Small volumes of relatively concentrated fluids (≥20,000 mg/kg TDS) have been encountered in Precambrian rocks in both the HDR wells (Grigsby et al., 1984) and in the WC23-4 well on Thompson Ridge in the western caldera moat (Shevenell et al., 1987, 1988). The origin of these fluids and their relation to more dilute but voluminous "reservoir" fluids is not yet resolved, but an association can be seen in the isotope plot of Fig. 16 (see also Table 3).

Turn around and return to NM-126. **0.1**

49.0 **Turn right** on NM-126. **4.3**

53.3 **Turn right** on NM-4 at La Cueva. **0.7**

54.0 Exposures of Banco Bonito Rhyolite over Battleship Rock Tuff on left side of upper San Diego Canyon. **1.3**

55.3 Contact of Permian Abo Formation (red beds) over Pennsylvanian Madera Limestone (buff rock). **1.0**

56.3 Mineral seeps in shale of Madera Limestone on right. **0.2**

56.5 **Turn left** into Battleship Rock picnic area (do not turn into Camp Shaver). Follow arrows to bridge and cross it. **0.2**

56.7 **STOP 5. Battleship Rock.** Park anywhere and walk past old restrooms to path that ascends the lower "prow" of Battleship Rock. Battleship Rock (Fig. 55) is a spectacular outcrop of columnar-jointed ignimbrite formed by a series of small eruptions that flowed down an ancestral drainage of the Jemez River. Subsequent erosion by new streams has formed canyons on either side of this beautiful example of reversed topography. San Antonio Creek drains the western caldera while East Fork Jemez River drains the eastern caldera, and the streams combine at Battleship Rock.

The ignimbrite is about 80 m thick and contains two main flow units that make up a single cooling unit (Bailey and Smith, 1978). Although the base is poorly consolidated, the center is densely welded and very striking in appearance. Abundant lithic and crystal fragments are found in the matrix of the ignimbrite along with glass shards and pumice. Chemical analyses of pumice lumps show that this ignimbrite is a rhyolite similar in composition to the youngest, more mafic group of moat rhyolites (Gardner et al., 1986). Self et al. (1988) consider the Battleship Rock Tuff to be part of the co-magmatic El Cajete Series and indicate an age of about 0.15 Ma. An age of 0.278 ± 0.052 Ma was obtained by K–Ar methods on sanidine separated from pumice lumps (F. Goff, unpubl. data 1986). In corehole VC-1, Banco Bonito Rhyolite directly overlies Battleship Rock Tuff; no El Cajete Pumice is found (Goff et al., 1986). Thus, the timing of the Battleship Rock Tuff with respect to other units is still in question.

If you examine the contact between ignimbrite and underlying rocks on the east side of Battleship Rock, note that the tuff overlies a small cliff of Pennsylvanian Madera Limestone. The limestone is extremely fossiliferous and includes crinoids, brachiopods, and bryozoans.

Return to NM-4. **0.3**

57.0 **Turn left** on NM-4. **0.5**

57.5 Smell of hydrogen sulfide and sight of bleached rock signify Hummingbird Fumarole on left of road but above level of Jemez River. **3.2**

60.7 **STOP 6. Soda Dam and Jemez fault zone.** Park in turnout on right side of road before crossing cattleguard. Walk up path to ledge overlooking the right (west) side of highway. The travertine dam (Fig. 56) across the gorge in Precambrian granite–gneiss was built by carbonated thermal waters that discharge from a strand of the Jemez fault zone. There are roughly 15 springs and seeps discharging in this area. About 20 years ago water discharged along the central fissure parallel to the trend of the dam, but the New Mexico State Highway Department eliminated the hump in the paved road by dynamiting a notch in the west end of the dam. This forever changed the plumbing of hot-spring water and today Soda Dam is slowly disintegrating.

The travertine deposits of Soda Dam proper have been dated by the U–Th technique and have a max-

FIGURE 55—Battleship Rock, a small-volume, postcaldera ignimbrite of the Valles Rhyolite that occupies the ancestral canyon of the Jemez River. Note radial cooling joints near the "prow."

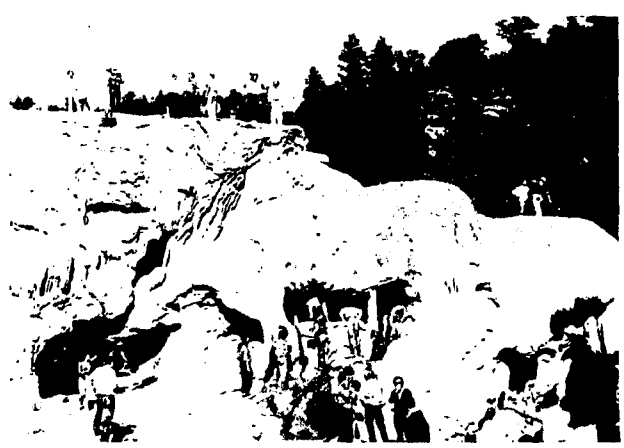

FIGURE 56—Soda Dam, a hot-spring deposit of travertine now undercut by the Jemez River (lower right). Narrow cavern in center of photo leads to Groto Spring. Main hot spring (48°C) issues along highway to left of photo.

imum age of about 5 Ka (Goff and Shevenell, 1987). Two older deposits at slightly higher elevation occur across the Jemez River (age = 60–110 Ka). On the west side of the gorge, roughly 30 m above the road, occurs an extremely large deposit of travertine that has an age range of about 0.48–1.0 Ma by evaluation with the U–U dating method. These older deposits do not overlie Bandelier Tuff; instead they lie directly on Paleozoic/Precambrian rocks. A discontinuous deposit of ancestral Jemez River gravels can be seen beneath the travertine and a large cave is located along the contact.

Hot-spring waters at Soda Dam have a maximum temperature of 48°C and contain about 1500 mg/kg Cl and substantial As, B, Br, Li, etc. (Table 3). They chemically resemble, but are more dilute than, reservoir water inside Valles caldera, and isotopically they appear to be mixtures of meteoric and reservoir water (Fig. 16). Several people have claimed that the hot waters follow the trace of the Jemez fault zone out of the caldera and mix with dilute ground waters (Dondanville, 1971; Trainer, 1974; Goff et al., 1981). By combining geochemistry of hot springs and aquifers throughout the southwestern perimeter of the caldera with other geologic data, Goff et al. (1988) showed that a major subsurface tongue of reservoir water flows out of the caldera on either side of the Jemez fault zone. During lateral flow, the waters dissolve Paleozoic limestone and become relatively rich in Ca and HCO_3. When these data are combined with the information on the travertine deposits, the age of the Valles hydrothermal system is estimated to be about 1.0 Ma.

The Jemez fault zone is very complex in this area. The main trace trends northeast across the highway and creates a 15 m scarp along the north side of the older travertine. Generally, displacement along the fault in Paleozoic rocks is about 200–250 m down-to-the-east. At Soda Dam, a local horst of sheared Precambrian granite–gneiss is uplifted and overlain by distorted Paleozoic rocks. The granite–gneiss is hydrothermally altered and contains secondary barite, galena, and sphalerite in veins and fracture fillings. The Jemez fault zone continues to the southwest and displaces the Tshirege Member of the Bandelier Tuff by about 50 m in the canyon wall.

If you gaze carefully at the upper east wall of San Diego Canyon, you can see a white band of Abiquiu Formation (late Oligocene) overlying orange Permian Yeso Formation sandstone and shale. The Abiquiu is overlain by volcanic units of the Paliza Canyon Formation (8–10 Ma?) and the mesa is capped by a thin layer of Tshirege Member, Bandelier Tuff. Looking northwest, the canyon wall is composed of Pennsylvanian Madera Limestone, Abo Formation, Abiquiu Formation, Paliza Canyon Formation, and both members of the Bandelier Tuff. The canyon is partly controlled by erosion along the Jemez fault zone and the stratigraphy is different on either canyon wall.

Return to vehicles and continue southwest (downstream) on NM-4. **0.2**

60.9 Outcrops of Precambrian granite–gneiss to left and right. **0.8**

61.7 Ruins of 17th century Spanish mission on left. **0.5**

62.2 **STOP 7. Jemez Springs and space-heating project. Turn right** just beyond Jemez Springs Police Station/Courthouse and drive to parking area by bathhouse. Jemez Springs is a small village with several religious institutions and several interesting hot springs. The bathhouse on the west side of the road is open to the public. Water is supplied mainly from an old, hand-dug well covered by the quaint gazebo. Temperature is about 55°C. Another curious spring (72°C) issues from a mound of travertine in the reeds near the Jemez River (Fig. 57). Others occur in the marshy area and discharge along the river. These springs are also derived from Valles reservoir fluids and are part of the hydrothermal plume (Table 3, Fig. 16).

In January 1979, the community of Jemez Springs drilled a well 255 m deep that penetrated the Madera Limestone and bottomed in Precambrian granite. They were seeking hot water for space heating. The hottest water (74°C) was at 25 m at the contact of alluvium and limestone. Another aquifer at 152 m has a cooler temperature of 62°C, indicating a typical temperature reversal beneath the hydrothermal plume (Goff et al., 1981). The town hall uses the aquifer at 25 m for space heating, but has problems with calcite scaling of the heat exchanger.

Return to NM-4. **0.1**

62.3 **Turn left** on NM-4 to return to Los Alamos (about 39 mi), or **turn right** on NM-4 to return to Albuquerque (about 50 mi); at San Ysidro **turn left** on NM-44; at Bernalillo **turn right** on I-25.

FIGURE 57—Travertine Mound Spring (72°C), the hottest spring outside the Valles caldera depression, is reported to contain an extremely rare species of alga. It is located in the reeds between the Jemez River and bathhouse at Jemez Springs.

Acknowledgments

This field-trip guide has evolved from the earlier guides published by Bailey and Smith (1978), Goff and Bolivar (1983), and Self et al. (1987), and from countless field trips led by the authors during the last 10 years. Many thanks to

all the explorers, developers, researchers, and graduate students, past and present, who have contributed to the general knowledge of the Jemez Mountains region. Much of the information incorporated in this paper was obtained from the geothermal efforts of UNOCAL (Santa Rosa, California), GEO Operator Corp. (San Mateo, California), and SUNEDCO (Dallas, Texas), and from the research and development efforts of the Hot Dry Rock project funded by the U.S. Department of Energy. The cooperation of the U.S. Forest Service, the Baca Land and Cattle Company, John Corbin of Sulphur Springs, and other landowners in the Jemez Mountains is gratefully appreciated. Marcia Jones and Anthony Garcia typed the manuscript and prepared many of the figures, respectively. This field-trip guide was funded by the U.S. Department of Energy, Office of Basic Energy Sciences, through the helpful efforts of George Kolstad, and by an Institutional Supporting Research grant from Los Alamos National Laboratory.

References

Aldrich, M. J., 1968, Tectonics of the Jemez lineament in the Jemez Mountains and the Rio Grande rift: Journal of Geophysical Research 91: 1753–1762.

Aldrich, M. J., Jr., and Laughlin, A. W., 1984, A model for the tectonic development of the southeastern Colorado Plateau boundary: Journal of Geophysical Research, 89: 10,207–10,218.

Ankeny, L. A., Braile, L. W., and Olsen, K. H., 1986, Upper crustal structure beneath the Jemez Mountains volcanic field, New Mexico, determined by three-dimensional simultaneous inversion of seismic refraction and earthquake data: Journal of Geophysical Research, 91: 6188–6198.

Bailey, R. A., and Smith, R. L., 1978, Volcanic geology of the Jemez Mountains, New Mexico; *in* Hawley, J. W. (ed.), Guidebook to the Rio Grande rift in New Mexico and Colorado: New Mexico Bureau of Mines & Mineral Resources, Circular 163: 184–196.

Bailey, R. A., Smith, R. L., and Ross, C. S., 1969, Stratigraphic nomenclature of volcanic rocks in the Jemez Mountains, New Mexico: U.S. Geological Survey, Bulletin 1274-P: 19 pp.

Baldridge, W. S., 1979, Petrology and petrogenesis of Plio-Pleistocene basaltic rocks from the central Rio Grande rift, New Mexico, and their relation to rift structure; *in* Riecker, R. E. (ed.), Rio Grande rift: Tectonics and magmatism: American Geophysical Union, Special Publication, pp. 323–353.

Baldridge, W. S., Perry, F. V., and Shafiqullah, M., 1987, Late Cenozoic volcanism in the southeastern Colorado Plateau: I. Volcanic geology of the Lucero area, New Mexico: Geological Society of America, Bulletin, 99: 463–470.

Baldridge, W. S., Damon, P. E., Shafiqullah, M., and Bridwell, R. J., 1980, Evolution of the central Rio Grande rift, New Mexico: New Potassium–Argon ages: Earth and Planetary Science Letters, 51: 309–321.

Barton, P., Bethke, P., Wetlaufer, P., Foley, N., Hayba, D., and Goss, J., 1982, Silver/base metal epithermal deposits; *in* Erickson, R. L. (ed.), Characteristics of mineral deposit occurrences: U.S. Geological Survey, Open-File Report 82-795: 127–130.

Bayhurst, G. K., and Janecky, D. R., 1987, Investigations of alteration mineralogy and geochemistry in CSDP hole VC-2A, Valles caldera, New Mexico: American Geophysical Union, Transactions, 68: 469.

Behrman, P. G., and Knapp, R. B., 1980, Structure of the Redondo Creek area, Baca prospect—Implications concerning the nature of permeability and control on production: Union Oil Company of California, Internal Report; also University of Utah Research Institute, Earth Science Laboratory, Open-File Report NM-Baca-101: 43 pp.

Brookins, D., and Laughlin, A. W., 1983, Rb–Sr geochronologic investigation of Precambrian samples from deep geothermal drill holes, Fenton Hill, New Mexico: Journal of Volcanology and Geothermal Research, 15: 43–58.

Budding, A. J., 1978, Gravity survey of the Pajarito Plateau, Los Alamos and Santa Fe counties, New Mexico: Los Alamos Scientific Laboratory, Report LA-7419-MS: 15 pp.

Chapin, C. E., 1979, Evolution of the Rio Grande rift: A summary; *in* Riecker, R. E. (ed.), Rio Grande rift: Tectonics and magmatism: American Geophysical Union, Special Publication, pp. 1–6.

Chapin, C. E., and Seager, W. R., 1975, Evolution of the Rio Grande rift in the Socorro and Las Cruces areas; *in* Seager, W. R., Clemons, R. E., and Callender, J. F. (eds.), Las Cruces country: New Mexico Geological Society, Guidebook 26: 297–321.

Charles, R. W., Vidale-Buden, R., and Goff, F., 1986, An interpretation of the alteration assemblages at Sulphur Springs, Valles caldera, New Mexico: Journal of Geophysical Research, 91: 1887–1898.

Cordell, L., 1978, Regional geophysical setting of the Rio Grande rift: Geological Society of America, Bulletin, 89: 1073–1090.

Dalrymple, G. B., Cox, A., Doell, R. R., and Grommé, C. S., 1967, Pliocene geomagnetic polarity epochs: Earth and Planetary Science Letters, 2: 163–173.

Dethier, D. P., and Manley, K., 1985, Geologic map of the Chili quadrangle, Rio Arriba County, New Mexico: U.S. Geological Survey, Map MF-1814, scale 1:24,000.

Dethier, D. P., Harrington, C. D., and Aldrich, M. J., 1988, Late Cenozoic rates of erosion in the Western Española basin, New Mexico: Evidence from geologic dating of erosion surfaces: Geological Society of America, Bulletin, 100: 928–937.

Doell, R. R., and Dalrymple, G. B., 1966, Geomagnetic polarity epochs, A new polarity event and the age of the Brunhes–Matuyama boundary: Science, 152: 1060–1072.

Doell, R. R., Dalrymple, G. B., Smith, R. L., and Bailey, R. A., 1968, Paleomagnetism, potassium–argon ages, and geology of rhyolites and associated rocks of the Valles caldera, New Mexico; *in* Coats, R. R., Hay, R. L., and Anderson, C. A. (eds.), Studies in volcanology: Geological Society of America, Memoir 116: 211–248.

Dondanville, R. F., 1971, The hydrothermal geology of the Valles caldera, Jemez Mountains, New Mexico: Union Oil Company, Santa Rosa, California, Open-File consultant report, 36 pp.

Dondanville, R. F., 1978, Geologic characteristics of the Valles caldera geothermal system: Geothermal Resources Council, Transactions, 2: 157–160.

Eichelberger, J. C., 1980, Vesiculation of magma during replenishment of silicic magma reservoirs: Nature, 288: 446–450.

Eichelberger, J. C., and Koch, F. G., 1979, Lithic fragments in the Bandelier Tuff, Jemez Mountains, New Mexico: Journal of Volcanology and Geothermal Research, 5: 115–134.

Faust, C. R., Mercer, J. W., and Thomas, S. D., 1984, Quantitative analysis of existing conditions and production strategies for the Baca geothermal system, New Mexico: Water Resources Research, 20: 601–618.

Fisher, R. V., 1979, Models for pyroclastic surges and pyroclastic flows: Journal of Volcanology and Geothermal Research, 6: 305–318.

Friedman, I., and Smith, R. L., 1958, The deuterium content of water in some volcanic glasses: Geochimica et Cosmochimica Acta, 15: 218–228.

Galusha, T., and Blick, J. C., 1971, Stratigraphy of the Santa Fe Group, New Mexico: American Museum of Natural History, Bulletin, 144: 1–128.

Gardner, J. N., 1985, Tectonic and petrologic evolution of the Keres Group: Implications for the development of the Jemez volcanic field, New Mexico: Unpublished Ph.D. dissertation, University of California, Davis, 295 pp.

Gardner, J. N., and Goff, F., 1984, Potassium–argon dates from the Jemez volcanic field: Implications for tectonic activity in the north-central Rio Grande rift; *in* Baldridge, W. S., Dickerson, P. W., Riecker, R. E., and Zidek, J. (eds.), Rio Grande rift: Northern New Mexico: New Mexico Geological Society, Guidebook 35: 75–81.

Gardner, J. N., and House, L., 1987, Seismic hazards investigations at Los Alamos National Laboratory, 1984 to 1985: Los Alamos National Laboratory, Report LA-11072-MS: 76 pp.

Gardner, J. N., Goff, F., Garcia, S., and Hagan, R. C., 1986, Stratigraphic

relations and lithologic variations in the Jemez volcanic field, New Mexico: Journal of Geophysical Research, 91: 1763–1778.

Geissman, J. W., 1988, Paleomagnetism and rock magnetism of Quaternary volcanic rocks and Late Paleozoic strata, VC-1 core hole, Valles caldera, New Mexico, with emphasis on remagnetization of Late Paleozoic strata: Journal of Geophysical Research, 93(B6): 6001–6026.

Ghazi, A., and Wampler, J., 1987, Potassium–argon dates of clays from brecciated and hydrothermally altered rocks from VC-1, Valles caldera, New Mexico: American Geophysical Union, Transactions, 68: 1515.

Gill, J. B., 1981, Orogenic andesites and plate tectonics: Springer-Verlag, New York, 390 pp.

Goff, F., 1983, Subsurface structure of Valles caldera: A resurgent cauldron in northern New Mexico (abs.): Geological Society of America, Abstracts with Programs, 15: 381.

Goff, F., and Bolivar, S. L., 1983, Field trip guide to the Valles caldera and its geothermal systems: Los Alamos National Laboratory, Report LA-9963-OBES: 53 pp.

Goff, F., and Gardner, J. N., 1980, Geologic map of the Sulphur Springs area, Valles caldera geothermal system, New Mexico: Los Alamos Scientific Laboratory, Map LA-8634-MAP (two sheets, scale 1:5000).

Goff, F., and Gardner, J. N., 1988, Valles caldera region, New Mexico, and the emerging Continental Scientific Drilling Program: Journal of Geophysical Research, 93(B6): 5997–6000.

Goff, F., and Grigsby, C. O., 1982, Valles caldera geothermal systems, New Mexico, USA: Journal of Hydrology, 56: 119–136.

Goff, F., and Nielson, D. L. (eds.), 1986, Caldera processes and magma-hydrothermal systems, Continental Scientific Drilling Program—Thermal Regimes, Valles caldera research, scientific and management plan: Los Alamos National Laboratory, Report LA-10737-OBES: 163 pp.

Goff, F., and Shevenell, L., 1987, Travertine deposits of Soda Dam, New Mexico, and their implications for the age and evolution of the Valles caldera hydrothermal system: Geological Society of America, Bulletin, 99: 292–302.

Goff, F., Gardner, J. N., Vidale, R., and Charles, R., 1985, Geochemistry and isotopes of fluids from Sulphur Springs, Valles caldera, New Mexico: Journal of Volcanology and Geothermal Research, 23: 2734–2797.

Goff, F., Grigsby, C., Trujillo, P., Counce, D., and Kron, A., 1981, Geology, water geochemistry, and geothermal potential of the Jemez Springs area, Cañon de San Diego, New Mexico: Journal of Volcanology and Geothermal Research, 10: 227–244.

Goff, F., Shevenell, L., Gardner, J. N., Vuataz, F. D., and Grigsby, C. O., 1988, The hydrothermal outflow plume of Valles caldera, New Mexico, and a comparison with other outflow plumes: Journal of Geophysical Research, 93(B6): 6041–6058.

Goff, F., Heiken, G., Tamanyu, S., Gardner, J., Self, S., Drake, R., and Shafiqullah, M., 1984, Location of Toledo caldera and formation of the Toledo embayment, Jemez Mountains, New Mexico: American Geophysical Union, Transactions, 65: 1145.

Goff, F., Nielson, D. L., Gardner, J. N., Hulen, J. B., Lysne, P., Shevenell, L., and Rowley, J. C., 1987, Scientific drilling at Sulphur Springs, Valles caldera, New Mexico: Corehole VC-2A: American Geophysical Union, Transactions, 68: 649, 661–662.

Goff, F., Rowley, J., Gardner, J. N., Hawkins, W., Goff, S., Charles, R., Wachs, D., Maassen, L., and Heiken, G., 1986, Initial results from VC-1: First Continental Scientific Drilling Program core hole in Valles caldera, New Mexico: Journal of Geophysical Research, 91: 1742–1752.

Goldstein, N. E., and Tsang, C. F., 1984, A review of lessons learned from the DOE/Union Baca geothermal project: Geothermal Resources Council, Bulletin 8: 7–12.

Golombek, M. P., 1983, Geology, structure, and tectonics of the Pajarito fault zone in the Española Basin of the Rio Grande rift, New Mexico: Geological Society of America, Bulletin, 94: 192–205.

Gonzalez, C. M., and McKibben, M. A., 1987, Thermal history of vein mineralization in CSDP corehole VC-2A, Valles caldera, New Mexico (abs.): Geological Society of America, Abstracts with Programs, 19: 679.

Griggs, R. L., 1964, Geology and groundwater resources of the Los Alamos area, New Mexico: U.S. Geological Survey, Water Supply Paper 1753: 107 pp.

Gribsby, C., Goff, F., Trujillo, P., and Counce, D., 1984, Geochemical behavior of a hot dry rock geothermal reservoir; *in* Baldridge, W. S., Dickerson, P. W., Riecker, R. E., and Zidek, J. (eds.), Rio Grande rift: Northern New Mexico: New Mexico Geological Society, Guidebook 35: 265–270.

Harrison, T. M., Morgan, P. M., and Blackwell, D. D., 1986, Constraints on the age of heating at the Fenton Hill site, Valles caldera, New Mexico: Journal of Geophysical Research, 91: 1899–1908.

Hayba, D. O., Bethke, P. M., Heald, P., and Foley, N. K., 1985, Geologic characteristics of volcanic-hosted epithermal precious-metal deposits: Reviews in Economic Geology, 2: 129–168.

Heiken, G. (ed.), 1985, Workshop on recent research in the Valles caldera: Los Alamos National Laboratory, Report LA-10339-C: 68 pp.

Heiken, G., and Goff, F., 1983, Hot dry rock geothermal energy in the Jemez volcanic field, New Mexico: Journal of Volcanology and Geothermal Research, 15: 223–246.

Heiken, G., Murphy, H., Nunz, G., Potter, R., and Grigsby, C., 1981, Hot dry rock geothermal energy: American Scientist, 69: 400–407.

Heiken, G., Goff, F., Stix, J., Tamanyu, S., Shafiqullah, M., Garcia, S., and Hagan, R., 1986, Intracaldera volcanic activity, Toledo caldera and embayment, Jemez Mountains, New Mexico: Journal of Geophysical Reserch, 91: 1799–1815.

Henley, R. W., and Ellis, A. J., 1983, Geothermal systems ancient and modern: A geochemical review: Earth-Science Reviews, 19: 1–50.

Hermance, J. F., and Pedersen, J., 1980, Deep structure of the Rio Grande rift: A magnetotelluric interpretation: Journal of Geophysical Research, 85: 3899–3912.

Hulen, J. B., and Nielson, D. L., 1986a, Hydrothermal alteration in the Baca geothermal system, Redondo dome, Valles caldera, New Mexico: Journal of Geophysical Research, 91: 1867–1886.

Hulen, J. B., and Nielson, D. L., 1986b, Stratigraphy and hydrothermal alteration in borehole Baca-8, Sulphur Springs area, Valles caldera, New Mexico: Geothermal Resources Council, Transactions, 10: 187–192.

Hulen, J. B., and Nielson, D. L., 1988a, Hydrothermal brecciation in the Jemez fault zone, Valles caldera, New Mexico: Results from Continental Scientific Drilling Program core hole VC-1: Journal of Geophysical Research, 93(B6): 6077–6090.

Hulen, J. B., and Nielson, D. L., 1988b, Clay mineralogy and zoning in CSDP core hole VC-2A—Further evidence for collapse of isotherms in the Valles caldera: Geothermal Resources Council, Transactions, 12: 291–298.

Hulen, J., Gardner, J. N., Nielson, D., and Goff, F., 1988, Stratigraphy, structure, hydrothermal alteration and ore mineralization encountered in CSPD core hole VC-2A, Sulphur Springs, Valles caldera, New Mexico: A detailed overview: University of Utah Research Institute, Report ESL-88001-TR: 44 pp.

Hulen, J., Nielson, D. L., Goff, F., Gardner, J. N., and Charles, R., 1987, Molybdenum mineralization in an active geothermal system, Valles caldera, New Mexico: Geology, 15: 748–752.

Iddings, J. P., 1890, On a group of rocks from the Tewan Mountains, New Mexico, and on the occurrence of primary quartz in certain basalts: U.S. Geological Survey, Bulletin 66: 34 pp.

Irvine, T. N., and Barager, W. R. A., 1971, A guide to the chemical classification of the common volcanic rocks: Canadian Journal of Earth Sciences, 8: 523–548.

Izett, G. A., Obradovich, C. W., Naeser, C. W., and Cebula, C. T., 1981, Potassium–argon and fission-track zircon ages of Cerro Toledo rhyolite tephra in the Jemez Mountains, New Mexico: U.S. Geological Survey, Professional Paper 1199-D: 37–43.

Janecky, D. R., Charles, R., and Goff, F., 1987, Geochemistry of molybdenum-bearing assemblages in CSDP well VC-2A, Valles caldera, New Mexico: American Geophysical Union, Transactions, 68: 469.

Keith, T. E. C., 1988, Alteration in the Madera Limestone and Sandia Formation from core hole VC-1, Valles caldera, New Mexico: Journal of Geophysical Research, 93: 6068–6076.

Kelley, V. C., Woodward, L. A., Kudo, A. M., and Callender, J. F., 1976, Guidebook to the Albuquerque Basin of the Rio Grande rift, New Mexico: New Mexico Bureau of Mines & Mineral Resources, Circular 153: 31 pp.

Kerr, R. A., 1982, Extracting geothermal energy can be hard: Science, 218: 668–669.

Kolstad, C. D., and McGetchin, T. R., 1978, Thermal evolution models for the Valles caldera with reference to a hot-dry-rock geothermal experiment: Journal of Volcanology and Geothermal Research, 3: 197–218.

Kuentz, D. C., 1986, The Otowi Member of the Bandelier Tuff: A study of the petrology, petrography, and geochemistry of an explosive silicic eruption, Jemez Mountains, New Mexico: Unpublished M.S. thesis, University of Texas at Arlington, 165 pp.

Lambert, S. J., and Epstein, S., 1980, Stable isotope investigations of an active geothermal system in Valles caldera, Jemez Mountains, New Mexico: Journal of Volcanology and Geothermal Research, 8: 111–129.

Laughlin, A. W., 1981, The geothermal system of the Jemez Mountains, New Mexico, and its exploration; *in* Rybach, L., and Muffler, L. J. P. (eds.), Geothermal systems: Principles and case histories: Wiley, New York, pp. 295–320.

Laughlin, A. W., Brookins, D. G., and Damon, P. E., 1976, Late-Cenozoic

basaltic volcanism along the Jemez zone of New Mexico and Arizona (abs.): Geological Society of America, Abstracts with Programs, 8: 598.

Laughlin, A. W., Eddy, A. C., Laney, R., and Aldrich, M. J., 1983, Geology of the Fenton Hill, New Mexico, hot dry rock site: Journal of Volcanology and Geothermal Research, 15: 21–41.

Lindgren, W., Graton, L. C., and Gorden, C. H., 1910, The ore deposits of New Mexico: U.S. Geological Survey, Professional Paper 68: 361 pp.

Loeffler, B. M., 1981, Major- and trace-element and strontium- and oxygen-isotope geochemistry of the Polvadera Group, Jemez volcanic field, New Mexico: Implications for the petrogenesis of the Polvadera Group: Unpublished Ph.D. dissertation, University of Colorado, Boulder, 259 pp.

Loeffler, B. M., Vaniman, D. T., Baldridge, W. S., and Shafiqullah, M., 1988, Neogene rhyolites of the northern Jemez volcanic field, New Mexico: Journal of Geophysical Research, 93(B6): 6157–6168.

Luedeke, R. G., and Smith, R. L., 1978, Map showing distribution, composition, and age of late Cenozoic volcanic centers in Arizona and New Mexico: U.S. Geological Survey, Miscellaneous Investigations Map I-1091-A, scale 1:1,000,000.

Luth, W., and Hardee, R., 1980, Comparative assessment of five potential sites for hydrothermal-magma systems: A summary: U.S. Department of Energy, Report DOE-TIC-11303: 51 pp.

Mahon, W. A. J., Klyen, L. E., and Rhode, M., 1980, Neutral sodium/bicarbonate/sulfate hot waters in geothermal systems: Japanese Geothermal Energy Association, Journal, 17: 11–24.

Manley, C. R., and Fink, J. H., 1987, Internal textures of rhyolite flows as revealed by research drilling: Geology, 15: 549–552.

Manley, K., 1976, K–Ar age determination on Pliocene basalts from the Española basin, New Mexico: Isochron/West, no. 16: 29–30.

Manley, K., 1982, Geologic map of the Cañones quadrangle, Rio Arriba County, New Mexico: U.S. Geological Survey, Map MF-1440, scale 1:24,000.

Mansfield, G. R., 1918, Sulphur in Jemez Canyon, Sandoval County: U.S. Geological Survey, Mineral Resources, 1918, pt. 2: 367.

Marvin, R. F., and Dobson, S. W., 1979, Radiometric ages: Compilation B: U.S. Geological Survey, Isochron West, no. 26: 3–32.

Mayo, E. G., 1958, Lineament tectonics and some ore districts of the southwest: Mining Engineering, 10: 1169–1175.

McDowell, D. S., and Elders, W. A., 1980, Authigenic layer silicate minerals in borehole Elmore 1, Salton Sea geothermal field, California, U.S.A.: Contributions to Mineralogy and Petrology, 74: 293–310.

Meeker, K., and Goff, F., 1988, Geochemistry of the 490-m 210°C aquifer in core hole VC-2A, Sulphur Springs and comparison with other hydrothermal fluids in Valles caldera, New Mexico: American Geophysical Union, Transactions, 69: 1049.

Mills, C., Winterkamp, J., and Marusak, N., 1987, Geosciences bibliography of the Valles Caldera: A CSDP information base: Los Alamos National Laboratory, Report LA-UR-84-3148 (Rev. 3): 235 pp.

Muffler, L. J. P., and White, D. E., 1969, Active metamorphism of upper Cenozoic sediments in the Salton Sea geothermal field and the Salton Trough, southeastern California: Geological Society of America, Bulletin, 80: 157–182.

Musgrave, J., Goff, F., Shevenell, L., Trujillo, P., Counce, D., Luedemann, G., Garcia, S., Dennis, B., Hulen, J., Janik, C., and Tomei, F., 1989, Selected data from Continental Scientific Drilling core holes VC-1 and VC-2A, Valles caldera, New Mexico: Los Alamos National Laboratory, Report, in press.

Nielsen, D. L., and Hulen, J. B., 1984, Internal geology and evolution of the Redondo dome, Valles caldera, New Mexico: Journal of Geophysical Research, 89: 8695–8711.

Olsen, K. H., Braile, L. W., Stewart, J. N., Daudt, C. R., Keller, G. R., Ankeny, L. A., and Wolff, J. J., 1986, Jemez Mountains volcanic field, New Mexico: Time term interpretation of the CARDEX seismic experiment and comparison with Bouguer gravity: Journal of Geophysical Research, 91: 6175–6187.

Pearson, F. J., and Truesdell, A. H., 1978, Tritium in the waters of Yellowstone National Park: U.S. Geological Survey, Open-File Report 78-701: 3 pp.

Perkins, P. C., 1973, Petrology of some rock types of the Precambrian basement near the Los Alamos Scientific Laboratory geothermal test site, Jemez Mountains, New Mexico: Los Alamos Scientific Laboratory, Report LA-5129-MS: 12 pp.

Phillips, F., Goff, F., Vuataz, F.-D., Bentley, H. W., Elmore, D., and Gove, H., 1984, ^{36}Cl as a tracer in geothermal systems: Example from Valles caldera, New Mexico: Geophysical Research Letters, 11: 1227–1230.

Potter, D. B., and Oberthal, C. M., 1983, Vent sites and flow directions of the Otowi ash flows (lower Bandlier Tuff), New Mexico: Geological Society of America, Bulletin, 98: 66–76.

Powell, J. W., 1961, The Exploration of the Colorado River and its canyons: Dover Publications, New York, 400 pp. (Republication of Canyons of the Colorado, Flood and Vincent, 1885.)

Reiter, M., Edwards, C. L., Hartman, H., and Weidman, C., 1975, Terrestrial heat flow along the Rio Grande rift, New Mexico and southern Colorado: Geological Society of America, Bulletin, 86: 811–818.

Reiter, M., Weidman, C., Edwards, C. L., and Hartman, H., 1976, Subsurface temperature data in Jemez Mountains, New Mexico: New Mexico Bureau of Mines & Mineral Resources, Circular 151: 16 pp.

Ross, C. S., and Smith, R. L., 1961, Ash-flow tuffs: Their origin, geologic relations and identification: U.S. Geological Survey, Professional Paper 366: 81 pp.

Sasada, M., 1987, Fluid inclusions from VC-2A core hole in Valles caldera, New Mexico, U.S.A.—Evidence for a transition from hot water-dominated to vapor-dominated system (abs.): Geothermal Research Society of Japan, Annual Meeting, Abstracts with Program.

Sasada, M., 1988a, Fluid inclusion evidence for recent temperature rising at Fenton Hill hot dry rock test site west of the Valles caldera, New Mexico, USA: *in* Exploration and Development of Geothermal Resources, International Symposium on Geothermal Energy, 1988: Geothermal Research Society of Japan, pp. 526–529.

Sasada, M., 1988b, Microthermometry of fluid inclusions from the VC-1 core hole in Valles caldera, New Mexico: Journal of Geophysical Research, 93(B6): 6091–6096.

Sass, J. H., and Morgan, P., 1988, Conductive heat flux in VC-1 and the thermal regime of Valles caldera, Jemez Mountains, New Mexico: Journal of Geophysical Research, 93(B6): 6027–6040.

Segar, R. L., 1974, Quantitative gravity interpretation, Valles caldera area, Sandoval and Rio Arriba counties, New Mexico: University of Utah Research Institute, Earch Science Laboratory, Open-File Report NM/BACA-27: 12 pp.

Self, S., Gardner, J. N., and Goff, F., 1987, A field guide to the Jemez Mountains volcanic field, New Mexico: *in* Davis, G. H., and Vonder Dolder, E. M. (eds.), Geologic diversity of Arizona and its margins: Excursions to choice areas: Arizona Bureau of Geology & Mining Technology, Special Paper 5: 95–112.

Self, S., Kircher, D. E., and Wolff, J. A., 1988, The El Cajete Series, Valles Caldera, New Mexico: Journal of Geophysical Research, 93(B6): 6113–6128.

Self, S., Goff, F., Gardner, J. N., Wright, J. V., and Kite, W. M., 1986, Explosive rhyolitic volcanism in the Jemez Mountains: Vent locations, caldera development and relation to regional structure: Journal of Geophysical Research, 91: 1779–1798.

Shevenell, L., Goff, F., Miles, D., Waibel, A., and Swanberg, C., 1988, Lithologic descriptions and temperature profiles of five wells in the southwestern Valles caldera region, New Mexico: Los Alamos National Laboratory, Report LA-11165-OBES: 43 pp.

Shevenell, L., Goff, F., Vuataz, F., Trujillo, P., Counce, D., Janik, C., and Evans, B., 1987, Hydrogeochemical data for thermal and nonthermal waters and gases of the Valles caldera, southern Jemez Mountains region, New Mexico: Los Alamos National Laboratory, Report LA-10923-OBES: 100 pp.

Singer, B. S., and Kudo, A. M., 1986, Assimilation–fractional crystallization of Polvadera Group rocks in the northwestern Jemez volcanic field, New Mexico: Contributions to Mineralogy and Petrology, 94: 374–386.

Smith, M. C., 1983, A history of hot dry rock geothermal energy systems: Journal of Volcanology and Geothermal Research, 15: 1–20.

Smith, R. L., 1979, Ash-flow magmatism: *in* Chapin, C. E., and Elston, W. E. (eds.), Ash-flow tuffs: Geological Society of America, Special Paper 180: 5–28.

Smith, R. L., and Bailey, R. A., 1966, The Bandelier Tuff—A study of ash-flow eruption cycles from zoned magma chambers: Bulletin of Volcanology, 29: 83–104.

Smith, R. L., and Bailey, R. A., 1968, Resurgent cauldrons: *in* Coats, R. R., Hay, R. L., and Anderson, C. A. (eds.), Studies in volcanology: Geological Society of America, Memoir 116: 613–662.

Smith, R. L., Bailey, R. A., and Ross, C. S., 1961, Structural evolution of the Valles caldera, New Mexico and its bearing on the emplacement of ring dikes: U.S. Geological Survey, Professional Paper 424-D: 145–149.

Smith, R. L., Bailey, R. A., and Ross, C. S., 1970, Geologic map of the Jemez Mountains, New Mexico: U.S. Geological Survey, Miscellaneous Geological Investigations Map I-571, scale 1:250,000.

Smith, S. P., and Kennedy, B. M., 1985, Noble gas evidence for two fluids in the Baca (Valles caldera) geothermal reservoir: Geochimica et

Cosmochimica Acta, 49: 893–902.

Sommer, M. A., 1977, Volatiles H_2O, CO_2, and CO in silicate melt inclusions in quartz phenocrysts from the rhyolitic Bandelier air-fall and ash-flow tuff, New Mexico: Journal of Geology, 85: 423–432.

Spell, T. L., 1987, Geochemistry of Valle Grande Member ring fracture rhyolites, Valles caldera, New Mexico: Unpublished M.S. thesis, New Mexico Institute of Mining & Technology, Socorro, New Mexico, 212 pp.

Spencer, R. K., and Tsang, C. F., 1984, Listing of scientific data on the Baca geothermal field: Lawrence Berkeley National Laboratory, Report LBL-17675: 138 pp.

Srodon, J., 1980, Precise identification of illite/smectite interstratifications by X-ray powder diffraction: Clays and Clay Minerals, 28: 401–411.

Srodon, J., and Eberl, D. D., 1984, Illite; *in* Bailey, S. W. (ed.), Micas: Mineralogical Society of America, Reviews in Mineralogy, 13: 498–544.

Stein, H. L., 1983, Geology of the Cochiti mining district, Jemez Mountains, New Mexico: Unpublished M.S. thesis, University of New Mexico, Albuquerque, 122 pp.

Steiner, A., 1968, Clay minerals in hydrothermally altered rocks at Wairakei, New Zealand: Clays and Clay Minerals, 16: 193–213.

Stix, J., Goff, F., Gorton, M. P., Heiken, G., and Garcia, S. R., 1988, Restoration of compositional zonation in the Bandelier silicic magma chamber between two caldera-forming eruptions: Geochemistry and origin of the Cerro Toledo Rhyolite, Jemez Mountains, New Mexico: Journal of Geophysical Research, 93(B6): 6129–6147.

Sturchio, N. C., and Binz, C. M., 1988, Uranium-series age determination of calcite veins, VC-1 drill core, Valles caldera, New Mexico: Journal of Geophysical Research, 93(B6): 6097–6102.

Suhr, G., 1981, Seismic crust anomaly under the Valles caldera in New Mexico, USA: Unpublished consultant report, PRAKLA-SEISMOS GMBH, Hannover, Federal Republic of Germany, 56 pp.

Summers, W. K., 1976, Catalog of thermal waters in New Mexico: New Mexico Bureau of Mines & Mineral Resources, Hydrologic Report 4: 80 pp.

Swanberg, C. A., 1983, Geothermal resources of rifts: A comparison of the Rio Grande rift and the Salton Trough: Tectonophysics, 94: 659–678.

Taschek, R. F., 1981, Scientific and operational plan for drilling in the Valles caldera, New Mexico: Continental Scientific Drilling Committee, National Science Foundation, Washington, D.C., Document 0491A: 45 pp.

Trainer, F. W., 1975, Mixing of thermal and nonthermal waters in the margin of the Rio Grande rift, Jemez Mountains, New Mexico; *in* Siemers, C. T., Woodward, L. A., and Callender, J. F. (eds.), Ghost Ranch: New Mexico Geological Society, Guidebook 25: 213–218.

Trainer, F. W., 1978, Geohydrologic data from the Jemez Mountains and vicinity, north-central New Mexico: U.S. Geological Survey, Water Resources Investigation 77-131: 146 pp.

Trainer, F. W., 1984, Thermal springs in Cañon de San Diego as a window into Valles caldera, New Mexico; *in* Baldridge, W. S., Dickerson, P. W., Riecker, R. E., and Zidek, J. (eds.), Rio Grande rift: Northern New Mexico: New Mexico Geological Society, Guidebook 35: 249–255.

Truesdell, A. H., and Janik, C. J., 1986, Reservoir processes and fluid origins in the Baca geothermal system, Valles caldera, New Mexico: Journal of Geophysical Research, 91: 1817–1833.

Turbeville, B. N., and Self, S., 1988, San Diego canyon ignimbrites: Pre-Bandelier tuff explosive rhyolitic volcanism in the Jemez Mountains, New Mexico: Journal of Geophysical Research, 93(B6): 6148–6156.

Vuataz, F.-D., and Goff, F., 1986, Isotope geochemistry of thermal and nonthermal waters in the Valles caldera, Jemez Mountains, northern New Mexico: Journal of Geophysical Research, 91: 1835–1853.

Vuataz, F. D., Goff, F., Fouillac, C., and Calvez, J. Y., 1988, A strontium isotope study of the VC-1 core hole and associated hydrothermal fluids and rocks from Valles Caldera, Jemez Mountains, New Mexico: Journal of Geophysical Research, 93(B6): 6059–6067.

Waresback, D. B., 1986, The Puye Formation, New Mexico: Analysis of a continental rift-filling volcaniclastic alluvial fan sequence: Unpublished M.S. thesis, University of Texas at Arlington, 269 pp.

Warshaw, C. M., and Smith, R. L., 1988, Pyroxenes and fayalites in the Bandelier Tuff, New Mexico: Temperatures and comparison with other rhyolites: American Mineralogist, 73: 1025–1037.

White, A. F., 1986, Chemical and isotopic characteristics of fluids within the Baca geothermal reservoir, Valles caldera, New Mexico: Journal of Geophysical Research, 91: 1855–1866.

White, D. E., and Heropoulous, C., 1983, Active and fossil hydrothermal convection systems of the Great Basin; *in* The role of heat in the development of energy and mineral resources in the northern Basin and Range province: Geothermal Resources Council, Special Report 13: 41–54.

White, D. E., Muffler, L. P. J., and Truesdell, A. H., 1971, Vapor-dominated hydrothermal systems compared with hot-water systems: Economic Geology, 66: 75–97.

Williston, McNeal and Associates, 1979, A time domain survey of the Los Alamos region, New Mexico: Los Alamos Scientific Laboratory, Report LA-7657-MS: 32 pp.

Wilt, M., and Vonder Haar, S., 1986, A geologic and geophysical appraisal of the Baca geothermal field, Valles caldera, New Mexico: Journal of Volcanology and Geothermal Research, 27: 349–370.

WoldeGabriel, G., 1989, Hydrothermal systems in two areas of the Jemez volcanic field: Sulphur Springs and the Cochiti minign district: Los Alamos National Laboratory, Report LA-11509-OBES: 66 pp.

WoldeGabriel, G., and Goff, F., 1989, Temporal relationships of volcanism and hydrothermal systems in two areas of the Jemez volcanic field, New Mexico: Geology (in press).

Wright, J. V., Smith, A. L., and Self, S., 1981, A terminology for pyroclastic deposits; *in* Self, S., and Sparks, R. S. J. (eds.), Tephra studies: D. Reidel Publishing Company, Boston, pp. 457–463.

Wronkiewicz, D., Norman, D., Parkinson, G., and Emanuel, K., 1984, Geology of the Cochiti mining district, Sandoval County, New Mexico; *in* Baldridge, W. S., Dickerson, P. W., Riecker, R. E., and Zidek, J. (eds.), Rio Grande rift: Northern New Mexico: New Mexico Geological Society, Guidebook 35: 219–22.

Zartman, R. E., 1979, Uranium, thorium, and lead concentrations and lead isotopic composition of biotite granodiorite (sample 9527-2b) from LASL drill hole GT-2: Los Alamos Scientific Laboratory, Report LA-7923-MS: 18 pp.

EXCURSION 18B:
Rio Grande rift volcanism: Northeastern Jemez zone, New Mexico

M. A. Dungan[1], R. A. Thompson[2], and J. S. Stormer[3], with a short contribution by J. M. O'Neill[2]

[1]Department of Geological Sciences, Southern Methodist University, Dallas, Texas 75275; [2]U.S. Geological Survey, Denver, Colorado 80225; [3]Department of Geology and Geophysics, Rice University, Houston, Texas 77251

Introduction

Magmatism, a predictable consequence of asthenospheric upwelling associated with lithospheric attenuation, is integral to continental rifting. The injection of mantle-derived magma into extending crust may have a profound effect on the rheology of the crust and therefore the style of deformation associated with extension (De Voogd et al., 1988). Rift-related magmatism encompasses much of the diversity of terrestrial-magma types. Compositions of mafic magmas range from tholeiite to some of the most silica-undersaturated magmas found on the continents, and their differentiates range over the entire spectrum of intermediate to salic compositions to include high-SiO_2 rhyolite, trachyte, and phonolite. Large effusive eruptions from fissures are typical of some rifts, whereas others may be dominated by central vent cones or even silicic caldera complexes. Most of these aspects of rift volcanism and a wide range of mafic to salic magma compositions are represented in the Rio Grande rift; many will be seen on this trip.

Geological setting of the Rio Grande rift

The Rio Grande rift is a late Cenozoic rift in continental crust of Proterozoic age (1.7–1.4 Ga) which, prior to rifting, experienced deformation during the Ancestral Rocky Mountain (late Paleozoic) and Laramide (Late Cretaceous–early Tertiary) orogenies. Rift basins have the same overall north–south trend as Laramide compressional structures in the Southern Rocky Mountains, and they are located near the eastern margin of the region affected by Laramide deformation. An extended episode of mid-Tertiary magmatism immediately preceded rifting. In the Southern Rocky Mountains, the eastern edge of the broad region of subduction-related calc-alkaline magmatism, which intermittently characterized the North American cordillera during early to mid-Tertiary time (Snyder et al., 1976; Coney and Reynolds, 1977; Cross and Pilger, 1978), coincides with the eastern limit of the uniquely broad and complex extensional regime that dominated late Cenozoic tectonics and volcanism of the western U.S.A. and northern Mexico. The Rio Grande rift lies close to the eastern edge of this mid-Tertiary magmatic arc, which is represented in Colorado and New Mexico by the San Juan and Mogollon–Datil volcanic fields (mainly 36–26 Ma). In fact, silicic to intermediate magmatism was still active in these fields at the time rift-related, dominantly basaltic volcanism was established in New Mexico at approximately 29–26 Ma. As with many continental rifts, the role of antecedent structures in controlling superimposed rift structures and the effects of prior magmatic events on subsequent rift-related magmatism are topics of considerable debate.

Physiography

The Rio Grande rift is a major physiographic and structural feature of the Southern Rocky Mountains, distinct from the Basin and Range provinces of southern Arizona and northern Mexico, Nevada, western Utah, southern Idaho, and eastern Oregon. However, as a well-defined volcano-tectonic province, it has been the object of concerted study for less than 20 years (Chapin, 1971, 1979; Lipman, 1969; Lipman and Mehnert, 1975, and other papers *in* Curtis, 1975; Chapin and Seager, 1975; Cordell, 1978; Seager and Morgan, 1979, and other papers *in* Riecker, 1979). The Rio Grande rift extends northward from a poorly defined terminus in northern Chihuahua, Mexico, through New Mexico into at least central Colorado (Tweto, 1979). Normal faulting, regional uplift, high heat flow (Decker et al., 1984), and scattered occurrences of volcanic rocks of late Cenozoic age are present as far north as southern Wyoming (e.g., Leucite Hills). The rift comprises two segments, the northern segment extending northward from Socorro, New Mexico, into Colorado and the southern segment extending south from Socorro into Mexico (Cordell, 1978). In the broader southern segment the tectonic style and physiography resemble the Basin and Range province: extension is distributed over several wide basins, lithospheric thinning and regional extension have reached an advanced stage, and regional elevations are lower than in the north. In the northern segment, rift basins are confined to a narrow axial zone superimposed on a region of high elevation. In effect, the rift basins of the northern Rio Grande rift separate the Colorado Plateau on the west from the High Plains to the east.

Proterozoic structures and crustal evolution

The Proterozoic history of western North America was apparently dominated by accretion of multiple exotic terranes (<2 Ga) onto a continental nucleus of Archean age. From northern Colorado to southern New Mexico and Arizona the ages of these accreted terranes decrease from about 1.8 Ga to 1.6 Ga (e.g., Reed et al., 1987; Karlstrom et al., 1987). Grambling et al. (1988) have identified six tectonostratigraphic terranes in northern and central New Mexico on the basis of differences in age (1.76–1.6 Ga), lithology, and metamorphic grade. All the rocks in these terranes are strongly deformed and display an early east–west fabric which has locally been overprinted by a northeast-trending crenulation cleavage (Montgomery, 1953; Nielsen, 1972; Nielsen and Scott, 1979; Holcombe and Callender, 1982; Holcombe et al., 1986; Grambling et al., 1988) that may be related to the Jemez lineament (see below). These terranes are locally intruded by 1.45 Ga granites.

Initiation of rifting and associated magmatism

There are four areas in the Rio Grande rift where the transition from Oligocene caldera-related magmatism to rift-related magmatism is well represented in the geologic record. They are the Trans-Pecos region of Texas, areas around Las Cruces and Socorro, New Mexico, and the San Luis Basin area of southern Colorado and northern New Mexico.